EPS-SG MicroWave Sounder (MWS) Science Plan

Prepared by the MWS Science Advisory Group

Contributors to the Science Plan:

MWS Scientific Advisory Group (SAG) Members:

Nigel Atkinson, UK Met Office
Niels Bormann, ECMWF
Fatima Karbou, Météo-France
Roger Randriamampianina, Met. Norway
Clemens Simmer, University of Bonn

External Experts:

Ralf Bennartz, Vanderbilt University
Sabatino Di Michele, EUMETSAT
Stephen English, ECMWF
Alan Geer, ECMWF
Marc Schröder, DWD
Nathalie Selbach, DWD
Sreerekha Thonipparambil, EUMETSAT

MWS SAG Co-chairs:

Dirk Schuettemeyer, ESA
Jörg Ackermann, EUMETSAT

Version 1.0
Date: 23/01/2019

Edited for the MWS Scientific Advisory Group by EUMETSAT, Eumetsat Allee 1, 64295 Darmstadt (Germany)

Table of contents:

EXECUTIVE SUMMARY ... 5
1 Introduction ... 7
1.1 Background and Role of the MWS Science Advisory Group ... 9
1.2 Purpose of the Science Plan ... 10
2 Mission objectives ... 11
2.1 Relevance of space based microwave measurements ... 11
2.2 MWS specific objectives and requirements ... 12
3 MWS Instrument ... 14
3.1 Evolution of Operational Microwave Sounding Instruments ... 14
3.2 Instrument Description ... 15
3.2.1 Requirements ... 15
3.2.2 MWS Design ... 19
3.2.2.1 Rotating mirror assembly, with scan control electronics ... 19
3.2.2.2 Quasi optics network and feedhorns ... 20
3.2.2.3 Receivers ... 21
3.2.2.4 Signal processing electronics ... 22
3.2.2.5 On-board calibration target ... 22
3.2.2.6 Other sub-systems ... 22
3.2.2.7 Implications of the design for science users ... 22
3.2.3 Radiometric Performance ... 23
3.2.3.1 NEΔT ... 23
3.2.3.2 Radiometric accuracy and stability ... 24
3.2.4 Temporal Sampling and Geometric Performance ... 26
4 MWS applications ... 30
4.1 Numerical Weather Forecast (data assimilation, expected impact on NWP models) ... 30
4.2 Regional Applications and Nowcasting ... 33
4.3 Climate Monitoring (Trends and future evolution of MWS retrieved geophysical parameters) ... 38
5 MWS Science and Products ... 41
5.1 Level 1 Products Generation (Radiances, Antenna Corrected Brightness Temperatures) ... 41
5.1.1 Calibration algorithm ... 41
5.1.1.1 Assumptions ... 41
5.1.1.2 Solving the calibration equations ... 41
5.1.1.3 The nonlinearity parameter ... 42
5.1.1.4 Variation of antenna reflectivity with scan angle ... 43
5.1.1.5 Lunar contamination of the space view ... 44
5.1.1.6 Other aspects of calibration processing ... 44
5.1.2 User customisation of Level 1 products ... 45
5.2 Use of Level 1 products in NWP ... 47
5.2.1 Radiative transfer model in NWP ... 47
5.2.2 Thinning, superobbing, modelling of spatial representativeness ... 48
5.2.3 Geophysical quality control ... 48
5.2.4 Treatment of systematic and random errors related to observations ... 49
5.2.5 All-sky developments and coupled data assimilation ... 49
5.2.6 Use of novel MWS channels ... 50
5.3 Level 2 Products ... 51
5.3.1 Total Column Water Vapor over Water ... 51
5.3.2 Total Column Water Vapor over Polar Areas ... 52
5.3.3 Cloud Liquid Water Content over Water ... 52
5.3.4 Sea Ice Concentration ... 53
5.3.5 Rain Rates ... 54
5.3.6 Land Surface Temperature ... 55
5.3.7 Cirrus Cloud Detection ... 55

5.3.8 Snow, Sea ice monitoring ... 56
5.3.9 Rainfall, Soil moisture ... 58
5.4 Product Monitoring ... 60
5.4.1 Monitoring of instrument parameters ... 60
5.4.1.1 NEΔT ... 60
5.4.1.2 Calibration view counts ... 61
5.4.1.3 Striping index ... 61
5.4.1.4 Instrument Temperature ... 61
5.4.2 Monitoring of Level 1 data against NWP fields ... 62
5.4.3 User notification ... 62
5.5 Synergy with other instruments ... 63
5.5.1 Instruments on the same platform ... 63
5.5.2 Instruments on different LEO platforms ... 65
5.5.3 Synergies with instruments on geostationary platforms ... 65
6 MWS research and Product development needs ... 67
6.1 Instrument Validation ... 67
6.1.1 Pre-launch Activities ... 67
6.1.1.1 Thermal vacuum calibration using precision calibration targets ... 67
6.1.1.2 Local oscillator frequency monitoring ... 69
6.1.1.3 Cross-channel interference ... 69
6.1.1.4 EMC testing ... 69
6.1.1.5 Antenna pattern determination ... 69
6.1.1.6 Pass-band characterisation ... 70
6.1.2 Post-launch Activities ... 71
6.1.2.1 Launch and early orbit phase (LEOP) ... 72
6.1.2.2 Satellite manoeuvres ... 72
6.1.2.3 Aircraft campaigns ... 74
6.1.2.4 Monitoring and use in NWP ... 74
6.2 Radiative transfer ... 75
6.2.2 Line-shape modelling ... 76
6.2.3 Issues in the 183 GHz band ... 76
6.2.4 Radiative transfer in clouds and precipitation ... 79
6.2.5 Ocean surface emissivity ... 80
6.2.6 Land surface emissivity ... 81
6.3 Identified research needs ... 85
Reference Documents ... 87
List of Acronyms ... 99

EXECUTIVE SUMMARY

The Microwave Sounder (MWS) on EPS-SG is a microwave radiometer with the primary objective to provide profile information on temperature and humidity in clear and cloudy regions, on liquid and ice clouds, as well as on some surface parameters like temperature and emissivity. It provides measurements in 24 channels, between 23.8 and 229 GHz, with 14 channels located in the 50-60 GHz oxygen band and five around the 183.31 GHz water vapour line. The instrument scans cross-track, providing 95 samples between scanning angles of ±49.31° (translating to a swath width of around 2210 km). The field-of-view sizes at nadir is 17 km for channels at 89 GHz and above, 20 km for channels in the 50-60 GHz band and 40 km for the remaining window channels. MWS has a strong heritage from similar sounders (MSU, AMSU-A, AMSU-B, MHS, ATMS, etc.), but also includes new lower surface/sounding channels never before available from space, namely two channels between 53 and 54 GHz for lower tropospheric sounding, and a new channel at 229 GHz for improved detection of ice clouds. The instrument design uses the heterodyne technique, and is subject to stringent requirements, particularly in terms of noise performance.

The Science Plan has been prepared by the MWS Scientific Advisory Group, convened jointly by EUMETSAT and ESA, and internal and external experts. It provides a framework for the scientific research and development that will be required to ensure that the MWS mission objectives are met and that the MWS instrument will be used to its full potential. It reviews the currently available scientific expertise in the application areas, in order to identify where research and development is needed. It also identifies areas where current and future studies may best be directed.

The main application areas for MWS are (see sections 4 and 5.3):

- Numerical Weather Prediction (NWP), both global and regional, for which microwave temperature and humidity sounders are leading providers of forecast skill;
- Climate monitoring, for which MWS continues key satellite-based observation records;
- Hydrology, through providing information on rainfall, cloud liquid water, snow and sea-ice.

Products will be produced to cater for these application areas, with Level 1 data being the primary product for NWP, and derived quantities such as total column water vapour, cloud liquid water content, rain rates or land products (land surface temperature, snow) used for various application areas. Level 1 processing will broadly follow the established principles of heritage instruments, relying on thorough pre-launch instrument characterisation and in-flight calibration information from space views and an on-board warm target (section 5.1). Traceability (as far as practical) as well as full documentation of the processing will be important, especially for climate studies. Software packages such as AAPP will need to be adapted to facilitate local processing of Level 1 data consistently with the central processing performed at EUMETSAT. Level 2 processing can build on established algorithms, with some adaptation, for instance to incorporate capabilities of the new channels (section 5.3).

Stringent instrument requirements from NWP (especially regarding noise performance) and climate monitoring (especially regarding stability) are driving the need for thorough pre-launch and in-flight instrument characterisation and validation. Required pre-launch characterisation is detailed in section 6.1.1, and includes thermal vacuum calibration characterisation using precise targets; determination of cross-channel interference; comprehensive antenna pattern characterisation; and detailed measurements of channel passbands.

- The SAG recommends that pre-launch characterisation of MWS should be thoroughly documented and made publicly available to ensure availability for future research.

Thorough calibration and validation after launch, combined with sustained monitoring of the Level 1 product and key instrument and processing parameters throughout the life-time of the mission will be essential for quality assurance. Such information is particularly useful for NWP and climate users. Requirements for calibration and validation tests are summarised in section 6.1.2, including campaign data, tailored satellite manoeuvres and monitoring in NWP, and they are further outlined in a dedicated Calibration/Validation Plan document.

- The SAG recommends making results of the life-time monitoring of level 1 characteristics and instrument parameters publicly available online for users in near-real-time (see section 5.4). User notifications of changes in the product should be provided as for heritage instruments.

Radiative transfer packages will need to be adapted to process MWS data. The technical adaptation of the fast radiative transfer package RTTOV is expected to be straightforward. However, continued scientific research and development for radiative transfer is very highly recommended, such as regarding line-by-line modelling, improved spectroscopic parameters, and fast radiative transfer modelling of clouds and precipitation (section 6.2).

NWP is a key driver for the MWS mission and processing requirements. While a basic use of microwave sounding data is fairly mature (concepts are reviewed in section 5.2), three key areas with very significant development in the recent two decades will have to be addressed for an optimised use of MWS measurements: 1) NWP systems are increasingly more accurate, with random errors in short-range forecasts for tropospheric temperature-sounding channels below the noise level of typical microwave sounders. 2) NWP systems make also use of cloud and rain-affected radiances, for initialisation of related variables, as well as improving microphysical parameterisations, in contrast to the traditional approach of rejecting observations with too large cloud/rain signals. 3) Coupled assimilation systems are emerging, in which an atmospheric model is more closely coupled to a land-surface or ocean model is offering opportunities to better use the surface information contained in the MWS radiances. These developments will potentially require significant adaptation for MWS, in order to achieve the full potential of the instrument.

The following main areas have been identified as priorities for research and development targeted at an optimised use of MWS data (section 6.3):

- Analysis of errors: Given that random errors in short-range forecasts from NWP for tropospheric temperature will be below the MWS instrument noise and given lower noise levels in MWS compared to heritage instruments, other sources contributing to the error budget will become more important (e.g. radiative transfer, cloud screening for clear-sky applications). To achieve the full potential of MWS, research is needed to identify and reduce these leading sources of error. Probabilistic approaches are one of the promising research activities; especially those focusing on nonlinearity handling and use of non-Gaussian errors. Extreme values representation is another important issue and it is necessary to better understand and characterize them.
- Improved radiative transfer modelling: Radiative transfer underpins all quantitative uses of MWS data, and continued research is needed to benefit all applications. Example areas with relevant uncertainties are line coupling aspects in the crucial 50-60 GHz range (particularly for clear-sky applications), and scattering properties (especially for frozen and mixed-phase particles) and modelling of 3-dimensional effects for cloud/precipitation-affected regions. Inter-comparison exercises of different models are also needed. This should encourage research towards more rigorous comparisons with in-situ measurements. For this, a proper treatment of scales for better match of observation and model representativity is also needed.
- The development of new techniques to improve the exploitation of MWS as part of a system of observations in perfect synergy not only with microwave sensors from other satellite missions (active or passive), but also with optical/infrared sensors and in-situ/airborne measurements.
- Better use of cloud/rain information, combination with MWI/ICI: MWS observations contain significant information on cloud and precipitation, particularly in the new MWS channels that have never been available from space. Developments are needed to make best use of this information to initialise clouds and the required dynamical environment in all-sky assimilation systems, capitalising on recent advancements in this area. The combined use of MWS with MWI/ICI allows unprecedented constraints on clouds and related fields for model initialisation and cloud parameterisation development, and it will require very significant research and development to fully realise this potential.
- Better use of surface information: MWS observations also include significant information on surface conditions (land surface, snow, sea-ice), but development is needed to best utilise this information for Earth System models, i.e. those assimilation systems that couple atmospheric and surface/ocean models. Such advances will improve the extraction of atmospheric information from lower tropospheric sounding channels, as well as benefit the of surface components initialisation of the Earth System models.

1 INTRODUCTION

Aim of the EUMETSAT Polar System - Second Generation (EPS-SG) System is to provide global information on geophysical variables of the atmosphere, the ocean and land surfaces derived from sensors (which cover a broad spectral range, from UV to MW) mounted on Low-Earth Orbit (LEO) satellites. To fulfil this goal it is required to deploy sustained capabilities to acquire, process, and to distribute to down-stream application users and second tier processing centres the environmental data derived from observations.. As such, EPS-SG will provide operational continuity and service enhancements to missions carried out by the Metop (Meteorological Operational satellite) satellites of the current EUMETSAT Polar System (EPS). The EPS-SG is planned for operation in the 2021-2041 timeframe and will contribute to the Joint Polar System Satellite (JPSS) being jointly set up with the National Oceanic and Atmospheric Administration (NOAA).

The space segment of the EPS-SG system will consist of a dual satellite configuration with three sounding and imaging satellites (A-series) and three microwave satellites (B-series). Each satellite is specified for a nominal life time (including commissioning) of 7.5 years. Like Metop, the satellites will be operated in a Sun synchronous, Low-Earth orbit at around 820 km altitude with an approximate equator crossing time at 09:30 Mean Local Solar Time in descending node.

The candidate EPS-SG missions were identified by the Post-EPS Mission Experts Team (PMET) and narrowed down after industrial Phase 0 studies in the Post-EPS Mission Definition Review. The payload complements have been confirmed through further feasibility studies at Phase A. As a result, the EPS-SG will encompass the following observation missions:

- The Infra-red Atmospheric Sounding – New Generation (IASI-NG) mission, covering a wide swath of hyper-spectral infra-red soundings in four spectral bands, covering the spectral domain from 3.62 to 15.5 μm at a spatial sampling of about 25 km;
- The Microwave Sounding (MWS) mission, allowing for all-weather soundings over a wide swath in the spectral region between 23 and 229 GHz, at a spatial sampling of about 30 km;
- The Scatterometry (SCA) mission, providing back-scattered signals in the 5.355 GHz band at a spatial resolution of 25 km;
- The Visible/Infra-red Imaging mission (VII) METimage, providing cross-purpose, moderate-resolution optical imaging in ≥20 spectral channels ranging from 0.443 to 13.345 μm with a spatial sampling of 500 m;
- The Microwave Imaging (MWI) mission, providing precipitation and cloud imaging in the spectral range from 18.7 to 183 GHz at a spatial sampling from about 8 km (highest frequency) to 12 km (lowest frequency);
- The Ice Cloud Imaging (ICI) mission, providing ice-cloud and water-vapour imaging in the spectral range from 183 to 664 GHz at a spatial sampling of < 15 km.
- The Radio Occultation (RO) mission, providing high vertical resolution, all-weather soundings by tracking GPS (Global Positioning System) and Galileo satellites;
- The Sentinel-5 Nadir-viewing Ultraviolet, Visible, Near-infra-red, Short-wave-infra-red sounding (UVNS) mission, providing hyper-spectral sounding with a spectral resolution from 0.05 to 1 nm within the spectral range from 0.27 to 2.4 μm at a spatial sampling of 7 km;
- The Multi-viewing Multi-channel Multi-polarisation Imaging (3MI) mission, providing moderate resolution aerosol imaging in the spectral region ranging from ultra-violet (0.342 μm) to short-wave infra-red (2.13 μm), at a spatial sampling of 4 km.

As consequence, the EPS-SG satellites will carry the instruments listed in Table 1.

Metop-SG payload	Metop-SG satellite
IASI-NG: Infrared Atmospheric Sounding Interferometer – New Generation	A
METimage: Visible-Infrared Imager (VII)	A
MWS: Microwave Sounder	A
Sentinel-5: UV-VIS-NIR-SWIR (UVNS) Sounder	A
3MI: Multi-viewing, -channel, -polarisation Imager	A
RO: Radio Occultation	A and B
SCA: Scatterometer	B
MWI: Microwave Imager	B
ICI: sub-mm wave Ice Cloud Imager	B
ARGOS A-DCS (Advanced Data Collection System) payload[1]	B

Table 1: Instruments embarked on the EPS-SG satellites.

This distribution of the payload complement between the two parallel satellites gives regard to the priority of the mid-morning sounding and imaging missions (IAS, MWS, RO, VII) and the need for co-registration of missions (IAS-VII, UVNS-VII, 3MI-VII, MWI-ICI).

In line with the above, the high level objectives of the EPS-SG programme are, in order of priority, as formulated in the EPS-SG End Users Requirements Document (EURD):

1. To support operational meteorology, continuing and enhancing the core relevant services provided by EPS, with a focus on advanced sounding capability in the mid-morning orbit and in accordance with agreed user needs and priorities, and taking into account World Meteorological Organization (WMO) requirements as far as possible;
2. To provide operational services in support of climate monitoring and detection of global climatic changes in the frame of relevant international initiatives, through cooperation and partnership, and taking into account the Global Climate Observing System (GCOS) requirements as far as possible;
3. To develop new environmental services covering the oceans, atmosphere, land and biosphere and natural disasters to the extent that they interact with, drive or are driven by meteorology and climate.

The operational objectives of the EPS-SG missions aim to provide a number of services throughout their operational lifetime, i.e. satisfying precise timeliness and availability requirements. Among the services to the users covered by the individual EPS-SG missions, the most relevant to the EURD are:

- Global data acquisition and generation;
- Regional data acquisition and generation;
- Level 1 (L1) Products generation;
- Level 2 (L2) Products generation;
- Near Real Time (NRT) data dissemination;
- Climate Data Records generation.

[1] ARGOS A-DCS is not considered an observation mission

In the following, focus will be given to the MWS mission and in particular, on the scientific part of the mission.

1.1 Background and Role of the MWS Science Advisory Group

The MWS instrument is part of the core payload of the future Metop-SG satellite A to be flown as part of the EPS-SG programme from 2021 onwards. MWS will contribute to primary mission objectives of EPS-SG in the areas of operational meteorology and climate monitoring. The objectives of the MWS mission are described in the EPS-SG End User Requirements Document, prepared by EUMETSAT and recapped in Section 2.2 of this document. Amongst other EPS-SG instruments, MWS is a so-called CPI (Contractor Provided Item) instrument, which means that in the framework of their responsibility for the prototype satellites, ESA is also responsible for the development of the MWS instrument. EUMETSAT is responsible for overall user requirements, procurement of the launchers and LEOP (Launch and Early Orbit Phase) services, the development of the ground segment, and also provides the operational service to the end-users.

For the scientific preparation of the MWS mission, ESA and EUMETSAT have established a MWS Science Advisory Group (SAG), composed of leading scientists in the application areas supported by this instrument. One of the primary tasks of this group is the preparation of a science plan (present document) to detail the scientific work, which is needed to meet the MWS mission objectives. The plan is prepared by the MWS SAG members with coordination support from EUMETSAT and ESA. As such, the science plan particularly focuses on the scientific requirements for MWS related components of the EPS-SG ground segment. The MWS SAG will accompany the MWS project at least to the end of the commissioning phase of the first flight model. Hence, the science plan is a living document and will be regularly reviewed and possibly updated. Besides the preparation of the science plan, the role of SAG is considered as beneficial in the following areas:

- Assisting ESA and EUMETSAT in the selection of the most suitable methods to be applied for the EPS-SG ground segment, covering both the central processing at EUMETSAT and the de-centralised processing in the network of the EUMETSAT Satellite Application Facilities;
- Advising ESA and EUMETSAT on requirements and methods for instrument calibration and post-launch validation activities;
- Identifying gaps that might exist in the proposed product processing, product format, archiving, dissemination, and reprocessing;
- Advising on the scientific requirements of the MWS system and instrument, taking into account constraints which are imposed by the status of design/development of the overall EPS-SG system and of the MWS instrument;
- Reviewing the progress and the results of scientific projects initiated in support of MWS, providing recommendations to ESA and EUMETSAT on the direction and focus of further work to be pursued within these projects;
- Reviewing the progress of the MWS project by supporting technical reviews and advise on implications of non-conformances for mission and scientific objectives;
- Providing recommendations for scientific studies which are needed to support the MWS project, and assisting the preparation of work statements and by reviewing results of initiated studies;
- Participating in the coordination of the MWS SAG activities with external science and user groups;
- Contributing to the draft of scientific reports and publications in the framework of the MWS SAG activities.

1.2 Purpose of the Science Plan

The Science Plan provides a framework for the scientific research and development that will be required to ensure that the MWS mission objectives are met. Furthermore, it identifies the main areas where scientific research and development activities are needed in order to achieve these mission objectives. It reviews the currently available scientific expertise in these areas, in order to identify where current and future studies may best be directed. By reviewing on-going activities related to product processing, software and databases, the level of compliance with the user needs can be established and the need for additional study and development identified. In this regard, it is anticipated that the MWS Science Plan will support:

- Definition of accuracies and utilisation of baseline products in respect to end user requirements;
- Identification and characterisation of potential higher level products to be derived from MWS, addressing capabilities and limitations of the MWS mission given by the current end user requirements;
- Selection and assessment of potential methods to generate higher level products,
- Identification, from a product processing point of view, of critical elements which specifically need to be addressed in the upcoming space/ground segment studies by industry within the Phases C/D of the programme;
- Identification and assessment of tools required for the preparation and/or validation of prototype code;
- Identification of pre- and post-launch science validation activities, and of elements for routine product monitoring;
- Promotion of ideas for extending and/or refining the proposed operational Level 1 product processing chain with respect to NWP and climate monitoring applications.

It is expected that in this regard the Science Plan will also provide useful information for the Satellite Application Facilities (SAF) when starting their planning on future MWS related pre and post launch activities.

The plan will not detail the tasks for routine operational verification and validation of the products and services for MWS. It will also not provide a detailed description of all end-to-end processing steps to be implemented into the facilities of the future EPS-SG ground. This is left to the associated Algorithm Theoretical Baseline Documents, Product Generation Specifications, Product Format Specifications, and Auxiliary Data Specifications.

2 MISSION OBJECTIVES

2.1 Relevance of space based microwave measurements

For several decades, microwave sounding observations from satellites in the so-called Low-Earth Orbit have significantly enhanced the National Meteorological Services' ability to initialise global and regional Numerical Weather Prediction (NWP) models with information on air temperature and humidity profiles, in particular for cloudy situations. With the evolution of NWP towards utilisation of rather high spatial resolution (<10 km) data, an improved representation of atmospheric processes encompassing the whole Earth system (including land and ocean) will be required. Hence, accurate knowledge of area-wide geophysical variables such as vertical profiles of temperature and humidity as well as surface parameters such as snow/ice coverage, and surface temperature will play an increasing role in a skilful weather forecast. In addition, the frequent availability of detailed air temperature and humidity soundings also contributes to fulfil other key requirements common to Nowcasting and Very Short Range Weather Forecast at regional scales such as, for example, convection initiation and cloud bulk, microphysical property evolution.

Moreover, the availability of microwave radiances is of primary importance for climate monitoring applications, due to the heritage of the temperature records from the Microwave Sounding Instrument (MSU) embarked on the American Polar-orbiting Operational Environmental satellites (POES) from Television Infrared Observation Satellite-Series N (TIROS-N) to NOAA-14, operational from 1979 to 1998, and those from its successor instruments Advanced Microwave Sounding Units A and B (AMSU-A, AMSU-B), Microwave Humidity Sounder (MHS), and Advanced Technology Microwave Sounder (ATMS). Climate observations are considered crucial for monitoring the Earth system under changing conditions. There is a societal need for a greater confidence in long-range climate projections that requires consistent and systematic high-quality observations as a basis for testing the predictive capabilities of climate models. This is particularly true for long-term studies of global change where the reliability of variables in the climate model projections need to be quantified. With the intent to support the United Nations Framework Convention on Climate Change (UNFCCC) and the Intergovernmental Panel on Climate Change (IPCC) the GCOS of the WMO introduced the list of the Essential Climate Variables (ECV) deemed technically and economically feasible for systematic observation (https://public.wmo.int/en/programmes/global-climate-observing-system?name=EssentialClimateVariables). The monitoring of several of these variables, in particular air temperature and humidity, rely to a large extent on observations in the microwave spectral range.

Space based microwave observations also contribute to several research areas in the atmospheric, land surface, oceanic and cryospheric sciences. Examples from the atmospheric sciences are the type, structure and dynamics of precipitating and non-precipitating clouds including in particular the thermodynamic environment in which they develop. Upper-tropospheric humidity is a very important climate change variable because of its high impact on the terrestrial radiation balance. For land surface sciences, including the interactions and exchange processes with the atmosphere, the high-quality surface information (emissivity) from the window channels might be explored also in view of so barely unexplored information on global land surface change including vegetation. The same holds for the ice cover (and potentially ice type) monitoring over polar latitudes and the sea surface temperature, near-surface wind.

For all these applications, space-based advanced microwave sounding instruments will be necessary to get this additional high resolution information on a global scale. This leads directly to the need for polar LEO satellites with highest benefit in regions where other kinds of observations are lacking or are only rather sparsely available (desert areas, oceans, mountain ranges, polar caps).

2.2 MWS specific objectives and requirements

The primary objective of the MWS mission is to support NWP at regional and global scales, through the provision of spectral radiance measurements, which contain information on:

- Atmospheric temperature profiles in clear and cloudy air;
- Atmospheric humidity profiles in clear and cloudy air;
- Cloud liquid water column contents (droplet size < 100 µm).

Consequently, the primary products to be derived from MWS observations include, in order of decreasing priority:

1. Temperature profile;
2. Humidity profile
3. Cloud liquid-water total column (droplet size < 100µm).

Further products to which MWS contributes are:

4. Cloud liquid-water profile (droplet size < 100 µm);
5. Cloud ice total column.

The level of fulfilment of these objectives will highly depend on the space-time resolution of the MWS mission. This is particularly critical at high latitudes where information from geostationary satellites is scarce or even unavailable.

Specific requirements relevant for all these applications are listed in the EURD where the end user requirements for the MWS mission are fully detailed. These requirements are briefly summarized below.

Dataset acquisition:

- The MWS shall generate simultaneously radiance samples for all its channels.

Quality:

- MWS measurements will be considered of good quality if data acquisition, timeliness, and spectral, radiometric and geometric accuracy requirements are met. In case of conflicts, radiometric requirements have higher priority than geometric requirements.

Level 1 Spectral Requirements:

- The maximum absolute shift of MWS centre frequencies is channel dependent and ranges between ±0.2 and ±130 MHz.
- The knowledge of the MWS spectral response function shapes shall be known with accuracy better than 0.1 dB at a frequency resolution less than Bandwidth/100.
- The channel-dependent measurement dynamic range of the MWS shall cover the top of atmosphere spectral radiances in terms of brightness temperatures and ranges between 80 K and 100 K for the minimum values and between 240 K and 315 K for the maximum values.
- The maximum acceptable values of MWS radiometric sensitivity are channel dependent and range between 0.25 K and 2.0 K. These values of NE∆T refer to scene temperatures less than 280 K, whereas for higher scene temperatures, the NE∆T can be increased up to 15% of the values.
- The MWS radiometric bias shall be less than 1 K for all channels and for the whole dynamic range.

- The orbit stability shall be such that variations of the radiometric bias of the measured MWS brightness temperature during any single orbit shall be less than 0.20 K.
- The lifetime stability shall be such that variations of the running average over one orbit of radiometric biases of the measured MWS brightness temperature shall be less than 0.20 K.
- Inter-channel radiometric bias differences between brightness temperatures of the same MWS spatial sample shall be less than 0.5 K.
- Radiometric bias differences between brightness temperatures of the same MWS spectral channel at different spatial samples shall be less than 0.3 K.
- Each MWS channel shall be linearly polarised and shall have a cross-polarisation error < 2%, with knowledge < 0.1% (Threshold), < 0.05% /Breakthrough).

Level 1 Geometric Requirements:

- The MWS shall provide measurements over a field of view ≥98°, perpendicular to the satellite velocity, symmetrical within 4° about the geodetic nadir direction.
- The MWS shall not expose spatial gaps due to calibration of the instrument.
- The MWS shall provide overlapping footprints for channels MWS-1 to MWS-16 and contiguous footprint sampling for channels MWS-17 to MWS-24.
- The MWS shall provide footprint sizes between 17 km and 40 km.
- The MWS geolocation shall be known with accuracy < 5 km at nadir and < 8 km at the swath edge.
- The MWS shall have a beam efficiency of 95% or greater. The wide beam efficiency shall be ≥97%. This shall be met for all channels and all valid beam positions.
- The beam shape shall be rotationally symmetric around the main-beam.
- All MWS channel co-registrations shall be done within 0.1° with knowledge of 0.05°.
- The MWS pointing knowledge shall be better than 0.25°.
- Within a scanline all the MWS spatial samples shall be with equal angular spacing. The angle between contiguous samples shall be equivalent to the spatial sampling distance at geodetic nadir of the MWS-17 channel.

In addition to the direct observation mission requirements summarised above, and yet the following objectives, essential to satisfy key user needs, have also to be fulfilled by each EPS-SG mission :

- Product generation;
- NRT Data Dissemination & Relay services to users;
- Non-NRT dissemination services;
- Long term archiving in the EUMETSAT Data Centre;
- Archived dataset retrieval services continue to be provided as part of the multi-mission EUMETSAT Data Centre services;
- User support services.

3 MWS INSTRUMENT

3.1 Evolution of Operational Microwave Sounding Instruments

The MWS instrument has a heritage of predecessor microwave cross-track sounders dating back to 1978. These are shown in Table 2. Note that some conical-scan microwave imagers also include a sounding capability (e.g. the Special Sensor Microwave Imager/Sounder SSMIS), but imagers are not discussed in this section. The features of the various instrument series are described below.

The first operational microwave sounder in the TIROS/NOAA satellite series was the MSU. It had only four channels, sounding the 50GHz oxygen band, and had coarse spatial resolution, though is to be bear in mind that 110 km is finer than the resolution of the global NWP models of the day. It was designed to operate in tandem with the infrared Stratospheric Sounding Unit (SSU). An earlier microwave sounder, the Nimbus-E Microwave Sounder (NEMS) with five channels was flown on the research satellite Nimbus-5.

A major advance, in 1998, was the Advanced Microwave Sounding Unit (AMSU), which comprised three physically separate instrument units (AMSU-A1, AMSU-A2 and AMSU-B). The spatial resolution was considerably enhanced compared with MSU, and many more channels were provided, giving coverage of both the troposphere and stratosphere. AMSU-B was later replaced with the MHS instruments, which was functionally similar to AMSU-B though of more modern design and with increased redundancy and reliability. AMSU was used on both the NOAA POES and Metop missions. For the National Polar-orbiting Operational Environmental Satellite System (NPOESS) Preparatory Programme (Suomi-NPP) and JPSS missions, a new microwave sounder was developed, the ATMS. ATMS constitutes the most recent passive microwave sounding instrument flying on an operational meteorological satellite. The channel set was slightly enhanced compared with AMSU, but a major difference was that all channels were combined into a single instrument (with 2 antennas), with significantly reduced volume and mass compared with AMSU+MHS.

Instrument	Agency responsible	Satellites	Time frame	Channels	Freq. range (GHz)	Footprint at nadir (km)
NEMS	NOAA	Nimbus-5	1973 - 1983	5	22.2 - 58.8	180
MSU	NOAA	TIROS-N to NOAA-14	1978 - 2007	4	50.3 - 57.95	110
AMSU-A	NOAA	NOAA-15/16/17/18/19; Metop-A/B/C	1998 - *2024*	15	23.8 - 89	48
AMSU-B	Met Office	NOAA-15/16/17	1998 - 2014	5	89 - 183.31	16
MHS	EUMETSAT	NOAA-18/19; Metop-A/B/C	2005 - *2024*	5	89 - 190.31	16
ATMS	NOAA	S-NPP; JPSS-1/2/3/4	2011 - *2038*	22	23.8 - 183.31	16 - 75
SAPHIR	CNES	Meghatropiques	2011 - *2018*	6	183.31	10
MWTS-1	CMA	FY-3A/3B	2008 - 2014	4	50.3 - 57.3	62
MWHS-1	CMA	FY-3A/3B	2008 - *2018*	5	150 - 183.31	16
MWTS-2	CMA	FY-3C to 3G	2013 - *2026*	13	50.3 - 57.3	32
MWHS-2	CMA	FY-3C to 3G	2013 - *2026*	15	89 - 183.31	16 - 32

Table 2: Cross-track microwave sounders providing heritage for MWS. Colour key: blue: temperature sounders; green: humidity sounders; red: combined temperature/humidity. Dates in italics are projected. The frequency range refers to channel centres.

The footprint of the 50 GHz channels was reduced (to 33 km) but the two low frequency channels were necessarily broader (75 km) as they no longer had a dedicated antenna. ATMS uses Monolithic Microwave Integrated Circuit (MMIC) technology for the front-end radio frequency modules (Muth et al., 2004).

The Chinese FY-3 satellites are equipped with microwave radiometers that are broadly similar to MSU/AMSU-B (on FY-3A/3B) and AMSU/MHS (FY-3C onwards). A significant difference is that the MWHS-2 instrument has a suite of channels at 118 GHz which potentially provides information on both temperature and cloud properties. These are assimilated operationally at some centres (e.g. European Centre for Medium-Range Weather Forecasts, ECMWF, Lawrence et al. 2018), but full scientific exploitation of these channels is still a developing area.

Finally, we note the *Sondeur Atmosphérique du Profil d'Humidité Intertropicale par Radiométrie* (SAPHIR) on the research mission Meghatropiques. SAPHIR designed to provide information on tropical water vapour, has a suite of channels centred on 183.31 GHz and it has a spatial footprint (10 km) smaller than any other microwave sounder to date.

The MWS instrument is designed both to maintain the existing microwave sounding capability and also to improve on certain areas, in line with evolved user requirements. The main areas of change compared with its predecessors are:

- Like ATMS, the instrument is contained in a single unit – thus minimising volume on the satellite and hence cost. Unlike ATMS, a single antenna is used, and this is significantly larger than the antennas on ATMS, providing improved spatial resolution (40 km at the lowest frequency);
- A new channel is added at 229 GHz, the purpose of which is to provide enhanced capability of detecting ice clouds (Sreerekha et al., 2010). Two channels are also added in the 53 GHz band;
- Noise equivalent delta temperature (NEΔT) is improved in order to meet the increasingly stringent requirements of NWP assimilation systems (Bell et al., 2010);
- It is designed to meet more stringent requirements for absolute accuracy;
- The design life of the instrument is increased to 7.5 years.

The MWS instrument is described in more detail in the following sections.

3.2 Instrument Description

This section is divided into two parts. In subsection 3.2.1 we first discuss the instrument requirements, as laid down in the EURD document, then in 3.2.2 we explain how those requirements have been translated to an actual design. Note that some parameters (e.g. polarisation) are left open in the EURD, but are defined fully in 3.2.2. Therefore it is important for the science user to read both parts in order to understand the characteristics of the MWS.

3.2.1 Requirements

The MWS instrument is a passive cross-track scanner capable of sensing radiance emitted by the Earth-atmosphere system, at high spatial resolution in specified spectral bands in the microwave region of the electromagnetic spectrum, from 23.8 GHz to 229 GHz.

The primary role of MWS is to provide temperature and humidity atmospheric soundings and total cloud liquid water column contents. The temperature sounding mainly exploits the oxygen band between 50 and 60 GHz, while the water vapour lines at 22.235 and 183.31 GHz are used for water vapour detection and profile retrieval.

MWS has a direct heritage from the Advanced TIROS Operational Vertical Sounder (ATOVS) instruments flying on the NOAA KLMN'-series satellites and on the EUMETSAT Metop satellites, namely AMSU and MHS. Observations from these instruments are directly assimilated at most NWP centres and constitute an important component of operational assimilation systems (English et al., 2013).

In addition to their importance for meteorology, microwave sounding instruments have also been widely used for climate studies, and they currently provide a very important contribution towards the development of long term climate records for global tropospheric and stratospheric temperature distributions (Zou, 2013).

The specified MWS spectral bands are presented in Table 3, together with other relevant requirements extracted from the EPS-SG EURD, where additional information on the EPS-SG microwave sounding mission can be found.

Channel	***Center frequency (GHz)***	***Bandwidth (MHz)***	***Center frequency stability (MHz)***	***NEΔT (K)***	***Polarisation***	***Nadir 3dB footprint size (IFOV) (km)***
MWS-1	23.8	270	±5	<0.25	QV or QH	40
MWS-2	31.4	180	±10	<0.35	QV or QH	40
MWS-3	50.3	180	±5	<0.5	QV or QH	20
MWS-4	52.8	400	±3	<0.35	QV or QH	20
MWS-5	53.246±0.08	2 x140	±5	<0.4	QH or QV	20
MWS-6	53.596±0.115	2 x 170	±2	<0.4	QH	20
MWS-7	53.948±0.081	2 x 142	±1	<0.4	QH or QV	20
MWS-8	54.4	400	±2	<0.35	QH or QV	20
MWS-9	54.94	400	±2	<0.35	QV or QH	20
MWS-10	55.5	330	±2	<0.4	QH or QV	20
MWS-11	57.290344	330	±0.5	<0.4	QH or QV	20
MWS-12	57.290344±0.217	2 x 78	±0.5	<0.55	QH or QV	20
MWS-13	57.290344±0.3222±0.048	4 x 36	±1.2	<0.6	QH or QV	20
MWS-14	57.290344±0.3222±0.022	4 x 16	±1.2	<0.9	QH or QV	20
MWS-15	57.290344±0.3222±0.010	4 x 8	±0.5	<1.2	QH or QV	20
MWS-16	57.290344±0.3222±0.0045	4 x 3	±0.2	<2.0	QH or QV	20
MWS-17	89	4000	±130	<0.25	QV or QH	17
MWS-18	165.5±0.725	2 x 1350	±40	<0.5	QV or QH	17
MWS-19	183.311±7.0	2 x 2000	±30	<0.4	QV or QH	17
MWS-20	183.311±4.5	2 x 2000	±30	<0.4	QV or QH	17
MWS-21	183.311±3.0	2 x 1000	±30	<0.6	QV or QH	17
MWS-22	183.311±1.8	2 x 1000	±30	<0.6	QV or QH	17
MWS-23	183.311±1.0	2 x 500	±30	<0.75	QV or QH	17
MWS-24	229.0	2000	±100	<0.7	QV or QH	17

Table 3: **Main MWS spectral and radiometric requirements**

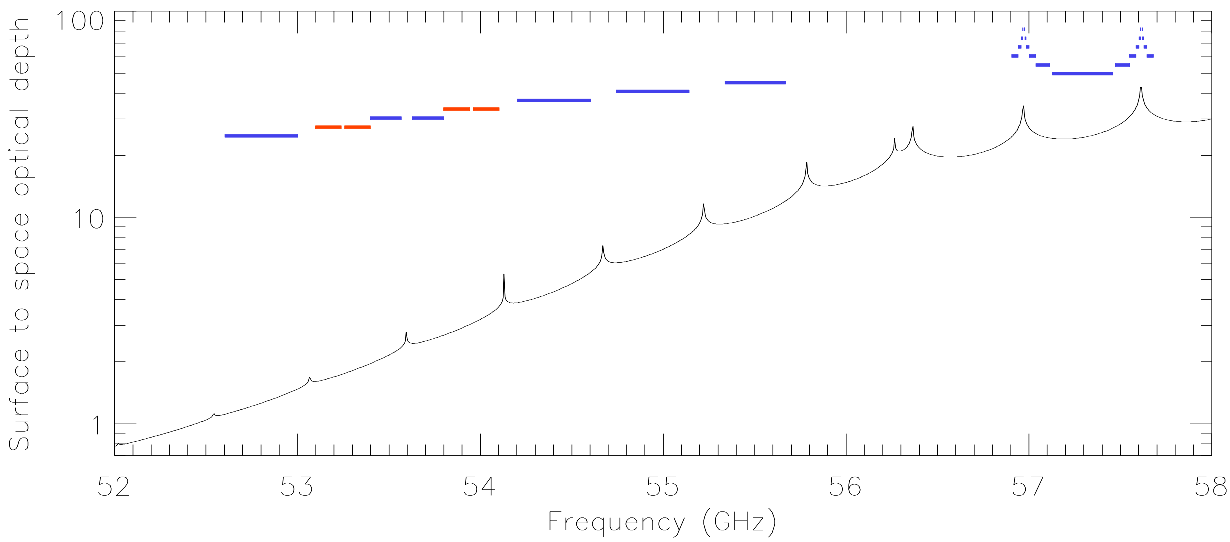

Figure 1: Location of MWS channels 4 to 16 relative to the oxygen spectrum. AMSU-A channels in blue, the new MWS channels in red. The optical depth was evaluated using a dry Arctic profile from the Radiative Transfer for TOVS (RTTOV) training set.

The 14 oxygen-band channels (MWS-3 to MWS-16) provide microwave temperature sounding for regions from the Earth's near surface up to about 42 kilometres, i.e. from surface pressure level to 2 hPa. Channels between 54 GHz and 57.5 GHz (MWS-8 to MWS-16) have a long-term heritage from predecessor instruments MSU operated on TIROS N, and NOAA-6 to 14, and AMSU-A1 flown onboard NOAA-15, 16, 17, 18, 19, National Aeronautics and Space Administration (NASA) Aqua, and EUMETSAT Metop satellites. Initially, the frequencies in this band were chosen to match closely with the weighting functions of the infrared sounding channels on the High Resolution Infrared Radiation Sounder (HIRS) instrument.

Below 54 GHz, the channel frequency specification is less obvious because the channels do not measure all the bandwidth between the spectral lines. Sreerekha et al. (2007) examined the optimal choice of frequencies below 54 GHz and showed some benefit from acquiring additional measurements to the established AMSU channel set. This result has suggested the new two channels MWS-5 and MWS-7 placed between 52 and 54 GHz, as shown in Figure 1.

Note that Sreerekha et al. (2007) assumed that these channels would be implemented via AMSU-A-like heterodyne technology, with an oscillator at each centre frequency, and hence a central stop-band. For MWS, such a configuration was not chosen (section 3.2.2), and there is no scientific requirement for the stop-bands as there are no oxygen lines near the band centres (unlike MWS-6). However, the stop bands were retained in the specification.

Channels MWS-19 to MWS-23 are sensitive to the 183 GHz water vapour line, therefore providing humidity sounding capability. In addition, the channels at 166 GHz (MWS-18), 23.8 GHz (MWS-1) and 31.4 GHz (MWS-2) yield information on the total column water vapour.

Surface-sensitive channels (including MWS-1, MWS-2, MWS-17 and MWS-24) allow checking measurements of other channels for contributions from surface emissivity and clouds. Channels MWS-4 to 6 are affected by cloud liquid water, therefore channels MWS-1 to 3 being also sensitive to cloud liquid water, are essential allowing the data to be screened. Cloud ice can affect MWS-4 to 8 in situations of severe convection: MWS-17, when used with MWS-1 and 2, allows identification of such conditions. The new channel at 229 GHz (MWS-24) provides enhanced sensitivity for the detection of cloud ice that would affect channels MWS-19 to 23. Noteworthy, the window channels also provide information about precipitation, sea ice and snow coverage (Ferraro et al., 2005).

The MWS set of channels is similar to the ones of ATMS, on-board the NOAA/NASA Suomi- NPP and JPSS-1 satellites, which has 22 channels with often similar or equal frequency bands compared to AMSU/MHS. Table 4 compares the radiometric specifications of MWS to the ones of ATMS and AMSU/MHS.

It is noted that for some channels, the polarisation is different, too. In order to make those channels comparable across instruments, a correction for the polarisation dependent (non unity) mirror reflectivity is deemed necessary – discussed in section 5.1.1.

AMSU/MHS			ATMS			MWS		
Ch.	*GHz*	*Pol.*	*Ch.*	*GHz*	*Pol.*	*Ch.*	*GHz*	*Pol.*
1	23.8	QV	1	23.8	QV	1	23.8	QH
2	31.4	QV	2	31.4	QV	2	31.4	QH
3	50.3	QV	3	50.3	QH	3	50.3	QH (QV)
			4	51.76	QH			
4	52.8	QV	5	52.8	QH	4	52.8	QH (QV)
						5	53.246 ± 0.08	QH (QV)
5	53.595±0.115	QH	6	53.596±0.115	QH	6	53.596±0.115	QH (QV)
						7	53.948 ± 0.081	QH (QV)
6	54.4	QH	7	54.4	QH	8	54.4	QH (QV)
7	54.94	QV	8	54.94	QH	9	54.94	QH (QV)
8	55.50	QH	9	55.50	QH	10	55.50	QH (QV)
9	57.290344	QH	10	57.290344	QH	11	57.290344	QH (QV)
10	57.290344±0.217	QH	11	57.290344±0.217	QH	12	57.290344±0.217	QH (QV)
11	57.290344 ±0.3222±0.048	QH	12	57.290344 ±0.3222±0.048	QH	13	57.290344 ±0.3222±0.048	QH (QV)
12	57.290344±0.3222±0.022	QH	13	57.290344±0.3222±0.022	QH	14	57.290344±0.3222±0.022	QH (QV)
13	57.290344±0.3222±0.010	QH	14	57.290344±0.3222±0.010	QH	15	57.290344±0.3222±0.010	QH (QV)
14	57.290344±0.3222±0.0045	QH	15	57.290344±0.3222±0.0045	QH	16	57.290344±0.3222±0.0045	QH (QV)
15	89.0	QV						
16	89.0	QV	16	88.2	QV	17	89.0	QV
17	157.0	QV	17	165.5	QH	18	164-167	QH
18	183.311±1.0	QH	22	183.311±1.0	QH	23	183.311±1.0	QV
			21	183.31 ± 1.8	QH	22	183.311±1.8	QV
19	183.311±3.0	QH	20	183.311±3.0	QH	21	183.311±3.0	QV
			19	183.311±4.5	QH	20	183.311±4.5	QV
20	191.31	QV	18	183.311±7.0	QH	19	183.311±7.0	QV
						24	229	QV

Matched Specificat.	Pol. is Different	Unique Passband	Pol. is Different and Unique Passband	New channel

Table 4: MWS (right) and ATMS (centre) characteristics compared to AMSU/MHS (left). Note that MWS polarizations correspond to the actual implementation (see Table 5).

The main design difference of MWS with respect to the ATOVS instruments is the inclusion of the complete range of radiometric frequency channels within a single instrument having a single main antenna. In addition, the two lowest frequency channels are over-sampled with respect to the footprint in the scanning direction, in order to allow the possibility of filtering out Radio Frequency Interference (RFI) observed in this spectral region (e.g. Kidd 2006). A schematic view of the MWS design is shown in Figure 2.

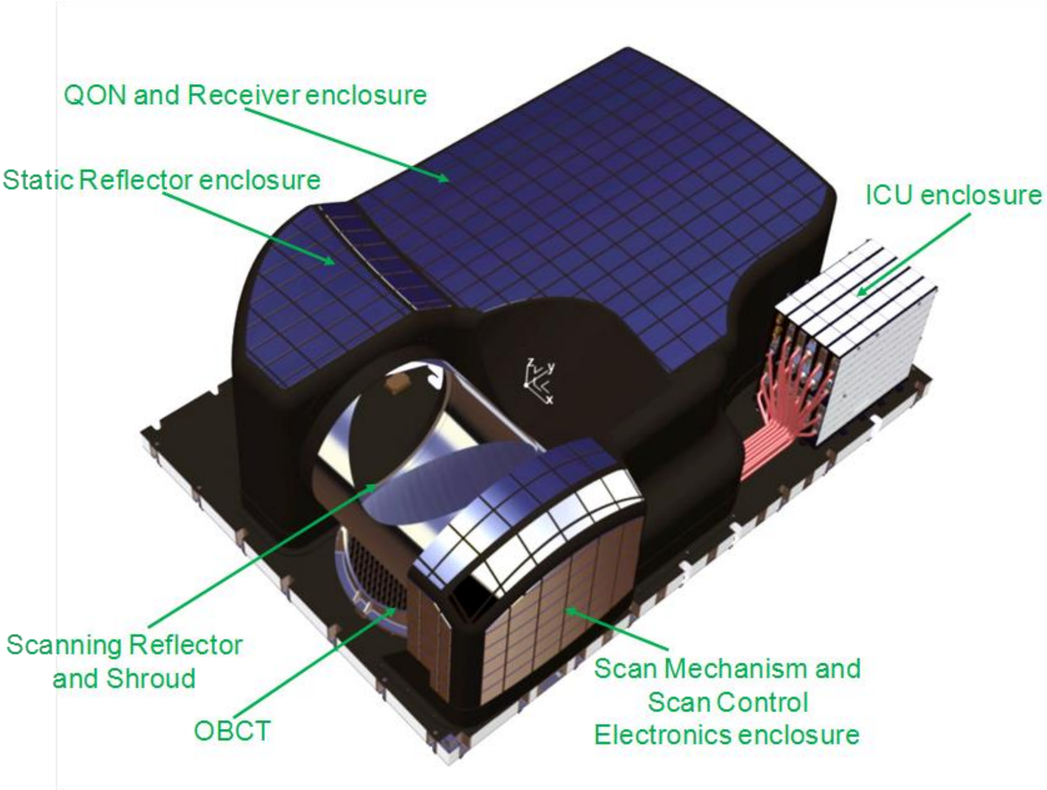

Figure 2: MWS instrument design

3.2.2 MWS Design

This section explains how the requirements of Section 2.2 are implemented in the design of the instrument. The various sub-systems of the MWS are detailed in dedicated sub-sections.

3.2.2.1 Rotating mirror assembly, with scan control electronics

A rotating drum and scan mirror, driven by a closed-loop controller, rotates in a plane perpendicular to the satellite motion (cross-track). As in MHS, the scan rate is optimised to spend over half the scan period viewing Earth, with rapid transitions to space views and blackbody views (Figure 3).

In the normal scan profile, there are 95 Earth samples per scan, 5 space samples and 5 blackbody samples. The maximum scan angle for Earth views is 49.31°, i.e. 1.049° per sample.

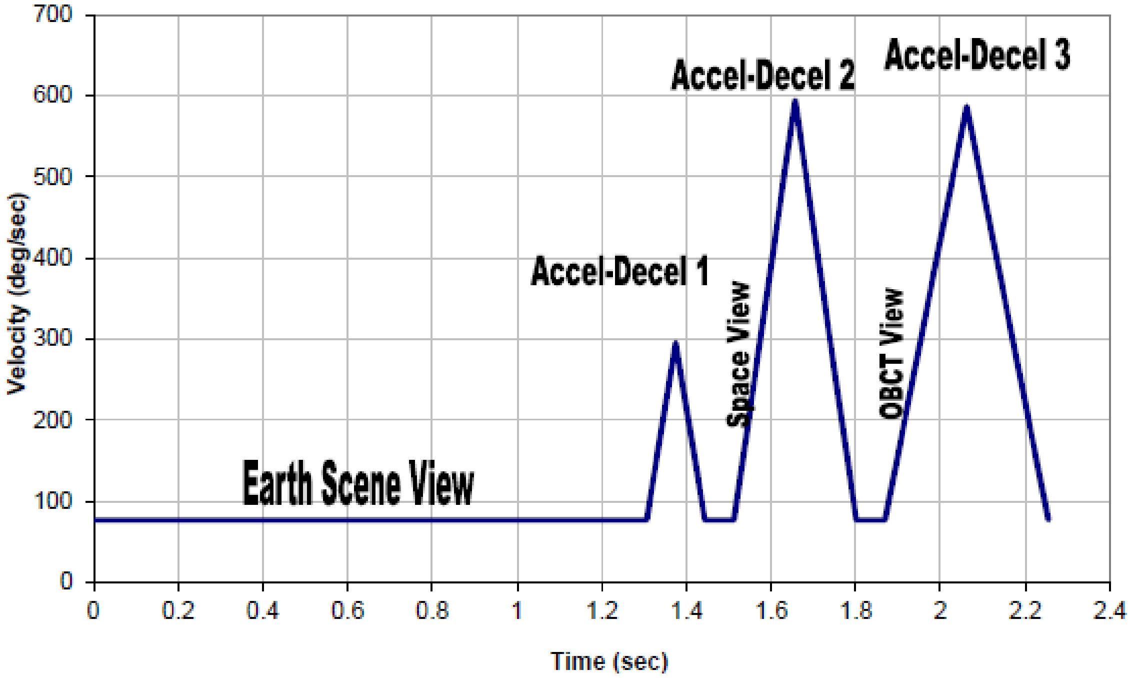

Figure 3: MWS scan profile (provisional)

The scan period is determined by the beam width of the narrowest channel: ≤ 17 km at nadir. The satellite ground-track velocity is 6.58 km/sec (for an orbit period 101.35 minutes), so the satellite covers a track of 14.8km during one scan. See section 3.2.4 for a more detailed discussion of the scan pattern.

The main reflector is made of carbon fibre with a metallic coating. (For comparison, ATMS has a nickel-plated beryllium reflector with 0.6μm gold coating (Yang et al., 2016), while AMSU-B was pure beryllium). This is discussed further in sections 3.2.3 and 5.1.1.

The diameter of the reflector aperture is mainly driven by the specification of the beamwidth of the 23.8 GHz channel (a 40km footprint at nadir is required) and the requirement for high beam efficiency. This leads to a diameter of 35 cm – significantly larger than that of heritage sensors.

The polarisation angle of the observed radiation (relative to the Earth surface) rotates with scan angle, as for other cross-track sensors (AMSU, MHS, etc.). QV means that when viewing nadir the instrument is sensitive to radiation having the E field perpendicular to the satellite track.

3.2.2.2 Quasi optics network and feedhorns

The incoming microwave radiation is split into 5 paths by a network of dichroic plates and mirrors, each path being directed into different feedhorns:

1. 23.8 and 31.4 GHz channels;
2. 54 GHz channels. This feedhorn has 2 separate outputs, one at QH polarisation (nominal) and one at QV polarisation (backup). This provides redundancy with no performance penalty;
3. 89 GHz;
4. 229 GHz;
5. 183 and 166 GHz.

3.2.2.3 Receivers

The 23.8, 31.4 and 89 GHz channels are direct detection, i.e. the RF signal is amplified, filtered and detected (converted to DC using a diode). The remaining channels use the heterodyne technique: each band has a phase-locked local oscillator (LO) and mixer to down-convert the signal.

- The 165/183/229 GHz channels are all mixed down with a LO at each centre frequency. They all have a central stop-band (including 229 GHz, which is implemented as 229±1 GHz).
- The 50-58 GHz channels are divided into 2 bands:
    - Channels 3-10 have an LO at 48.2 GHz (the lower sideband is suppressed).
    - Channels 11-16 have an LO at 55 GHz (again, the lower sideband is suppressed).

The down-converted signals are amplified, filtered and detected.

There are two sets of 50-58 GHz receivers: one set for the normal polarisation and a second set taking the backup polarisation from the feedhorn. *This provides redundancy in the event of failure or degradation in one set of 50-58 GHz channels.* Note that the implementation of the 50-58 GHz receivers is significantly different from AMSU-A (with individual LOs at 50.3, 52.8, 53.596, 54.4, 54.94, 55.5 and 57.290344 GHz) and ATMS (a single LO at 57.290344 GHz – Muth et al., 2004). The MWS channel implementation is shown in Table 5.

Channel	*Center frequency (GHz)*	*Bandwidth (MHz)*	*Polarisation*	*LO freq (GHz)*
MWS-1	23.8	270	QH	-
MWS-2	31.4	180	QH	-
MWS-3	50.3	180	QH (QV)	48.2
MWS-4	52.8	400	QH (QV)	
MWS-5	53.246±0.08	2 x140	QH (QV)	
MWS-6	53.596±0.115	2 x 170	QH (QV)	
MWS-7	53.948±0.081	2 x 142	QH (QV)	
MWS-8	54.4	400	QH (QV)	
MWS-9	54.94	400	QH (QV)	
MWS-10	55.5	330	QH (QV)	
MWS-11	57.290344	330	QH (QV)	55.0
MWS-12	57.290344±0.217	2 x 78	QH (QV)	
MWS-13	57.290344±0.3222±0.048	4 x 36	QH (QV)	
MWS-14	57.290344±0.3222±0.022	4 x 16	QH (QV)	
MWS-15	57.290344±0.3222±0.010	4 x 8	QH (QV)	
MWS-16	57.290344±0.3222±0.0045	4 x 3	QH (QV)	
MWS-17	89	4000	QV	-
MWS-18	165.5±0.725	2 x 1350	QH	82.75
MWS-19	183.311±7.0	2 x 2000	QV	91.655
MWS-20	183.311±4.5	2 x 2000	QV	
MWS-21	183.311±3.0	2 x 1000	QV	
MWS-22	183.311±1.8	2 x 1000	QV	
MWS-23	183.311±1.0	2 x 500	QV	
MWS-24	229.0±1.0	2 x 1000	QV	114.5

Table 5: MWS channels as implemented

3.2.2.4 Signal processing electronics

The signal processing stage comprises additional post-detection amplifiers (with configurable gains and offsets) and analogue to digital converters (ADC). The raw digital sampling is at a rate of 16 times the nominal sampling rate; in the case of channels 3-24 the 16 individual samples are summed. For channels 1-2 the raw samples are passed to downstream systems in case they are needed for RFI detection.

The ADC outputs are assembled into packets and passed to downstream systems.

3.2.2.5 On-board calibration target

The on-board calibration target is viewed for approximately 0.1 s in every scan, as shown in Figure 3, and provides the warm reference point in the 2-point radiometric calibration (section 5.1.1). The target design is similar to that of MHS and AMSU, but the size is significantly larger (37 cm diameter, 16 kg in mass) due to much larger antenna size of MWS compared to MHS/AMSU. The surface is an array of pyramidal spines, with a thin coating of microwave absorber applied on top of an aluminium substrate. The target is populated with 12 (6 nominal and 6 redundant) precision temperature sensors. A close-fitting baffle shields the target from external thermal radiation which would otherwise be liable to cause temperature gradients. Thermal control is passive.

3.2.2.6 Other sub-systems

Other sub-systems, which are not directly related to the science of the instrument, include (i) power systems, (ii) thermal control systems, (iii) mechanical structure and harness, and (iv) instrument control and monitoring systems.

3.2.2.7 Implications of the design for science users

The following points are of particular note:

- For channels 3-10 (50.3-55.5 GHz) and, separately, for channels 11-16 (57.29 GHz), radiative transfer models should be able to switch readily between QH and QV polarisation, depending on the configuration of the instrument. It is assumed that there will be a flag in the telemetry indicating which configuration is being used. Note that brightness temperatures at QV and QH will be identical at scan angles of 0 (nadir) and ±45°, but at other angles they will differ, especially for surface-sensitive channels over ocean.
- For heterodyne channels with a central stop band (i.e. channels at 165, 183 and 229 GHz), there will be some uncertainty in sideband imbalance. See Atkinson and Rayer (2015). Sideband imbalance has not historically been seen as a significant issue for AMSU-B or MHS, but as NWP model representation of humidity improves then small errors in RT modelling for these channels could become more important. Sideband imbalance is not an issue for the 50-57 GHz channels because the lower sideband is rejected.
- The nonlinearity correction used in the Level 1 processing should properly take account of the post-detection gain settings. It is assumed that most of the nonlinearity originates in the power detector. This is discussed in detail in section 5.1.1.3.

3.2.3 Radiometric Performance

3.2.3.1 NEΔT

A key radiometric performance indicator is the Noise Equivalent Delta Temperature, or NEΔT. For end users, it tells them what level of instrument noise to expect in the data, which is crucial to the effective use of the data in NWP assimilation. For the manufacturer, it is an important part of the instrument specification, and meeting this specification is usually considered high priority. Long-term monitoring of NEΔT is essential for understanding how the characteristics of the instrument change with time.

At a fundamental level, the NEΔT can be defined using the ideal noise equation for a total power radiometer (Ulaby et al., 1981, equ. 6.64 with calibration term added):

$$\Delta T = \left(T_{sys} + T_{scene}\right)\left[\frac{1}{B\,\tau} + \left(\frac{\Delta G}{G}\right)^2 + \frac{1}{B\,N\,\tau_c}\right]^{\frac{1}{2}} \qquad \textbf{(1)}$$

where T_{sys} is the system noise temperature, B is the bandwidth, τ is the integration time, $\Delta G/G$ represents instrument gain fluctuations and τ_c is the integration time for each of the N calibration views. Normally, the first term dominates (i.e. noise is largely random).

In the MWS specification, the integration time τ, is defined as the time to sweep out the 3 dB beamwidth for the channel concerned. It is *not* the single-sample integration time (which is commonly used in other satellite programmes). MWS specific conversion factors are shown in **Table 6**, assuming contiguous sampling for channels 17-24.

Channels	Nominal footprint (km)	Single sample NEΔT relative to spec
1-2	40	1.53
3-16	20	1.085
17-24	17	1.0

Table 6: NEΔT conversion factors for MWS, assuming NEΔT is proportional to $\tau^{-1/2}$

Although T_{sys} can be measured pre-launch, it is not measured directly in orbit, so instead the variability of the warm and cold calibration counts has to be used in order to estimate NEΔT. In-orbit monitoring of NEΔT is discussed in detail in section 5.4.

It should be noted that NEΔT specifications in the EURD (see Reference Documents) are defined at a scene temperature of 280K, for consistency with post-launch measurements of the variability of the warm calibration view (the warm target being typically close to 280K). For microwave instruments, the NEΔT increases with scene temperature; the rate of increase varies from channel to channel, depending on the size of T_{sys} relative to T_{scene}. The EURD permits an increase of up to 15% when the scene temperature exceeds 280K. By monitoring the NEΔT for both the warm calibration view and the cold view, the user can interpolate to get the effective NEΔT at other temperatures.

Receiver gain fluctuations introduce so-called "1/f" or "flicker" noise (Voss, 1979), which is associated with a "striping" in the channel brightness-temperature images for instruments such as ATMS (Doherty et al., 2014). Striping can be minimised through careful choice of semiconductor material, and it is expected that MWS will perform well in this regard. It can be monitored via a "striping index" (related to the ratio of along-track to cross-track variability for calibration view counts, see section 5.4).

When using sounder data in NWP or climate applications, it is common practice to perform spatial averaging in order to reduce instrument noise (e.g. 3×3 samples for ATMS: Doherty et al., 2014). One might expect that a 3×3 averaging would reduce noise by a factor 0.33 relative to un-averaged data. But striping can degrade the ability to reduce noise through spatial averaging. In the extreme case, where striping noise dominates and nearly all the noise is in the scan-to-scan variability, the ratio of 3×3 NEΔT to single-sample NEΔT could be as large as $1/\sqrt{3} = 0.58$. Monitoring of effective NEΔT for spatially averaged fields is discussed in section 5.4.

If 1/f noise for MWS turns out to be significant, then a technique is available for removing the unwanted noise via signal processing (Ma and Zou, 2015). In brief, for each channel the 2-dimensional array of brightness temperatures $BT_{k,i}$ (scan k, spot i, total N spots) is first decomposed into N principal components (PC):

$$BT_{k,i} = \sum_{j=1}^{N} e_{j,i} u_{k,j} \tag{2}$$

where e are the eigenvectors and u are the PC coefficients. Then the first PC coefficient (representing along-track variability) is smoothed using a suitable filter, and the decomposition is reversed to give a modified brightness temperature field. At the time of writing, the technique shows potential but has not been fully tested in an operational environment. More research would be needed if this technique were to be considered for use with MWS. However, as stated previously, the expectation is that striping mitigation will not be needed.

3.2.3.2 Radiometric accuracy and stability

There are a number of specifications in the EURD related to accuracy and stability:

- Radiometric bias < 1 K for all channels;
- Bias variation over an orbit < 0.2 K;
- Lifetime stability of orbital-mean bias < 0.2 K;
- Inter-channel bias differences, for the same sample < 0.5 K;
- Bias differences across the scan, for a given channel < 0.3 K.

These specifications apply to the Level 1 data, after calibration processing has been performed. There are many factors that can cause radiometric biases. The main factors are summarised in Table 7.

Factor	Bias characteristic	Warm or cold bias, if uncorrected?
Accuracy of thermometry for the warm load, and its thermal uniformity	Bias at warm scene temperatures.	Either
Warm load microwave emissivity and the shielding of the warm load cavity from the space environment	Bias at warm scene temperatures.	Depends on the radiometric temperature of the cavity. Cold if shielding from space is inadequate.
Accuracy of modelling the radiance of the cold space calibration view, including contamination by the Earth limb and the satellite	Bias at cold scene temperatures.	Warm
Accuracy of the antenna pattern correction for Earth views (influence of cold space)	Bias largest at the edge of scan and for warm scene temperatures.	Cold
Knowledge of the nonlinearity for each channel	Bias at mid-range scene temperatures	Either
Accuracy of modelling the antenna reflectivity and the variation of the reflectivity with polarisation	Scan-dependent bias, largest at nadir for cold scene temperatures.	Cold for QV channels, warm for QH channels.
Cross-polarisation sensitivity	Bias for window channels when viewing ocean, symmetric about scan axis. Zero at nadir and 45° scan angle	Depends on scan angle and polarisation
Polarisation twist	Bias for window channels when viewing ocean, asymmetric about scan axis. Zero at nadir.	Either
Oscillator frequency drift	Depends on channel. Varies with time. May be correlated with instrument temperature.	Either
Radio frequency interference	Unpredictable	Either
Cold calibration counts too close to lower limit of ADC range	Large, variable bias at cold scene temperatures.	Warm
Warm calibration counts too close to upper limit of ADC range	Large, variable bias at warm scene temperatures	Cold

Table 7: Factors influencing radiometric bias

Clearly there are many factors that need to be taken account in formulating the instrument error budget. Some of these factors (e.g. antenna pattern) produce significant errors if uncorrected, but are reduced to acceptable levels in the calibration processing, using pre-launch characterisation data (see section 6.1.1). Other factors are reliant on good instrument design, e.g. stability of the oscillators.

Taking antenna pattern as an example, in the past some very simple models have been taken to correct for antenna sidelobes. For example, Hewison and Saunders (1996) created a simple model of the spacecraft and Earth, as seen by the AMSU-B instrument, and used it to create fixed cold calibration offsets for each channel. The offsets were between 0.5 K and 1 K, depending on channel. Antenna pattern corrections were also estimated for the Earth views, of up to 0.6 K. A similar procedure was carried out for AMSU-A by Tsan Mo (1999), who found space-view offsets of 0.7–2K. For MWS, a more sophisticated procedure is planned, based on a more realistic model of the Earth, with a radiative transfer model used to predict the Earth emission at each channel, and taking account of latitudinal variations. This should help to ensure that the specifications for radiometric accuracy are met.

The emissivity of the main reflector is mentioned in Section 5.1.1. In the past, the issue has tended to be ignored. Saunders et al. (1996) noted a cold offset of 0.4K in their thermal vacuum tests, and this was later explained as a polarisation-dependent emissivity (Labrot et al., 2011). But corrections are not routinely applied to AMSU-B or MHS data. For ATMS, Weng and Yang (2016) found that the antenna emissivity was higher than expected, and found that the predicted difference between nadir and edge-of-scan bias, for scenes at the temperature of cold space, was as large as 0.8 K (at 23.8 GHz). It is expected that MWS will have an antenna emissivity lower than that of ATMS; nevertheless it is clear that this effect needs to be modelled. Therefore it is planned to apply the correction as an integral part of the level 1 processing, not as an afterthought. Details are given in section 5.1.1.

3.2.4 Temporal Sampling and Geometric Performance

The MWS scanning principle is illustrated in Figure 4. The instrument collects the radiation coming from the Earth by means of a scanning flat mirror (rotating reflector, RR), which reflects the energy to the feed-horn assembly through a static parabolic reflector. The rotation of the mirror around an axis which is nearly parallel to the flight direction of the orbiter results in the cross-track sensing of the instrument. During nominal operations, the MWS scanning reflector rotates anti-clockwise, i.e. from the left to the right, when viewed from the platform anti-velocity side, through 360° in each scan cycle. Thus, the spin vector points in the negative x-direction while the spacecraft moves along the positive x-direction. Since Metop-SG will be operated in a morning orbit (descending node), this scanning configuration allows MWS viewing the cold space in the desired anti-Sun direction.

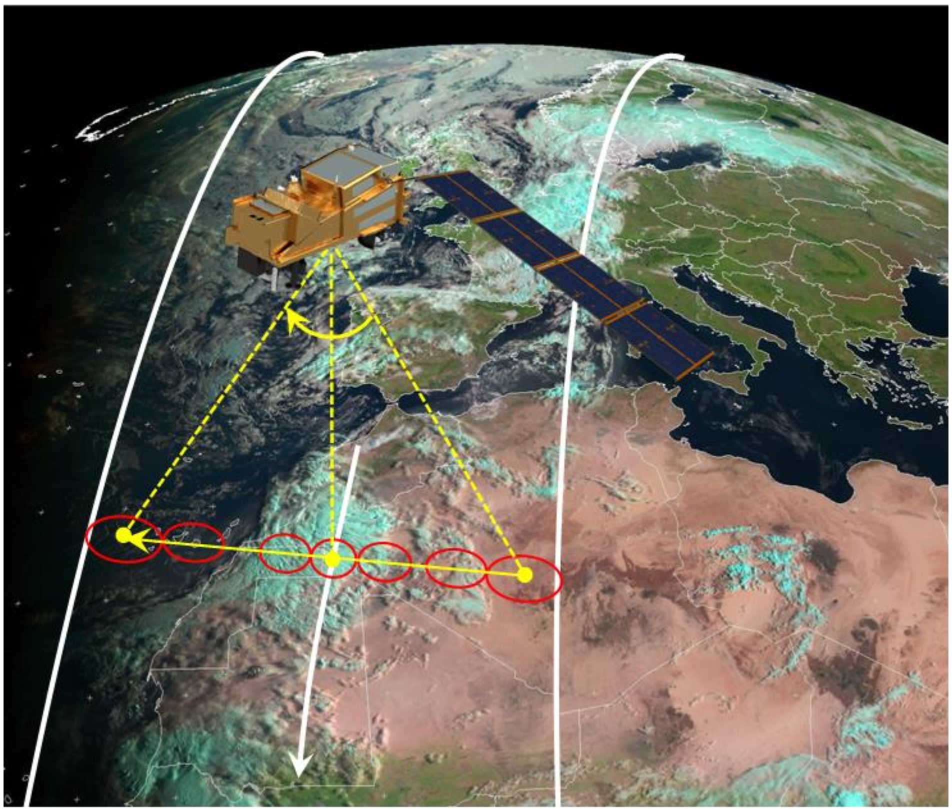

Figure 4: MWS scanning geometry

The Earth is viewed at different scanning angles, symmetric around the nadir direction. The scan speed is constant during the Earth view thus providing equally spaced measurements in viewing angle. In this manner, each MWS Earth scene will have equal integration time. The scan duration and integration time are chosen to provide nearly contiguous footprints at nadir along-track and across-track, for the channels having the smallest instantaneous footprint sizes (diameter of 17 km for MWS-17 to MWS-24). The instantaneous footprint, which should be circular at Nadir, is determined by the half-power beamwidth (HPBW) for each channel. The diameter of the footprint increases for the lower frequency channels (MWS-1 to MWS-16), thus resulting in overlapping footprints for these channels through the scan cycle. Observations should be acquired within an angle greater of ± 49° relative to Nadir, equivalent to a swath of about 2100 km. In addition, a minimum number of 86 samples for each scan is required. In accordance with the outcome of the MWS instrument Critical Design Review in 2018, the following scanning properties are obtained: the scan duration is 2.254 seconds, and the angular sampling amounts 1.04919°. Thus, to cover at least ±49°, the number of Earth view pixel per scan is 95 resulting in a maximum scanning angle of 49.31°.

This results in a swatch width of about 2210 km in mid-latitude regions. Nominally, Metop-SG satellite-A series will be operated in the yaw steering mode. The main impact of yaw steering control on the acquisition geometry is a shift of the scene viewing angle (in Azimuth) by a value corresponding to the value of the yaw steering angle, since the axis (Nadir direction) is the same for both rotations (the yaw axis of the satellite coincides with the radiometer scan axis, see Figure 4). The impact of yaw steering has its maximum at the equator, where the yaw angle amounts to about +3.95° and -3.95° for the descending and the ascending crossing, respectively. The minimum angle of 0° occurs near the Northernmost and the Southernmost positions of the satellite.

Results of MWS scan simulations using the above-mentioned scan properties are shown from Figure 5 to Figure 8. Using a simulated descending satellite overpass of South Europe, the scan patterns of selected channels (MWS-1, MWS-3, MWS-17) with different ground resolutions are plotted. Footprint sampling and extension are also displayed in Figure 8 for nadir (left panels) and scan edge (right panels). From top to bottom, the three instantaneous footprint sizes of Table 3 are considered.

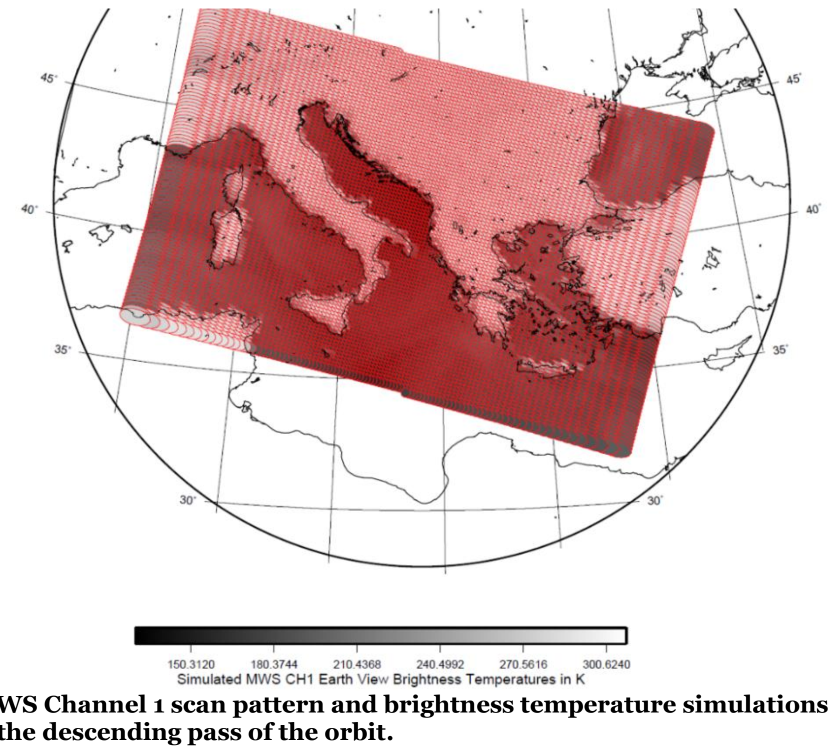

Figure 5: MWS Channel 1 scan pattern and brightness temperature simulations for a polar satellite on the descending pass of the orbit.

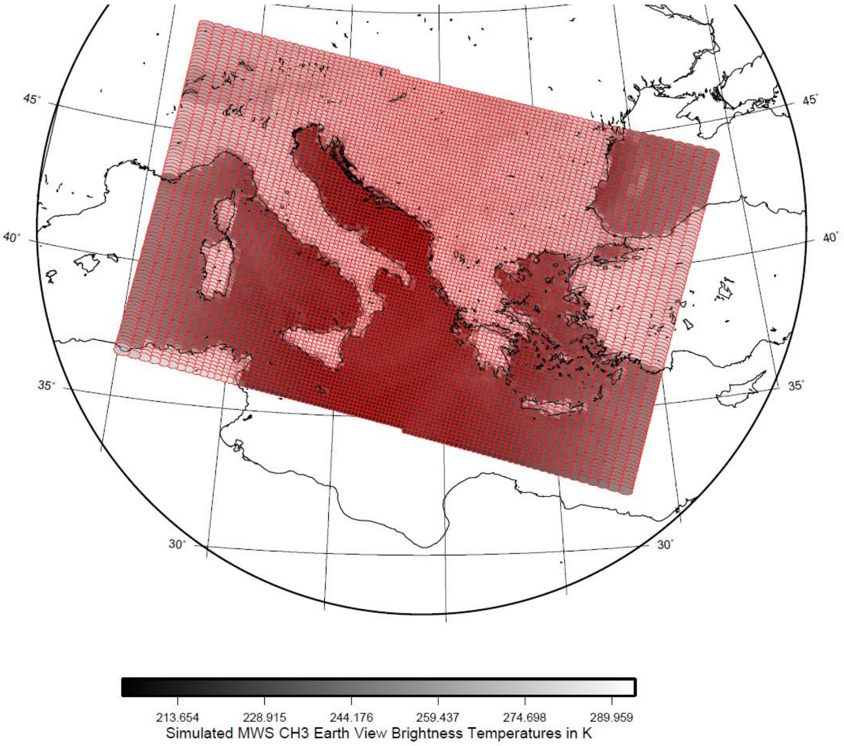

Figure 6: ***As*** **Figure 5,** ***but relative to*** **MWS Channel 3.**

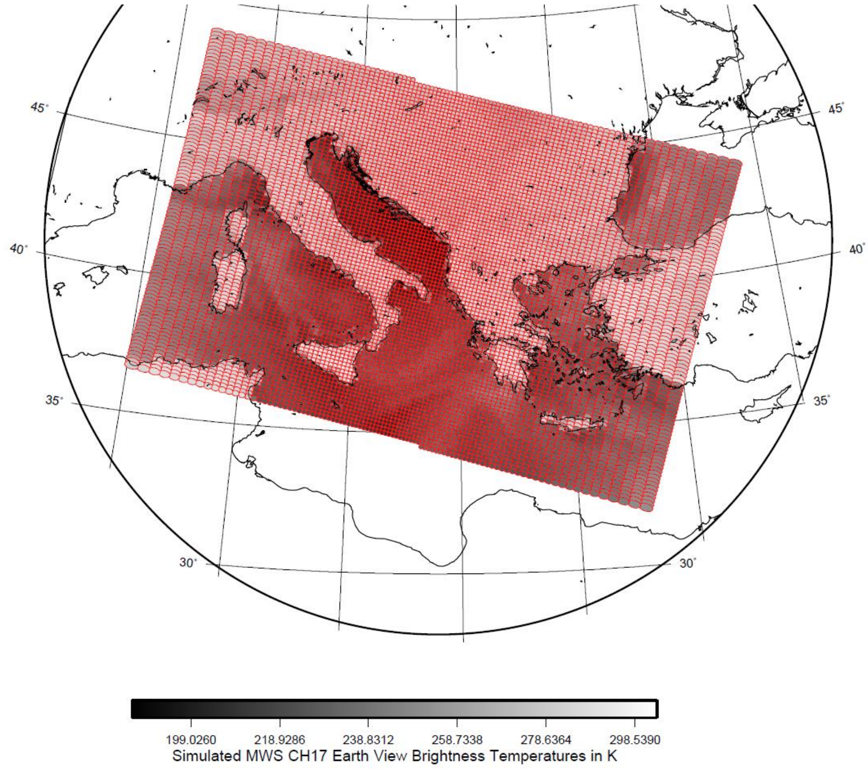

Figure 7: ***As*** **Figure 5,** ***but relative to*** **MWS Channel 17.**

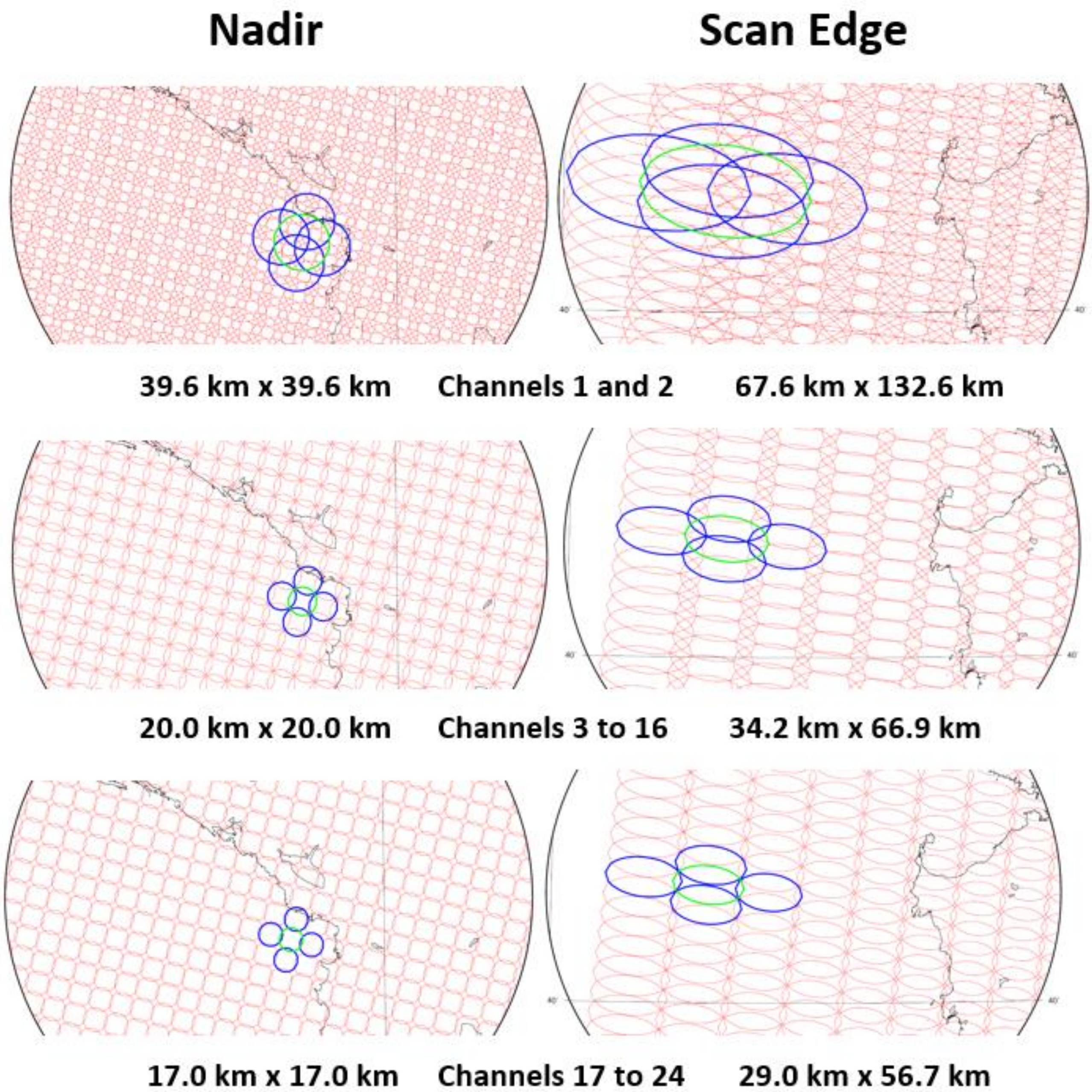

Figure 8: ***Schematic view and extension of instantaneous MWS footprints near nadir (left panels) and at the scan edge (right panels).The geographical regions are bordered by the large black brackets, whereas the corresponding scan patterns are drawn in red. For clarity, one individual center ellipse within each region is highlighted in green, and the pixels immediately adjacent to the center pixel (along and across) are drawn in blue. The approximate footprint sizes in kilometres are also given.***

4 MWS APPLICATIONS

4.1 Numerical Weather Forecast (data assimilation, expected impact on NWP models)

One of the key application areas for level 1 data from MWS will be the assimilation in Numerical Weather Prediction (NWP) systems, particularly at global, but also at regional scales. This will build on the strong heritage of previous microwave sounders such as AMSU-A, AMSU-B, MHS, and ATMS. Data from these sounders are currently available from a number of satellites from the Metop and NOAA series and S-NPP, and they are routinely assimilated at all major global and regional NWP centres (e.g. Doherty et al. 2015, Bormann et al. 2013, English et al. 2000).

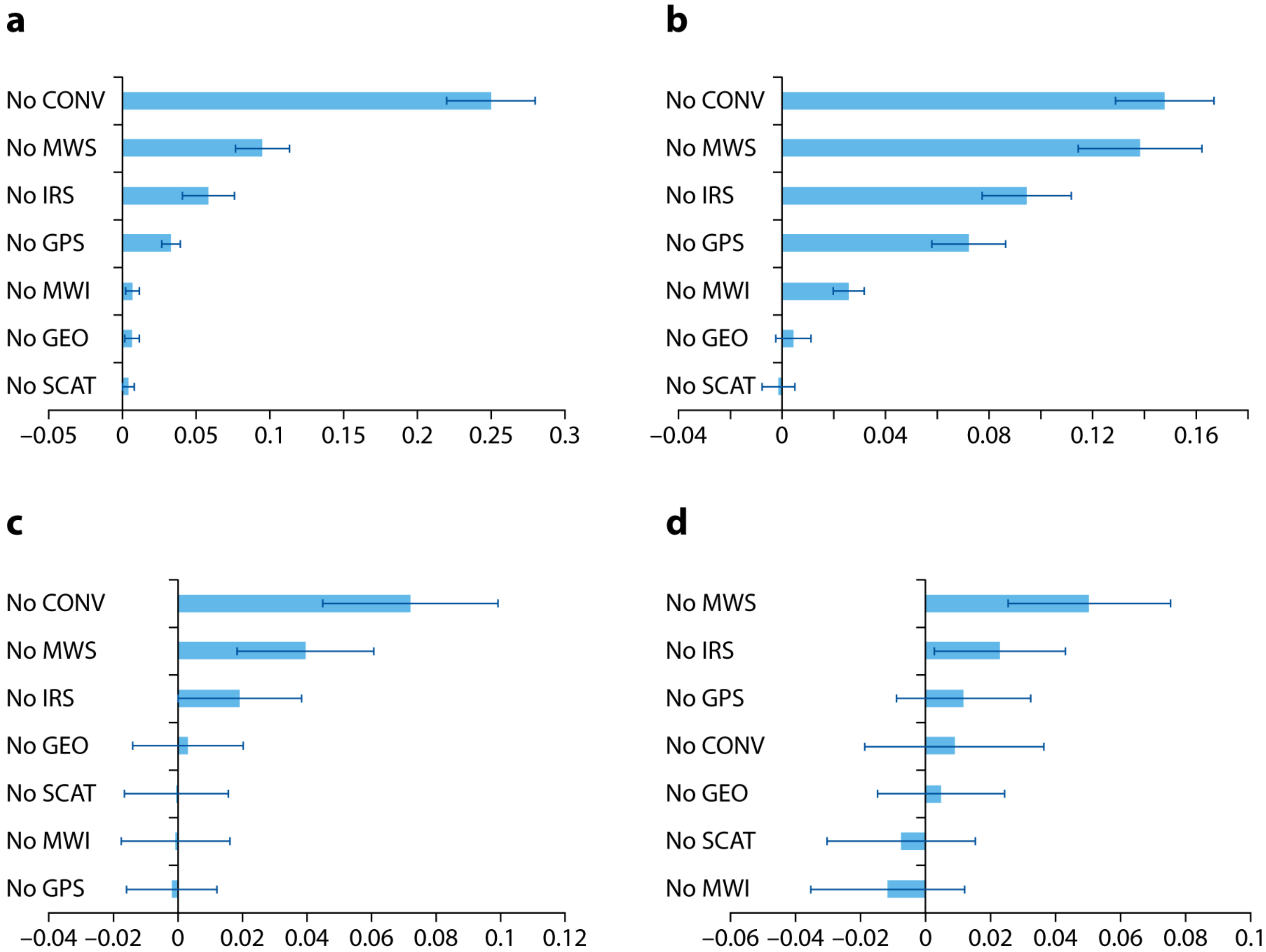

Figure 9: a) Normalised increase in the day-1 (T+24h) 500 hPa geopotential forecast error over the Northern Hemisphere resulting from denying various observing systems in the ECMWF NWP system. The observing systems are: CONV: conventional observations, MWS: microwave sounders (7 AMSU-A, 4 MHS, 1 ATMS), IRS: infrared sounders (2 IASI, 1 AIRS, 1 HIRS), GPS: radio occultation observations, MWI: microwave imagers, GEO: data from geostationary satellites (AMVs and radiances) and SCAT: scatterometer observations (2 ASCAT). The period covered is 1 March – 30 June 2014, with the experiments using the version of the ECMWF system operational at the time, but run at the lower spatial resolution of T511 (approx. 40 km). Forecasts have been verified against the operational ECMWF analysis. b) As a), but for the Southern Hemisphere. c) As a), but for the day-6 forecast (T+144h). d) As c), but for the Southern Hemisphere. Courtesy McNally et al (2014).

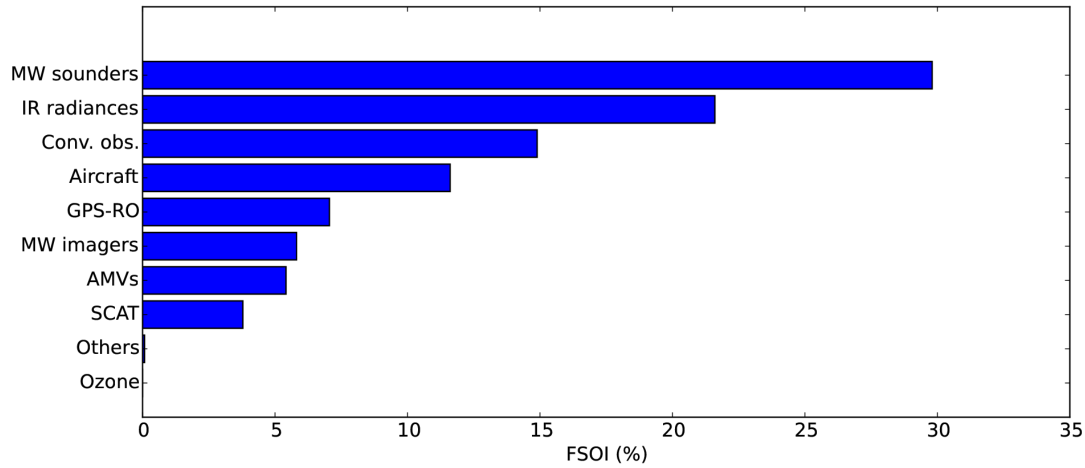

Figure 10: Relative contribution to the reduction in short-range forecast errors for various observing systems as estimated through Forecast Sensitivity Observation Impact (FSOI) diagnostics, for ECMWF's operational 4DVAR system, covering the period 1 Nov 2015 to 7 March 2016. "MW sounders" includes data from 6 AMSU-A, 4 MHS, F-17 SSMIS (sounder channels), ATMS, and MWHS.

Observing System Experiments as well as Forecast Sensitivity diagnostics from a range of NWP centres consistently show that these observations combined provide the largest forecast impact for medium-range global weather forecasts (e.g. Andersson and Sato 2012, Gelaro et al 2010). An example of such results is shown in Figure 9 and Figure 10 for an estimate of the relative forecast impact of various observing systems at ECMWF. The aim is that MWS continues this strong forecast impact.

Data assimilation systems are designed to provide the best estimate of the current state of the atmosphere for use in NWP, by combining a large variety of different observations and our knowledge of the evolution of the atmosphere simulated by numerical weather prediction models. The most common methods in use today at operational centres are 3- or 4-dimensional variational systems which are particularly suited to satellite radiance assimilation (e.g. Rawlins et al. 2007, Andersson et al 1994). Ensemble methods are increasingly attracting attention, especially for the characterisation of the situation-dependent uncertainty in the short-range forecasts that are used to carry forward in time the information from previously assimilated observations (e.g. Buehner et al. 2013, Clayton et al. 2013, Bonavita et al. 2012).

The strong forecast impact of the 50-60 GHz temperature-sounding channels is primarily the result of constraining the large-scale mass field through highly accurate information on relatively deep temperature layers. A key capability here is that MWS provides this information also in situations that are weakly affected by clouds, unlike infrared sounders which cannot sense through clouds. In the extra-tropics, approximate geostrophic balance ensures that the temperature information also translates to information on the wind field. A key prerequisite of this strong forecast impact is the high precision required for the data. Today's short-range forecasts show random uncertainties of around 0.1 K in terms of MWS-like tropospheric temperature-sounding channels, and this uncertainty is expected to be even lower in the EPS-SG time-frame (e.g. Bell et al. 2010). Even though this uncertainty in short-range forecasts cannot be directly interpreted as a requirement for MWS observations, it gives an indication that stringent noise requirements for MWS are critical to be able to improve short-range forecasts through the assimilation of MWS data.

The improvement in the accuracy of NWP systems, leading to particularly stringent requirements for the temperature-sounding channels and their use, is further highlighted in Figure 11. It shows the evolution of standard deviations of differences between observations and operational short-range

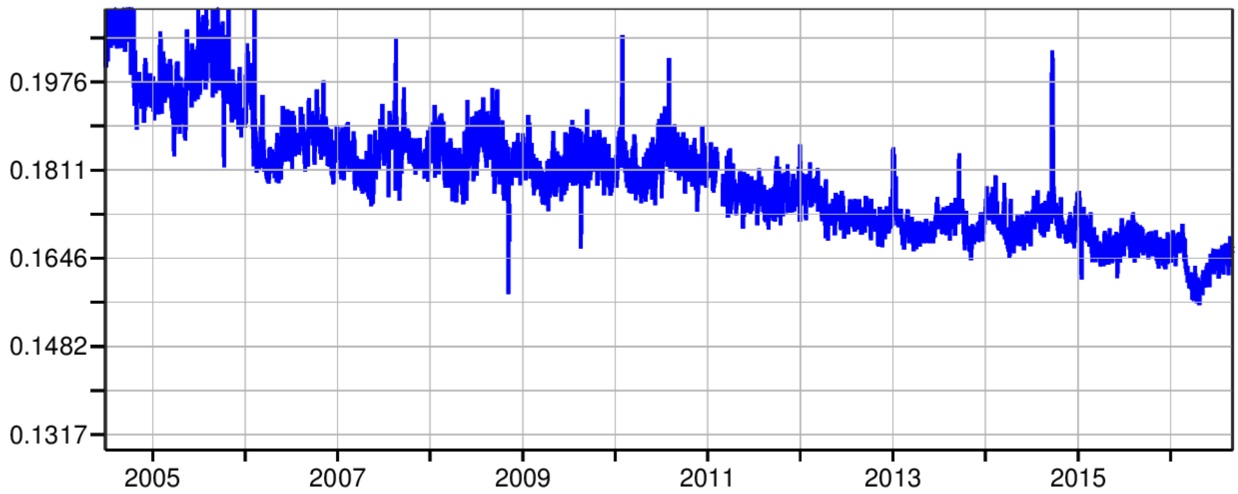

Figure 11: Evolution of the standard deviation of differences between observations and short-range forecast equivalents (K, after bias correction) for assimilated observations from channel 8 of the Aqua AMSU-A, taken from the operational ECMWF system.

forecasts from ECMWF for AMSU-A channel 8 from the Aqua instrument over a 12-year period. Since 2005, the fit to these observations has decreased from 0.21 K to around 0.16 K today. This means that these standard deviations are now mostly dominated by the instrument noise of this channel (around 0.14-0.15 K), whereas contributions from random uncertainties in short-range forecasts have decreased to well below the instrument noise. The assimilation therefore needs to make smaller and smaller adjustments to correct errors in short-range forecasts, and this places ever more demands on the accuracy of the observations and their use in NWP. Errors that in the past may have been considered negligible are now becoming more important. These aspects will be reviewed in more detail in section 5.2.

The forecast impact of the 183 GHz humidity-sounding channels is more complex. When used in clear-sky regions only, they add direct information on mid- and upper tropospheric humidity layers. However, the temporal evolution of these also allows the derivation of dynamical information during the assimilation of the data. This is, for instance, achieved in 4-dimensional variational assimilation systems, which consider the temporal evolution of the atmosphere over a 6-12-hour time window, enabling a “tracing” of humidity structures (e.g. Geer et al 2014, Andersson et al 1994). Such tracing can be particularly powerful if data is provided at several temporal intervals (e.g. Peubey and McNally 2009). MWS will therefore act in the context of the wider observing system to provide similar dynamical information. Extracting information on wind from these channels plays a key role in obtaining medium-range forecast impact from the data.

In recent years, significant progress has been made in extending the use of microwave sounder radiances to regions that are considerably affected by clouds or precipitation (e.g. Bauer et al. 2011, Geer et al. 2018). This so-called “all-sky” approach is expected to be a more common application in the EPS-SG time-frame. While cloud-effects are smaller for microwave sounding channels than in the infrared, strongly cloud/precipitation-affected observations are nevertheless traditionally screened out for the assimilation of microwave sounder radiances. Given improvements in the representation of clouds in forecast and radiative transfer models (e.g. Geer and Baordo 2014, Geer et al. 2009), approaches have been developed in which cloud- and precipitation-affected observations are also assimilated and allowed to provide information on model clouds (Guerbette et al. 2016, Geer et al. 2014). This has been shown to give strong benefits in terms of forecast skill, particularly for the 183 GHz channels, and is used operationally at some NWP centres. At ECMWF, treating humidity-sensitive microwave radiances in an all-sky framework has been an important factor in getting their forecast impact to approach that of the microwave temperature sounding observations.

Similar to the assimilation of humidity information, a key mechanism for translating the impact from all-sky observations into improved forecast skill in the medium range is the improvement of the dynamical analysis resulting from adjustments to support the observed cloud evolution (Geer et al. 2014). For these applications, instrument noise is not a crucial factor for current instruments, but rather the description of representation errors. Several challenges and possibilities for improvement still remain for all-sky applications, not least in terms of radiative transfer improvements and treatment of uncertainties in the representation of clouds and precipitation in forecast models.

An all-sky use appears particularly attractive for the new lower temperature sounding channels of MWS (MWS-5 and -7), as well as the new 229 GHz channel. As no similar channels have previously been available, new approaches for assimilation may need to be developed. In addition, synergies with cloud information available from MWI and ICI in an all-sky context will be a significant advancement over the capabilities of the first generation EPS. As no comparable observations exist presently, these synergies have not been explored before, and significant development is likely to be necessary to make the best use of the combination of these observations.

Another application area with considerable research activity is the use of surface-sensitive data over land and sea-ice (e.g. Karbou et al. 2010). The use of surface-sensitive data over land and sea-ice hinges on the adequate description of the surface emissivity and skin temperature, which is particularly complex over snow-covered or sea-ice surfaces. With the advent of coupled atmosphere/land-surface data assimilation schemes, simultaneously extracting atmospheric as well as surface information from surface-sensitive channels will undoubtedly be a more widespread activity in the EPS-SG time frame. Presently, these two Earth-System components are mostly treated separately, leading to aliasing of surface-related errors into atmospheric analyses and vice versa. Coupling systems offer a more consistent exploitation of the data in this respect, with significant opportunities and challenges.

A more detailed review of the scientific and practical aspects of the data use in NWP will be provided in Section 5.2.

4.2 Regional Applications and Nowcasting

Similarly to global application, the Level 1 radiances are widely used in regional models. From a data assimilation point of view, the same technique is used in global and regional models for the radiance assimilation, including microwave data. In case of regional model, however, the access to observations from polar orbiting satellite depends on the geographical location and on the extension of the model domain. Furthermore, the observations (satellite paths) can cover different parts of the model domain at different assimilation times. As a consequence, different numbers of radiance observations are available at different assimilation times. According to Randriamampianina et al. (2011), the usual way of the computation and update of the radiance bias correction coefficients, cycling through the assimilation (Auligné et al. 2007), is not efficient for radiance assimilation in regional models. Instead, they proposed a daily aggregation of the bias statistics for each assimilation time.

Many studies reported positive impact of the microwave radiances in limited area models (LAM) (Zhang et al. 2014, Zou et al. 2013, Randriamampianina, 2006). Storto and Randriamampianina (2010) applied a moist total energy norm-based diagnostic technique to evaluate the impact of ATOVS (AMSU-A and AMSU-B/MHS) radiances assimilated together with other satellite and conventional observations in a regional model (

Figure 12). They found that while the conventional observations have higher impact on the very short-range forecasts, the impact of the ATOVS radiances is higher for longer forecast ranges. They also evaluated the impact of each assimilated ATOVS channel on the LAM forecasts (Figure 13), and studied the impact of each channel to tropospheric (low: 850-600 hPa, middle: 600-350 hPa and high: 350-150 hPa), and stratospheric (150-20 hPa) layers based on the total (full terms, Ehrendorfer et al., 1999) and only moist part of the energy norm. Figure 13 shows that the troposphere-sensitive AMSU-A channels (5 to 8, respectively 53 to 55 GHz) and AMSU-B/MHS channels (3 to 5, respectively 183 to 191 GHz) have considerable impact on the short-range forecasts.

A recent study (Randriamampianina et al. 2017), performed over the Arctic, using the HARMONIE-AROME (HIRLAM–ALADIN Research on Mesoscale Operational NWP in Euromed, Applications of Research to Operations at Mesoscale) shows similar impact of the ATOVS radiances on LAM analyses and forecasts (Figure 12), although, the following restrictions were applied in this study: 1) the low-peaking channels (5 and 6 from AMSU-A, and channel 5 from AMSU-B/MHS) were not used over land, and 2) no radiance assimilation was applied over sea ice. We expect the equivalent MWS channels with the two new ones (5 and 7) to be similarly valuable for regional applications.

Nowcasting systems are often associated with warning of severe weather conditions. Early systems used the extrapolation of radar or satellite images. Recently, more meteorological centres dedicate resources in developing NWP-based nowcasting system thanks to the progress in mesoscale data assimilation, short-range NWP and efficient computing systems. The impact ATOVS radiances in such a nowcasting system (called ‘rapid refresh’) using the HARMONIE-AROME mesoscale model is shown in Figure 14 and Figure 15.

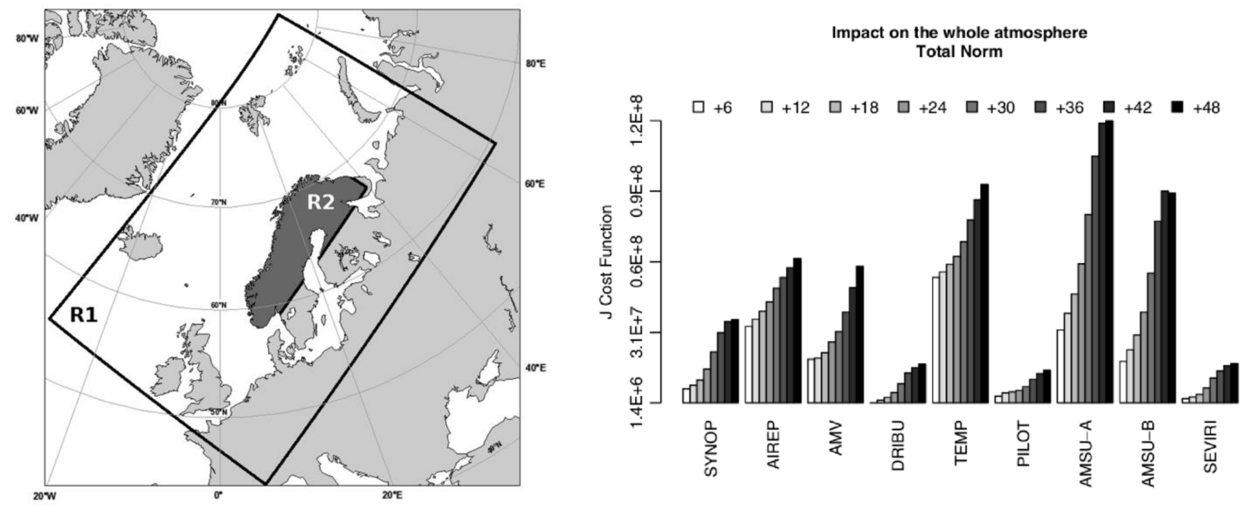

Figure 12: The domain of the ALADIN LAM (left). The graph in the right shows the sensitivity cost function defined as the total moist energy norm differences between the forecasts issued with full set of observations and the ones without the diagnosed set of observations. The comparison was done for the whole atmosphere over the whole domain (region R1). The observations’ nomenclature is as follows: SYNOP for synoptic reports over land and sea; AIREP for airborne in situ observations; AMV for atmospheric motion vectors deducted from cloud-drift images; DRIBU, oceanographic buoys and drifting buoys; TEMP for the radiosondes network; PILOT for the wind profilers; AMSU-A for the microwave radiances from the AMSU-A sounding units; AMSU-B for the microwave radiances from the AMSU-B and MHS sounding units; SEVIRI for the infrared radiances from the MSG-2/SEVIRI imager. The histograms for each observation type refer to different forecast length, as specified in the legend. See Storto and Randriamampianina (2010) regarding the impact of ATOVS on region R2.

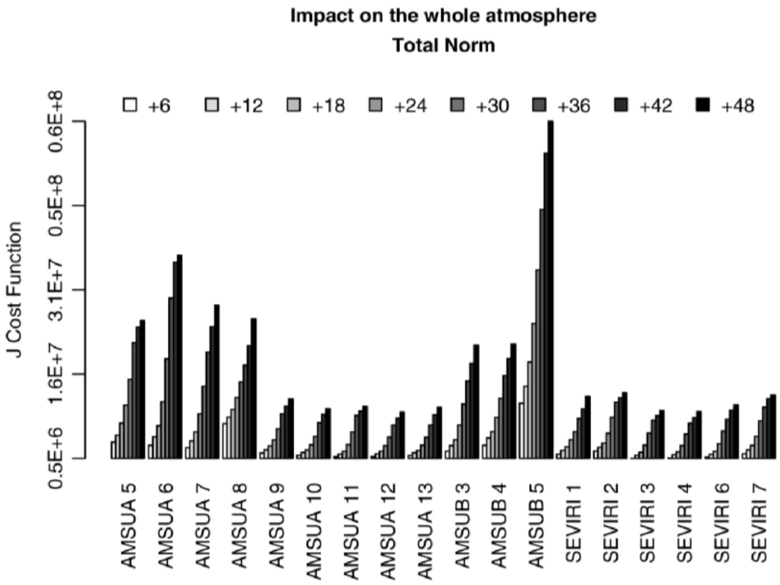

Figure 13: Sensitivity cost function defined as the total moist energy norm differences between the forecasts issued with full set of observations and the ones without the diagnosed set of observations. The diagnostic was calculated for the whole atmosphere and individually for each satellite channels.

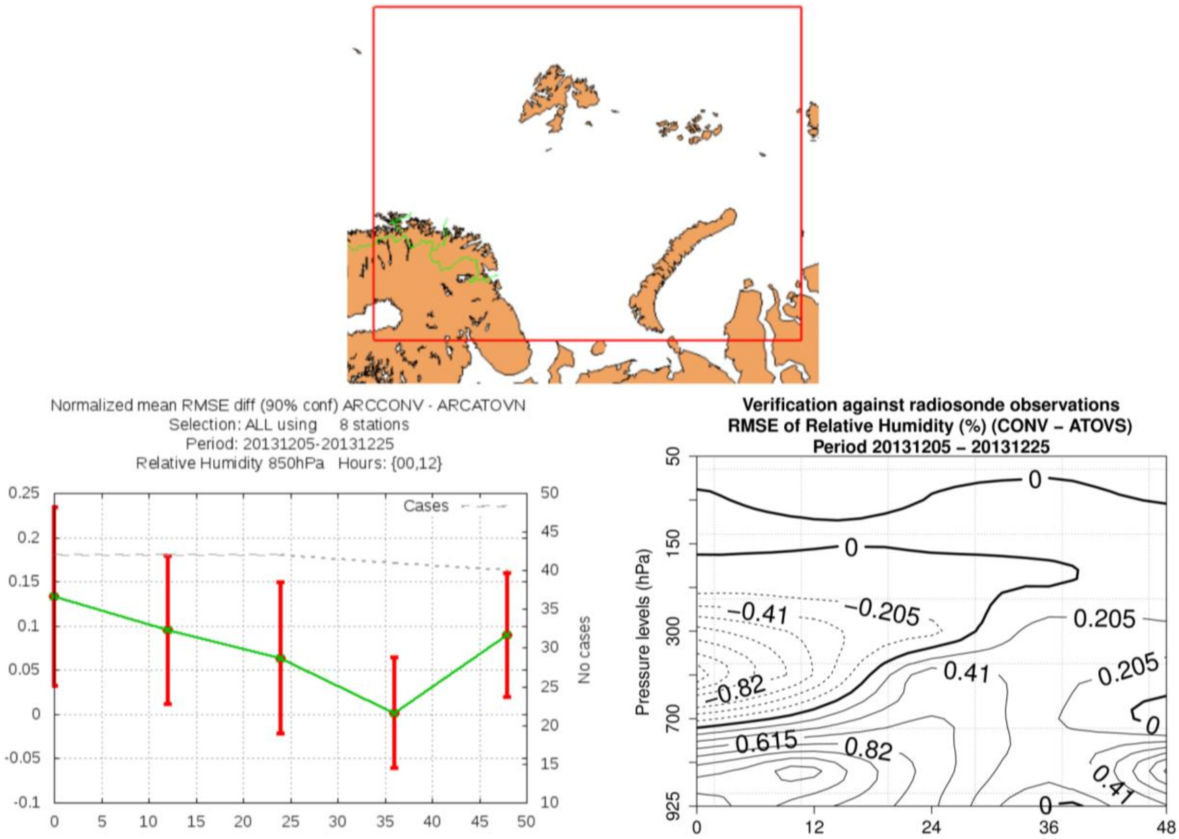

Figure 14: The domain of the HARMONIE-AROME (called AROME-Arctic) (top graph). The verification of analyses and forecasts of relative humidity against observations is shown in the lower graphs with the vertical cross-section of the difference between the RMSE of runs with and without ATOVS radiances (right graph) and the corresponding significance test at 850 hPa (left graph). Positive (negative) values mean positive (negative) impact of the ATOVS radiances. For both graphs, horizontal axe shows the forecast lengths.

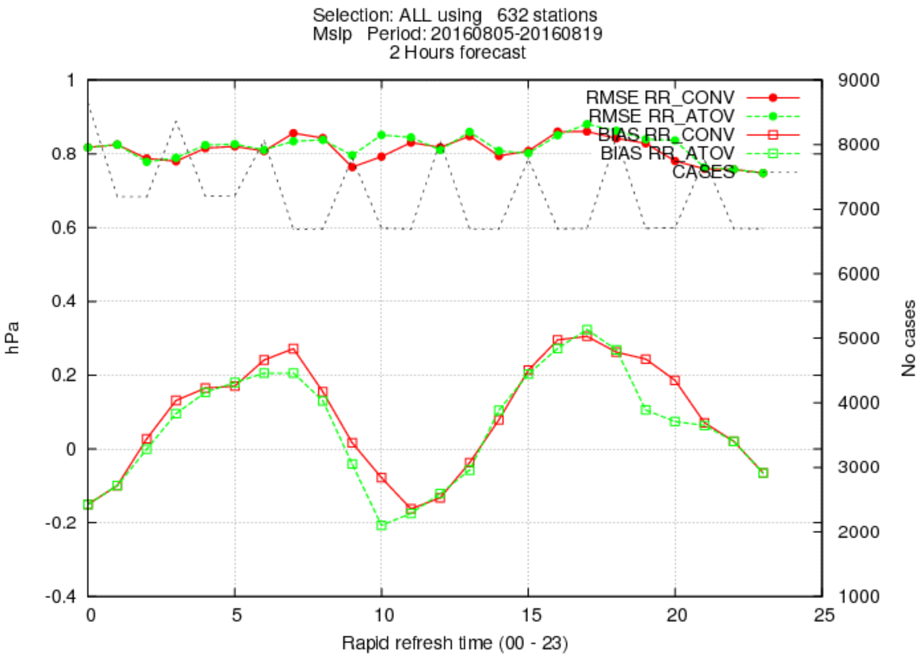

Figure 15:Verification against surface synop observations comparing 2-hours forecasts from two rapid refresh experiments with (RR_ATOV) and without ATOVS (RR_CON). The assimilation system in both cases is 3D-VAR. Lines with stars show the root-mean-square error (RMSE) and those with squares show the bias (BIAS). The experiments were performed over the MetCoOp domain (over Scandinavia).

Nowcasting systems are built over restricted regional domains, set up with hourly or even sub-hourly frequency update with data assimilation, and hence constrained with very short cut-off time (e.g. 15 minutes). These conditions lead to a limited access to data from instruments on board polar orbing satellites like MWS. But, more frequent observations are accessible in a system over high latitude compared to mid-latitude or tropical domains. For example, for a system with a domain spanning high latitudes, 12 of 24 hourly rapid refresh times get advantage of polar microwave radiances using NOAA and Metop satellites (Table 8), while for a system over the mid-latitudes most satellite radiances can only be used at least 1 h after the observation time (Auger et al., 2015). Nonetheless, microwave radiances were successfully used in several nowcasting systems (Auger et al., 2015, Ballard et al., 2016). No study reports a clear impact of microwave radiances on nowcasting systems. Performing experiments with and without the ATOVS radiances in the above mentioned HARMONIE-AROME with 1-hour rapid refresh system over the Scandinavia for a period of 15 days showed significant negative impact on the mean sea level pressure and neutral impact to surface parameters like 2m temperature, 2m relative humidity and 10m wind but positive impact on accumulated precipitation (Figure 14). It is important to notice that this verification was done with point comparison. Fields verification would show better and fairer comparison, especially for precipitation verification. Many reasons can be responsible for this weak impact of ATOVS on hourly rapid refresh system. One of them can be the non-optimality of the applied variational bias correction, where the applied coefficients need to be better defined and the lack of anchors observations may also cause serious problem. Efficient solutions must be found to handle properly biased observations in nowcasting systems.

Most of the temporally and spatially frequent observations (e.g. radar, aircraft Mode-S, ground-based GPS), which play principal roles in nowcasting systems, sense primarily the troposphere. Even though the tops of mesoscale models are often lower compared to those of the global models, stratospheric observations like by the 54 and 55 GHz MWS data can be very important to support a

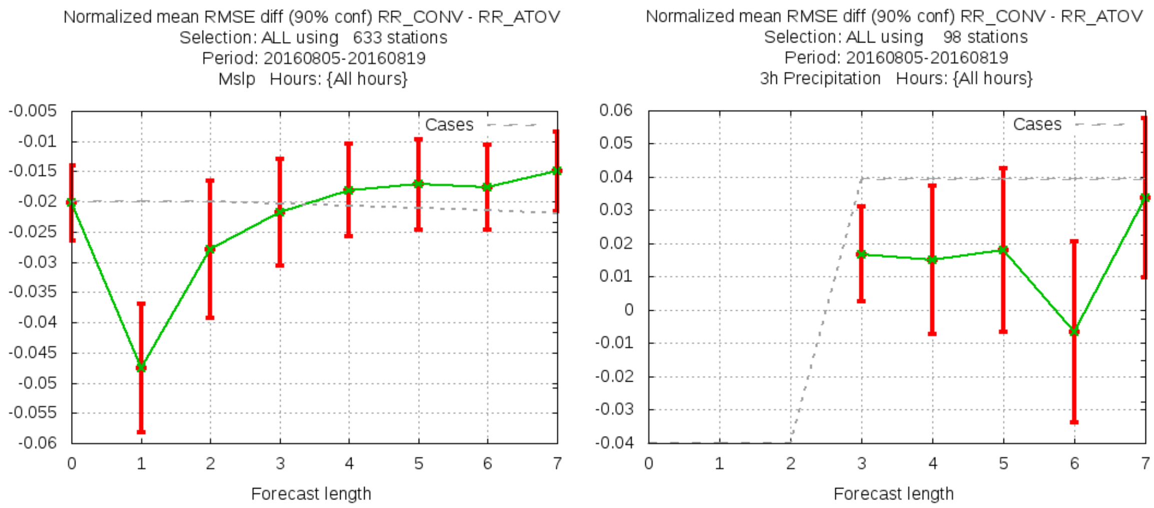

Figure 16: **Significance test of normalised mean root-mean-square error difference between runs with (RR_ATOV) and without (RR_CONV) ATOVS data for mean sea level pressure (left) and 3-hourly accumulated precipitation (right). Positive (negative) values mean positive (negative) impact of the ATOVS radiances on rapid refresh system. The statistics shown here are from all the 24 runs per day.**

good balance in the analysis and to ensure that physical processes are realistically represented in the very short-range NWP forecasts. This is important because very often, at certain analysis time, in case the surface or low-stratospheric observations are dominating in the assimilation, as prescribed by the background error statistics, upper-level increments are created during the assimilation. Since the background error statistics are computed with some assumptions, they cannot provide good analysis balance for all meteorological conditions. Hence better balance between the driving variables (called control variables) is reached, in case of the above example, when upper-tropospheric or stratospheric observations are also assimilated. This is true when radiosonde observations, which are important for stratospheric level analyses are not available in nowcasting system because of the very short cut-off time.

The availability of ATOVS radiances is shown in Table 8**.** One can see for some nowcasting times positive impact on bias of MSLP, but the main conclusion from this study is that for optimal use of radiances in rapid refresh system, appropriate or well computed bias correction coefficients are needed for each nowcasting time. Significance test of the differences for the 2-hours forecasts is shown on Figure 16.

Limited range of radar data in space (for example not available over sea) and variable amounts of aircraft (e.g. Mode-S) observations in time (day and night), may restrict the impact of these data in nowcasting systems. When MWS radiances are available, they can be assimilated with the improved all-sky approach (Geer et al 2014, see also the section 5.2.5). Such improvement aims at providing better fits of the all-sky approach with the mescoscale model physics. Assimilated in such a system, the MWS data can complement the above cited observations and can provide efficient impact also in cases of cloudy and precipitating events. This concept requires further development of the all-sky approach together with improving the fit of the MWS radiances in the mesoscale model space by accounting for their footprints. The later development, aiming at reducing the representativeness error of radiances in mesoscale data assimilation, is needed because the resolution of the mesoscale models is much higher than that of any channels of the MWS instrument.

More and more NWP centres found solutions for affordable mesoscale ensemble-based forecast systems (e.g. UK MOGREPS-UK, Germany KENDA, Norway and Sweden MEPS, Denmark COMEPS, France AROME-EPS). Zhang et al. (2012) showed that ensemble assimilation of precipitation-affected microwave radiances improves the quality of precipitation analyses in terms of spatial distribution and intensity in accumulated surface rainfall. Similarly, cloud- and precipitation-affected MWS radiances assimilated in a mesoscale ensemble variational (EnVAR) system have the potential of providing a more reliable nowcasting and very short-range forecasts of the probability of intense events.

Nowcasting time (UTC)	Available microwave data	Nowcasting time (UTC)	Available microwave data
00		13	
01		14	NOAA-19
03		15	NOAA-18
04	NOAA-19	16	
05	NOAA-18	17	
06	NOAA-19	18	
07	NOAA-18	19	Metop-B
08		20	Metop-A
09	Metop-B, NOAA-19	21	Metop-B
10	Metop-A, NOAA-18	22	
11	Metop-B NOAA-19	23	
12			

Table 8: Availability of the ATOVS radiances in an hourly rapid-refresh system over the METCOOP domain:

4.3 Climate Monitoring (Trends and future evolution of MWS retrieved geophysical parameters)

Microwave satellite sensors such as MWS provide valuable humidity observations in the upper troposphere using the 183.31 GHz channels. Several studies have compared AMSU/MHS derived Upper Tropospheric Humidity (UTH) with some target validation data (Buehler and John (2005), Moradi et al. (2010)). Buhler et al. 2008, describe a global database of UTH making use of AMSU-B/MHS data from several satellites. Brogniez et al. describe a SAPHIR based algorithm to derive UTH over tropical regions. MWS offers an unprecedented set of humidity channels close to the 183.31 GHz water vapour line. These channels are of great interest for long-term studies of UTH, weather and climate (see for instance Garot et al. 2017 who examined the distribution of UTH from the SAPHIR instrument in Indian Ocean and its links with the phase of the Madden–Julian oscillation and large-scale advection versus local production of humidity).

Climate observations, and especially long-term studies of the climate system, have a value in themselves for the monitoring of climate under changing conditions. However, there is also the need for a monitoring program that can build the basis for testing the capabilities of climate models and create greater confidence in long-range climate projections (Goody et al., 2002). The GCOS programme has identified a set of Essential Climate Variables (ECVs) that are feasible for systematic observation and for which observations are needed, in particular to support to the work of the United Nations Framework Convention on Climate Change (UNFCCC) and the Intergovernmental Panel on Climate Change (IPCC). A detailed list of the currently 52 ECVs (plus potential future ECVs) covering atmosphere, terrestrial and ocean domains and their product requirements can be found in GCOS (2016). Data from operational and research satellites provide a valuable data source for the generation of climate data records (CDRs) of such ECVs due to their space time-coverage and observing capabilities. MWS data will be an important input for satellite-based climate monitoring and reanalyses by further extending the data record of previous polar-orbiting microwave sounders such as AMSU- A and –B, MHS and ATMS flying on the different NOAA POES, JPSS and EUMETSAT Metop satellites. The length of the microwave sounder record for some channels will approach 50 years by the end of the EPS-SG programme, and this will provide one of the backbones of satellite-based climate monitoring and reanalysis quality.

Several GCOS ECVs, such as temperature and water vapour profiles, total column water vapour (TCWV), cloud liquid water column, precipitation and land surface temperature can be derived from MWS and will extend the existing time series of these parameters. CDRs from currently available sensors are already available from different CDR programs (e.g. NOAA CDR program, EUMETSAT Satellite Application Facilities (esp. Satellite Application Facility on Climate Monitoring (CM SAF)) based on the predecessors. For example, a monthly mean map of total precipitable water vapour (TPW) and the associated standard deviation from the CM SAF ATOVS data record (Courcoux and Schröder, 2013, 2015) is shown in Figure 17. MWS will contribute to the extension of such ECVs. At the same time the addition of more frequencies, which are not yet available with current systems, and the increased spatial resolution will introduce new observing capabilities, which will enhance the climate monitoring potential.

Reanalysis builds on the assimilation infrastructure developed for NWP to produce consistent best-estimates of the atmospheric state by using the same state-of-the-art assimilation system and the most complete set of observations over an extended period of time. Several such projects on the global scale exist, for instance at ECMWF, JMA or NCEP (e.g. Dee et al. 2011, Uppala et al 2005). Also higher-resolved regional mesoscale reanalyses are generated for various purposes e.g. sustainable energy generation applications (e.g. Bollmeier et al. 2015, Wahl et al. 2017).

Satellite-based climate monitoring as well as global and regional reanalyses are widely used for trend and process studies or to produce reliable climatologies. In general, full traceability of operational processing from level 0 to level 1b and further from level 1b via level 2 to level 3 data (including information on processor version, auxiliary data, etc.) together with a thorough geolocation of the data is important. The input flow, all processing steps, quality control and all other steps as well as known issues and changes must be fully documented and made publically available. Changes in the behaviour of the instrument (e.g. ageing effects) or changes in the Level 1 algorithms might erroneously be interpreted as a signal of climate change and can disrupt trend monitoring. In order to avoid a false interpretation of data and to remove the potential corruption of the time series,

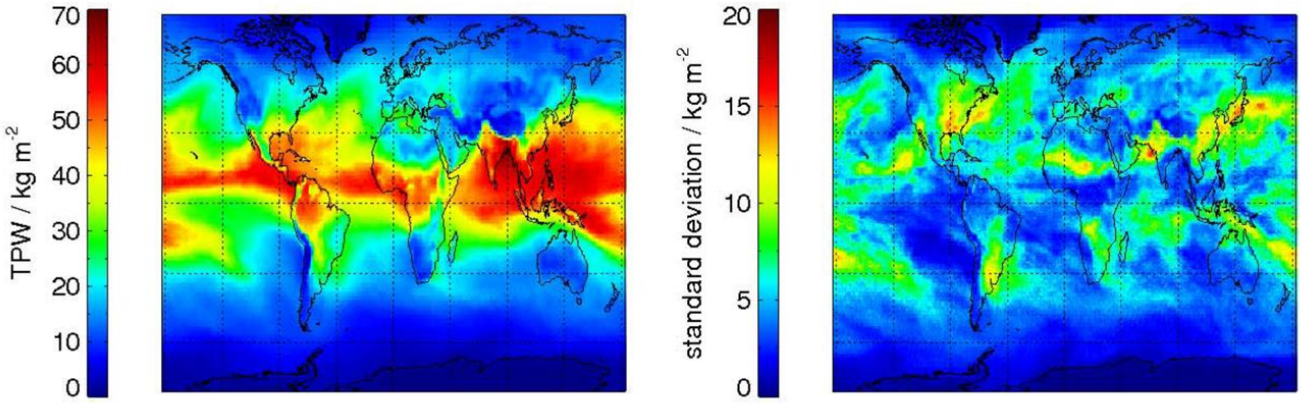

Figure 17: Mean TPW and associated standard deviation for September 2007 (from Courcoux and Schröder, 2015).

reprocessing of the MWS data is expected to be an integral task of producing a reliable and consistent climate record. So-called "fundamental climate data records" are the critical basis for the generation of ECV datasets (Bojinski et al (2014), Chander et al (2013)). Such datasets will be highly beneficial for reanalysis activities and climate monitoring applications.

Changes in instrument behaviour due to, e.g., ageing effects, or for identification of pre- and post-launch differences in instrument characteristics, can be characterized by roll manoeuvres which allow monitoring of changes in instrument characteristics by "seeing" stable space (without any atmospheric contributions). Also pitch manoeuvres can support the identification of changes in scan-angle behaviour or cross-track asymmetries as e.g. done with NOAA-14 (Kleespies et al., 2007) or Suomi-NPP (Weng and Yang, 2016). These manoeuvres are highly beneficial for a solid characterization of the sensor during the life-time of the instrument, which is of extreme importance for climate applications.

The generation of climate data records needed for climate applications relies on careful cross-calibration activities. In case of MWS, sufficient temporal overlap with heritage instruments ATMS and MHS is crucial for reliable cross-calibration. The overlap with heritage sensors should be large enough to allow for the identification of jumps, drifts and offsets between the instruments (e.g. Weatherhead et al (2017). An overlap of at least one year to cover the full yearly cycle would be beneficial (e.g. Ohring et al, 2005), while even longer overlap times would allow for an even better characterization of instrument differences. Back-propagating the new cross-calibration to even older heritage instruments, i.e. AMSU and even MSU is a next step in order to achieve maximum temporal coverage. Of particular note is that the MWS design features phase-locked local oscillators, ensuring stable central pass-band frequencies for all MWS channels. Uncertainties in the pass-band characteristics provide a considerable source of systematic error for today's generation of microwave sounders (e.g. Zou and Wang 2011, Lu and Bell 2014). Provided other sources of uncertainty are small, this improved capability of MWS may enable an independent characterisation of pass-band characteristics of older sensors such as AMSU-A. This will allow to further test the recent hypothesis that considerable pass-band shifts occurred for some of these sensors during or after launch.

A sound validation of the Level 1 data is needed and additionally independent assessments of Level 1 data would give valuable feedback on the achieved quality and compliance with user requirements. It is essential that the recalibration of MWS, the cross-calibration with heritage instruments and the validation is carried out in a sustained environment. Again, this requires also traceability and needs to be fully documented and made available. The Global Space-based Inter-Calibration System (GSICS) is an international collaborative effort by the WMO and the Coordinated Group for Meteorological Satellites (CGMS) to establish a consistent (inter-)calibration of satellite measurements from different instruments on different satellites. The Microwave Subgroup (MWSG) of the GSICS Research Working group aims to develop radiometric corrections for passive microwave sounders (GSICS 2015, 2016). It is expected, that GSICS will include MWS in its activities. A close collaboration with GSICS should be envisaged.

From a backward looking climate monitoring perspective newly developed/adapted retrieval schemes for MHS, ATMS, AMSU and/or MSU are required such that CDRs of ECVs such as TCWV, water and temperature profiles and precipitation can be generated. In addition and from a forward looking climate monitoring perspective retrieval schemes that make full use of the new capabilities of MWS are beneficial as well in view of the life time of EPS-SG satellites. Finally, reprocessing of the full archive including heritage instruments to generate ECVs and the evaluation of related CDRs will provide valuable feedback to the calibration, recalibration and cross-calibration teams. Such feedback loops have proven to be important elements to remove potential issues in level 1 data which occasionally become evident only in level 2 or level 3 space and with that to improve the quality of the level 1 data and the CDRs.

5 MWS SCIENCE AND PRODUCTS

5.1 Level 1 Products Generation (Radiances, Antenna Corrected Brightness Temperatures)

5.1.1 Calibration algorithm

5.1.1.1 Assumptions

The fundamental assumptions underpinning the level 1 calibration algorithm are (see Atkinson, 2016):

- The incoming radiation is reflected off an imperfect scan mirror, of reflectivity R_θ, where θ is the scan angle;
- There are cold and warm calibration views: cold space and the on-board black-body calibration target;
- The energy entering the receiver is related to the counts, C, from the analogue to digital converter (ADC) via a quadratic transfer function. Thus, for the Earth view (subscript E):

$$a_0 + a_1 C_E + a_2 C_{E^2} = (1 - R_\theta) B_{REF} + R_\theta B_E \quad (3)$$

where B_{REF} is the black body radiance at the temperature of the reflector and B_E is the radiance of the Earth scene. We assume that the a_0 , a_1 and a_2, coefficients do not depend on scan angle. Similar equations can be written for the space view (subscript SP) and internal black-body view (subscript bb):

$$a_0 + a_1 C_{SP} + a_2 C_{SP^2} = (1 - R_\theta) B_{REF} + R_\theta B_{SP} \quad (4)$$

$$a_0 + a_1 C_{bb} + a_2 C_{bb^2} = (1 - R_\theta) B_{REF} + R_\theta B_{bb} \quad (5)$$

5.1.1.2 Solving the calibration equations

There are various ways to solve the above three calibration equations to derive a_0 and a_1 for each scan line (a_2 is discussed later).

Method 1

The method recommended for implementation in the operational ground segment is to use (4) and (5) to derive expressions for a_0 and a_1, in terms of calibration measurements:

$$a_0 = B_{bb} R_{bb} - C_{bb} \frac{A}{G} + a_2 C_{SP} C_{bb} + B_{REF}(1 - R_{bb}) \quad (6)$$

$$a_1 = \frac{A}{G} - a_2(C_{bb} + C_{SP}) \tag{7}$$

where:

$$G = \frac{C_{bb} - C_{SP}}{B_{bb} - B_{SP}} \tag{8}$$

and:

$$A = \frac{R_{bb}(B_{bb} - B_{REF}) - R_{SP}(B_{SP} - B_{REF})}{B_{bb} - B_{SP}} \tag{9}$$

Note that the variable A is very close to 1. Then use (3) to obtain B_E for each sample. So for each scan line we would have the values of a_0, a_1, a_2 and the reflector temperature, while the reflectivity values would be obtained from a look-up table or a reflectivity model. An advantage of this approach is that it closely mirrors the existing approach for AMSU, but is modified to correctly take account of the reflector (Atkinson, 2016). Computation of the polynomial coefficients can be delegated to a calibration task, while application of the coefficients to raw Earth-view counts, to generate antenna temperatures, is straightforward. The approach also maintains the useful concept of gain, *G*. It is useful to monitor the gain and calibration coefficients as indicators of instrument stability.

The antenna reflectivity (as a function of scan angle) is derived either from pre-launch measurements or from a satellite manoeuvre in which the instrument views only cold space (see section 6.1.2). The black-body radiance of the reflector (B_{REF}) must be estimated from a thermal model, since it is rotating and its temperature cannot be easily measured.

Method 2

Another method (which is mathematically equivalent in terms of the result) is to express B_E as a function of the raw counts and the calibration parameters, without computing the polynomial coefficients explicitly. It can be shown that (see derivation in Atkinson, 2016):

$$\begin{aligned} B_E = {} & \left(1 - (1-x)\frac{R_{SP}}{R_\theta} - x\frac{R_{bb}}{R_\theta}\right)B_{REF} + x\frac{R_{bb}}{R_\theta}B_{bb} + (1-x)\frac{R_{SP}}{R_\theta}B_{SP} \\ & - \frac{a_2}{R_\theta}x(1-x)(C_{bb} - C_{SP})^2 \end{aligned} \tag{10}$$

where $x = (C_E - C_{\mathrm{SP}})/(C_{\mathrm{bb}} - C_{\mathrm{SP}})$. If the antenna reflectivity (R) does not vary with scan angle then the first term vanishes and we obtain the familiar transfer function used for AMSU. If the antenna reflectivity does vary then we obtain the radiometric offsets discussed in section 3.2.3.

Method 3

A third possibility is to compute the calibration coefficients using the "classical" (AMSU/MHS) approach, initially ignoring antenna reflectivity. Then a reflectivity correction can be added as a second step (as in Labrot et al. 2011). This is less satisfying from the theoretical viewpoint, even though in practice it is expected to yield satisfactory accuracy – the reflectivity corrections being small.

5.1.1.3 The nonlinearity parameter

The nonlinearity parameter a_2 needs to be determined before launch, and we need to find its correct formulation post launch. We make the following assumptions:

1. Nonlinearity arises primarily in the power detector;
2. The characteristics of the power detector do not change with time.

We also recognise that there may be an amplifier between the detector and the analogue to digital converter, with the gain being configurable by ground command (e.g. in steps of 1dB).

Let γ be the gain of the configurable post-detection amplifier, i.e. $\gamma = 10^{(\mathrm{dB}/10)}$, and g be the gain of the receiver front-end (subject to possible drift as the instrument ages). The system gain G is proportional to $g\gamma$.

Neglecting the antenna, let us consider the signal at different parts of the receiver:

- Feedhorn: signal = x
- Output of RF Amplifier: xg
- Output of detector: $a + b(xg) + c(xg)^2$
- Output of post-detection amplifier (proportional to count C): $\gamma(a + b(xg) + c(xg)^2)$

So $\mathrm{d}^2C/\mathrm{d}x^2$ is proportional to γg^2.

Neglecting antenna emission, and assuming the nonlinearity is small, we can invert Eq. (3) to give

$$
\begin{aligned}
C &= \frac{B - a_0}{a_1} - \frac{a_2}{a_1} C^2 \\
&\approx \frac{B - a_0}{a_1} - \frac{a_2}{a_1}\left(\frac{B - a_0}{a_1}\right)^2
\end{aligned}
$$

From which, $\mathrm{d}^2C/\mathrm{d}B^2$ is proportional to $a_2/a_1^3 = a_2G^3$ (since G is proportional to $1/a_1$). Comparing with the expression for $\mathrm{d}^2C/\mathrm{d}x^2$ from the receiver model, we see that a_2G^3 is proportional to γg^2; a_2 is proportional to $\gamma g^2/G^3 = 1/(\gamma G)$. Hence,

$$a_2 = \frac{\mu}{G\gamma} \tag{11}$$

where the parameter μ is determined pre-launch for each channel, as a function of instrument temperature. The units of μ are *inverse counts*.

Note that this formulation differs from that used operationally in the AMSU and MHS level 1 processors (Robel et al., 2009), which assume $a_2 = \mu/G^2$, with μ having units of *inverse radiance*. The MWS formulation proposed above is expected to be more realistic as it correctly takes account of post-detector gain and possible ageing of the receiver front-end. It will be important that the level 1 processor has access to the γ values (channel-dependent).

5.1.1.4 Variation of antenna reflectivity with scan angle

The Level 1 processor aims to achieve a correct radiometric calibration for an *unpolarised scene*. Under these conditions, the effective reflectivity at a scan angle θ from nadir is given by:

$$R_\theta = R_0 cos^2\theta + R_{90} sin^2\theta \tag{12}$$

Let r_h be the antenna reflectivity, at 45° incidence angle, for radiation with electric vector parallel to the plane of the reflector surface and r_v be the antenna reflectivity for the orthogonal polarisation. According to Yang et al. (2016):

$$r_h{}^2 = r_v \tag{13}$$

i.e. r_v is always smaller than r_h. For a channel with quasi-vertical (QV) polarisation, $R_0 = r_h$ and $R_{90} = r_v$. Similarly, for a channel with quasi-horizontal (QH) polarisation, $R_0 = r_v$ and $R_{90} = r_h$. So to estimate the reflectivity as a function of scan angle, we just need a single free parameter r_h, for each channel, with:

$$R_{\theta,QV} = r_h cos^2\theta + r_h{}^2 sin^2\theta \tag{14}$$

$$R_{\theta,QH} = r_h{}^2 cos^2\theta + r_h sin^2\theta \tag{15}$$

The parameter r_h can be determined either from pre-launch testing or from a post-launch manoeuvre (section 6.1.2). The parameter could depend on instrument temperature. If the scene itself is polarised (e.g. a quasi-window channel over ocean), then mirror reflectivity may result in additional errors (Weng and Yang, 2016). But accounting for this effect is not considered part of the level 1 processing.

5.1.1.5 Lunar contamination of the space view

At certain times of the month the Moon can approach the MWS space views. If uncorrected, errors of several Kelvin can result. It is recommended that MWS processing follows an approach similar to that used for ATMS (Yang and Weng, 2016), i.e., in brief:

- The lunar position is computed;
- Space samples are considered lunar-contaminated if the angular separation from the Moon is less than a specified multiple of the beam width. The result will vary from channel to channel;
- If there are some Moon-free space samples then these are used in the normal calibration process;
- If all samples are lunar-contaminated then the sample furthest away from the Moon is chosen, and the lunar correction is estimated and applied to that sample.

This process will tend to increase random noise in the calibrated radiances, but this is better than allowing the radiances to be biased.

The parameters are expected to be tuned during post-launch commissioning.

5.1.1.6 Other aspects of calibration processing

In other respects, the calibration procedure for MWS is conventional:

- Warm and cold calibration counts are averaged to reduce noise. The number of scan lines to be used in the averaging can be determined pre-launch or during commissioning;

- Warm target radiance may include temperature corrections (e.g. for thermometry errors);
- Cold space radiance includes the antenna correction;
- An Earth-view antenna correction is applied as a final step.

Regarding the averaging of calibration samples for successive scans, Atkinson (2015) shows that some averaging will almost certainly be required; if there is no averaging across scans (i.e. if only the 5 cold/warm samples within a scan are averaged) then there is a noise penalty of about 10%. It is expected that the optimum number of scans will be of order 7 (as in the current AMSU scheme).

For AMSU and MHS, the Earth-view antenna correction is obtained from the "efficiencies" (for each spot) integrated over the Earth (f_e), cold space (f_{sp}), and satellite platform (f_{sat}) (Mo 1999, Hewison and Saunders 1996). The efficiencies are tabulated in an AAPP data file. (Note that these efficiencies are not the same as the *beam efficiency* and *wide-beam efficiency* defined in the EURD). Assuming the platform is at the same temperature as the Earth (a questionable assumption), AAPP defines the corrected radiance as:

$$R' = \frac{R - f_{sp}B_{sp}}{f_e + f_{sat}} \tag{16}$$

In other words, for AMSU and MHS there is a fixed linear relationship between R' and R, and similarly between the corresponding *brightness temperature* and *antenna temperature*.

As mentioned in section 3.2.3, for MWS a more sophisticated model is planned. The degree of sophistication is an open issue, e.g. does it need to be continually updated with the latest estimate of atmospheric state and satellite position, or is climatology adequate? This needs to be addressed before the design of the level 1 processing software is finalized. A key point is that the final algorithm must be equally applicable to the core ground segment and to direct broadcast applications (i.e. should not rely on the availability of full-orbit data), and the algorithm should not be so complex that the timeliness of the product is adversely affected.

Consistency of Level 1 products between global and direct-broadcast applications is important. It is expected that MWS will become part of the *Direct Broadcast Network (DBNet) for near real-time relay of low Earth orbit satellite data* (WMO 2015). NWP centres will use a combination of DBNet data (delivered with 30 minutes of acquisition), and global data (usually delivered later, due to the delay in dumping the global data to a high-latitude ground station). The brightness temperatures need to be consistent, to much better than the accuracy specification of the instrument; 10% of the specification is suggested as a goal in the DBNet Guide. In this case, the relevant EURD specification is the bias variation over an orbit (0.2 K) – because DBNet products are typically a small fraction of an orbit and are expected to be consistent with the global products. This suggests that the goal for global-local consistency should be 0.02 K, which seems reasonable.

5.1.2 User customisation of Level 1 products

The level 1 product disseminated by EUMETSAT will contain the calibrated brightness temperatures measured by the instrument, at the native sampling and resolution of each channel. This will be fine for many applications; however for some applications users will want to modify the product before using it. Common reasons are:

- to reduce noise, especially for the temperature sounding channels;
- to make all channels have the same effective footprint.

The microwave community is already familiar with this issue through use of ATMS data. Noise reduction is typically required for global NWP; for temperature-sounding channels, background errors are already comparable with, or less than, the NEΔT of the instrument (Bell et al. 2010). On the other hand, for high-resolution regional modelling the key requirement is to capture the atmospheric structures (e.g. clouds and humidity) at the highest possible spatial resolution.

There are different methods in operational use for handling noise reduction and footprint equalisation. Some centres use the Fourier Transform method implemented in AAPP (Atkinson, 2011). This has the capability of broadening the high-frequency channels and also of narrowing (~7%) the low-frequency channels (see Figure 18). Other centres prefer to use a simple 3×3 average to achieve a broadening of the beam.

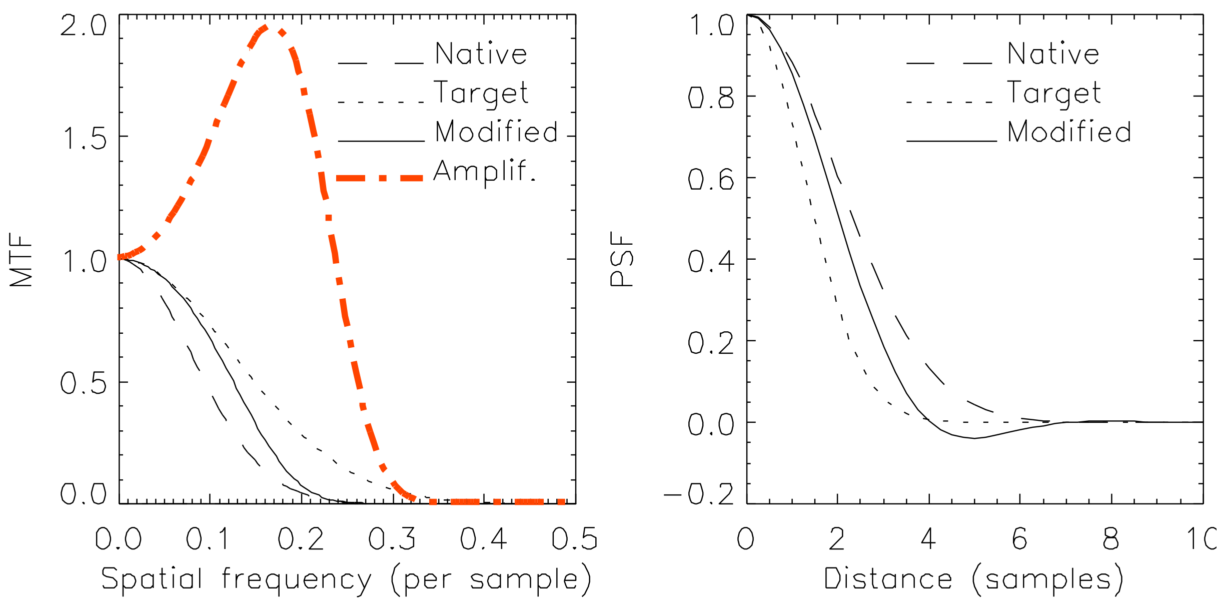

Figure 18: Attempt to synthesise an AMSU-A-like beam width (3.3°) from an ATMS channel with width 5.2° (from Atkinson, 2011). Left: amplification in the spatial-frequency domain; right: original and modified beam shape.

For MWS, the native footprint sizes are about 40% smaller than ATMS at frequencies below 60 GHz. On the other hand, NWP model grid spacing will also be significantly smaller in the EPS-SG era than they were when ATMS was specified. So it seems likely that techniques developed for ATMS will also be used for MWS.

Another consideration is that some centres assimilate different instruments separately (or even groups of channels within the same instrument), while others (e.g. the Met Office) use a 1DVAR pre-processor to generate initial profiles based on all channels, which are then used as a starting point for 4DVAR. In the latter case, beamwidth consistency between the different channels is important. These different approaches are expected to continue.

In conclusion, the spatial filtering capabilities available in AAPP for ATMS are likely to be applicable for MWS also, and the extension of AAPP should be supported. At the same time, any additional user requirement for the filtered product (e.g. output format) should be fed into the NWPSAF planning process.

5.2 Use of Level 1 products in NWP

The use of level 1 products in NWP will be one of the driving applications of MWS data, as already outlined in section 4.1. The use of level 1 data (rather than level 2 retrievals) has a strong track-record and the use of MWS can build on a good heritage from similar instruments (e.g. Doherty et al. 2015, Bormann et al. 2013, English et al. 2000).

At the same time, the accuracy of NWP systems and the sophistication of assimilation methods is continuously improving (e.g. Figure 11): the standard deviations of differences between observations in the 50 GHz tropospheric channels and short-range forecast equivalents used to be 0.25 K when ATOVS was first introduced (e.g. English et al. 2000), whereas nowadays these have been reduced to around 0.15 K. This reflects large improvements in short-range forecasts. It means that uncertainties that have not mattered in the past may become important and need to either be reduced or better taken into account. The best impact from MWS in NWP will hence only be achievable with considerable adaptation and optimisation of current methods.

To address the increasingly stringent requirements from NWP, MWS is expected to deliver observations with significantly lower noise over equivalent spatial footprints than heritage sensors. This will be a significant advancement for NWP applications. However, to fully exploit this may mean that the treatment of other uncertainties will become relatively more important. An optimised exploitation of MWS data in NWP hence may require similar improvements in:

- Radiative transfer involved in the assimilation,
- Quality control,
- Treatment of systematic and random errors.

5.2.1 Radiative transfer model in NWP

An accurate and fast radiative transfer model is essential for NWP applications of MWS data, with one of the leading models being Radiative Transfer for the Television InfraRed Observation Satellite (TIROS) Operational Vertical Sounder (RTTOV), developed by the NWP-SAF (Saunders et al. 1999, Saunders et al. 2013). Developments in radiative transfer, described in section 6.2 will hence directly benefit NWP applications. Given the very significant improvements in the accuracy of NWP forecasts, developments in the underlying modelling of line characteristics, as described earlier, may well be necessary to maintain the relative importance of MWS for NWP. It is expected that the use of cloud and precipitation-affected observations in NWP centres will increase in the next few years, so better capabilities to represent effects due to clouds and hydrometeors will be particularly crucial, in synergy with developments for MWI and ICI.

An additional aspect for NWP applications is the treatment of the viewing geometry in radiative transfer. MWS combines lower instrument noise with a wider swath, larger zenith angles and hence more extreme viewing geometries compared to heritage sensors such as AMSU-A. The slanted viewing geometry is commonly neglected in NWP applications, where instead fields are spatially interpolated to a nadir-profile to calculate model equivalents. As shown by Bormann (2017), this leads to errors that are already significant for the ATMS instrument. In an assimilation system, the effect can be taken into account through appropriate interpolation along the viewing path (Bormann 2017). Additional 3D radiative transfer effects play a role in the presence of cloud and rain, and further work in this area is likely to see benefits in an all-sky assimilation context.

5.2.2 Thinning, superobbing, modelling of spatial representativeness

Instrument noise and spatial representativeness will mean that the spatial characteristics of MWS data will require some consideration. For ATMS, global NWP centres presently assimilate data that is a spatial average over several footprints, either by performing a simple averaging over 9 neighbouring footprints (so-called 3x3 averaging) or by more sophisticated averaging involving a Fourier transform (e.g. Doherty et al. 2015, Bormann et al. 2013). This averaging of footprints is also referred to as superobbing, and for ATMS the main purpose is to reduce the noise in the assimilated data. This is needed as the instrument noise for temperature-sounding channels from a single ATMS footprint is considered to be too high compared to the uncertainties in a short-range forecast from a state-of-the-art NWP system.

While MWS is expected to have a better noise performance than ATMS (when considering comparable footprints), improvements in the accuracy of short-range forecasts will mean that NWP centres are likely to nevertheless consider similar superobbing of MWS footprints. At the same time, such spatial averaging will need to be traded off against the error arising from the mismatch of the scales represented in the observations and the NWP system. With nominal spatial resolutions of global NWP models approaching 5 km in the MWS time-frame (and regional models much lower than that), some explicit modelling of the spatial footprint when calculating observation equivalents from model fields may become desirable, primarily for all-sky applications.

5.2.3 Geophysical quality control

Geophysical quality control will be needed for successful assimilation, aimed at rejecting observations that cannot be adequately represented in the assimilation system. For instance, today, many NWP systems still do not assimilate observations that are significantly affected by clouds, or observations that are significantly affected by the land surface, as in both cases the uncertainties in the respective observation operators are larger. In these cases, affected observations need to be identified and rejected.

For clear-sky assimilation, a number of methods exist to identify observations that are significantly affected by clouds (e.g. Bormann et al 2013, Bell et al. 2008), and it is expected that these will be adapted to MWS data. They aim to limit the contribution from clouds or precipitation to the observed radiances by considering differences between window channel observations against clear-sky model equivalents, empirical liquid water path retrievals (e.g. Grody et al. 2001), or scattering indices that aim to detect the presence of ice clouds. Maximum-likelihood approaches have also been developed that estimate the likelihood that a combination of channels is cloud-affected, e.g., English et al. (1999).

The new 229 GHz channel on MWS will offer new capabilities for screening cirrus clouds in a clear-sky assimilation approach (e.g. Sreerekha et al. 2008). The previously available window channels at 89 and 166 GHz show only very weak sensitivity to ice hydrometeors smaller than 200 µm, and this is not always sufficient to detect the influence of cirrus clouds in the wings of the 183 GHz water vapour line. The inclusion of the 229 GHz channel in cloud screening for clear-sky systems will therefore allow a more reliable detection. This in turn will mean reduced uncertainty in the assimilation of the 183 GHz channels, allowing more weight to be put on these observations, with possible gains in forecast impact.

Some adaptation of cloud detection methods is likely to be needed, to reflect instrument characteristics and growing accuracy demands of NWP centres. Cloud or precipitation contamination that may be tolerable for higher noise instruments such as AMSU-A may need to be taken into account for MWS, either through quality control or through an appropriate treatment of the associated uncertainty in the observation error assignment.

As mentioned earlier, all-sky assimilation of microwave data is currently becoming more wide-spread and is expected to become standard at many NWP centres in the MWS time-frame (e.g. Geer et al. 2014). This makes the detection of cloud or rain-affected observations obsolete. However, some cloud-related quality control may still be necessary, for instance, for regions in which the model clouds show too large deficiencies. This is for instance presently done at ECMWF for cold-air outbreak regions which are currently rejected (Lonitz and Geer 2015).

5.2.4 Treatment of systematic and random errors related to observations

The precision requirements for the microwave temperature sounding channels are very stringent, bearing in mind that the precision of short-range forecasts from NWP systems is expected to be, on average, well below 0.1 K for most tropospheric channels in the MWS time-frame. If other systematic errors are present, they will need to be treated separately during the assimilation, as they will otherwise lead to significant degradations. Such systematic errors can arise, for instance, from the data processing, the instrument characterisation, or the radiative transfer model used for the assimilation.

Today's NWP systems are capable of handling systematic errors whose structures are stable or vary only very slowly in time. Correction of such biases is normally achieved through an appropriate model of the systematic error. The free parameters of this model are evaluated either during the assimilation, or based on statistics of differences between observations and model equivalents (see Auligné et al. 2007 and references therein). Nevertheless, the identification and correction of systematic errors introduces extra uncertainty that can limit the impact of the observations. This is expected to become increasingly important as the precision of short-range forecasts from NWP centres is increasing. The presence of systematic errors should therefore be limited at source as far as practical.

An effort has been made as part of the instrument specification to limit systematic errors in MWS observations, and to limit these errors to be slowly varying. A number of innovations are foreseen as part of the pre-launch instrument characterisation, for instance, through very accurate antenna pattern treatments or the provision of detailed measured spectral response functions. To further reduce systematic errors arising from radiative transfer, additional developments may become necessary as outlined in section 6.2.

Random observational uncertainties need to be taken into account during the assimilation by assigning an observation error for each observation. This needs to take into account the uncertainty inherent in the observations (e.g. instrument noise), but also the uncertainty in the modelling of these observations (e.g. from a radiative transfer model). The assigned observation error should hence reflect the situation-dependent uncertainty, for instance, arising from surface sensitivity or neglected clouds. For current microwave temperature-sounding channels in clear-sky regions, the random observational uncertainty is presently dominated by the instrument noise (Bormann and Bauer 2010), and many observation error values used currently at NWP centres reflect this. However, in the MWS time-frame the modelling of other uncertainties (e.g. from radiative transfer), including their spectral or spatial correlations, may be required. For all-sky assimilation, situation-dependent observation error assignment plays a particularly important role, as it describes the larger uncertainties involved in the presence of clouds. In many ways, the observation error assignment takes the place of geophysical quality control previously needed for clear-sky assimilation.

5.2.5 All-sky developments and coupled data assimilation

The assimilation of microwave sounder radiances in cloudy and precipitating scenes as well as in clear-sky conditions is currently a very active field of research and operational development, with significant progress, but also many open challenges (e.g. Geer et al 2018). ECMWF operationally assimilates humidity sounding radiances around 183 GHz from a range of sounders in all-sky conditions (Geer et al. 2014), as well as temperature-sounding channels around 118 GHz from the Chinese MWHS-2 instrument (Lawrence et al. 2018). Assimilation of 50-60 GHz temperature-sounding channels in all-sky conditions is being investigated (Geer et al. 2012), and NCEP is using AMSU-A observations in non-precipitating cloudy scenes operationally (Zhu et al. 2016). For global NWP, one attraction of all-sky assimilation is to infer dynamical information in meteorologically active regions around clouds in 4DVAR, and this dynamical information is crucial for translating the impact into improved medium-range forecast skill.

There are many aspects of all-sky assimilation that have not yet been fully explored, and areas with significant development potential and relevance to MWS are:

- Direct assimilation of more channels, such as the new MWS channels (see below), but also the window channels typically included for microwave sounders. These will provide better constraints on clouds;
- Better radiative transfer models, including a better treatment of 3-dimensional effects, better description of optical properties of hydrometeors, etc. (see also section 6.2)
- Better treatment of the characteristics of the representation error, either in the assignment of observational uncertainty (e.g. including correlations, dependence of different cloud situations) or as model error;
- Further developments in assimilation methodology, such as an appropriate treatment of background errors for cloud fields.

Another area that is expected to see growing attention in the MWS time-frame is the increased use of coupled data assimilation systems, that is, systems in which atmospheric models are coupled with models of other aspects of the Earth system (e.g. land surface models) and used together in assimilation systems. The approach is not unlike the move from clear-sky to all-sky assimilation, in which previously discarded or approximated observational information is instead used to infer more information on a wider range of geophysical variables in a physically consistent way. MWS offers some potential in this area, for instance, for the assimilation of information on land-surface conditions (including snow) or sea-ice. Currently, most of the emphasis in assimilation is on extracting atmospheric information from microwave sounders; information on surface conditions is partially estimated, but then discarded, through methods such as surface emissivity retrievals (Karbou et al. 2010). Systems with increased coupling to land or ocean surface schemes will offer more possibilities for extraction of additional information from surface-sensitive channels (incl. sea-ice, snow), with benefits for the extraction of atmospheric information. This is expected to be an area with substantial development in the EPS-SG time-frame (e.g. ECMWF strategy 2016-2025).

5.2.6 Use of novel MWS channels

MWS offers three additional channels that have not previously been available on heritage sensors, e.g. two lower temperature sounding channels (MWS-5 and -7) and a channel at 229 GHz. The two lower sounding channels are positioned between AMSU-A channel 4 and 5, and 5 and 6, respectively, i.e., they are sounding channels with considerable sensitivity to the surface and to clouds. They hence have the potential to provide extra information on the lower-most temperature structure of the atmosphere (e.g. Sreerekha et al. 2007), as well as clouds and some surface conditions. As there is no experience with the assimilation of these channels, approaches to use these will need to be developed. They are prime candidates for an all-sky use.

Similarly, the 229 GHz channel will provide previously unavailable information, especially on ice-clouds. As mentioned earlier, approaches have already been developed to use this for a more reliable detection of cirrus clouds for clear-sky assimilation (e.g. Sreerekha et al. 2008). In an all-sky assimilation of the MWS data, the channel offers new capabilities to distinguish between liquid and ice clouds with potential benefits for the analysis of clouds, but also dynamical features, as the channel is expected to reduce some of the ambiguities in the dynamical cloud evolution. These aspects ought to be explored in tandem with the new ICI instrument on-board EPS-SG.

The synergistic use of MWS, MWI, and ICI data in an all-sky assimilation system is so far entirely unexplored, and has the potential to be a very significant advancement over heritage polar systems. However, successful use will require substantial development in various areas, especially for the use of ICI data.

5.3 Level 2 Products

5.3.1 Total Column Water Vapour over Water

The total column water content (TCWV) is determined preferably over ice-free water surfaces. Current algorithms use mainly brightness temperatures at 23.8 GHz (MWS Channel 1) and at 31.4 GHz (MWS Channel 2) in combination with the forecasted surface temperature and wind field (not mandatory as input, but improves product quality). The retrieved TCWV constitute not only a separate product, but can also serve as useful input for a subset of cloud detection tests of VIS and IR imaging radiometers, which rely on differences in brightness temperatures of individual channels (for example, combinations of channels at 3.7 μm, 10.8 μm, and 12 μm). Figure 19 illustrates the global distribution of TCWV derived from AMSU-A onboard Metop-A measurements of eight subsequent orbits during 31. August 2008.

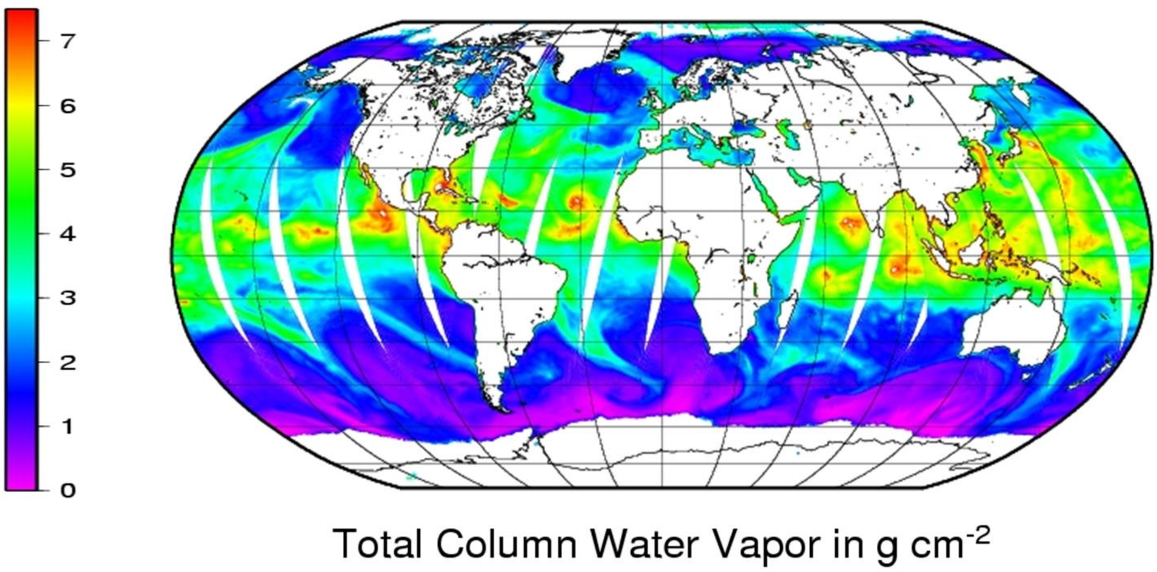

Figure 19: Total Column Water Vapor retrieved from Metop-A AMSU-A data of 31. August 2008.

5.3.2 Total Column Water Vapour over Polar Areas

Among other measurements, MWS will provide information in the microwave frequency domains currently covered by the Microwave Humidity Sounder MHS onboard Metop-A/B, and its predecessor instrument AMSU-B which has similar channel characteristics than MHS and is embarked on the NOAA KLM satellites. Therefore, after adaption and careful validation, algorithms originally developed for MHS and/or AMSU-B will also be applicable to MWS data. One example is a TCWV algorithm proposed by Melsheimer and Heygster (2008), which is used for polar areas and therefore essentially fills the gaps in TCWV not covered by the algorithm previously presented: depending on actual brightness temperature differences between channels at frequencies of 89 GHz, 157 GHz , 189±1 GHz, 189±3 GHz and 189±7 GHz (numbers of equivalent MWS channels are 17, 18, 23, 21, and 19 respectively), a scan-angle dependent regression equation is used to convert these differences into a TCWV value. The original version of the algorithm is limited to water vapour contents of up to 15 kg m^{-2} (= 1.5 g cm^{-2}) over the Arctic and 7 kg m^{-2} over Antarctica, respectively. Figure 20 shows the TCWV results derived from MHS data of eight subsequent Metop-A orbits from the 31. August 2008.

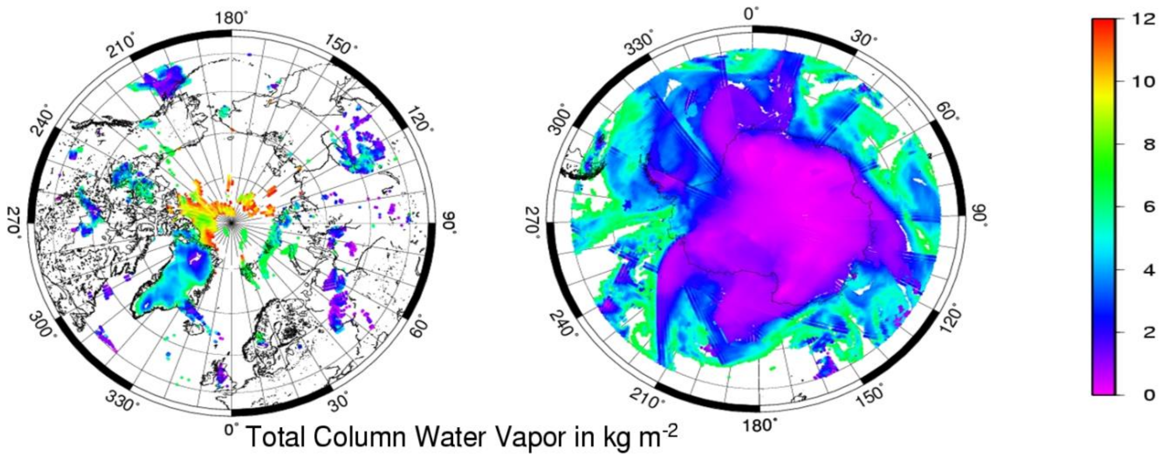

Figure 20: Total Column Water Vapour over polar areas retrieved from Metop-A MHS data of 31. August 2008.

5.3.3 Cloud Liquid Water Content over Water

Concurrent with the calculations of TCWV, the cloud liquid water content (CLW) over water surfaces can be derived from standalone microwave sounder measurements. The input data sets are the same as the ones used for the TCWV determination. Also, the equations applied to the measured brightness temperatures, have the same terms in both algorithms, but the mass absorption coefficients for the considered microwave frequencies are different. The resulting CLW's are reliable for values lower than about 0.4 mm. Figure 21 displays the results for the same Metop-A AMSU-A data, which were also used to derive the TCWV values.

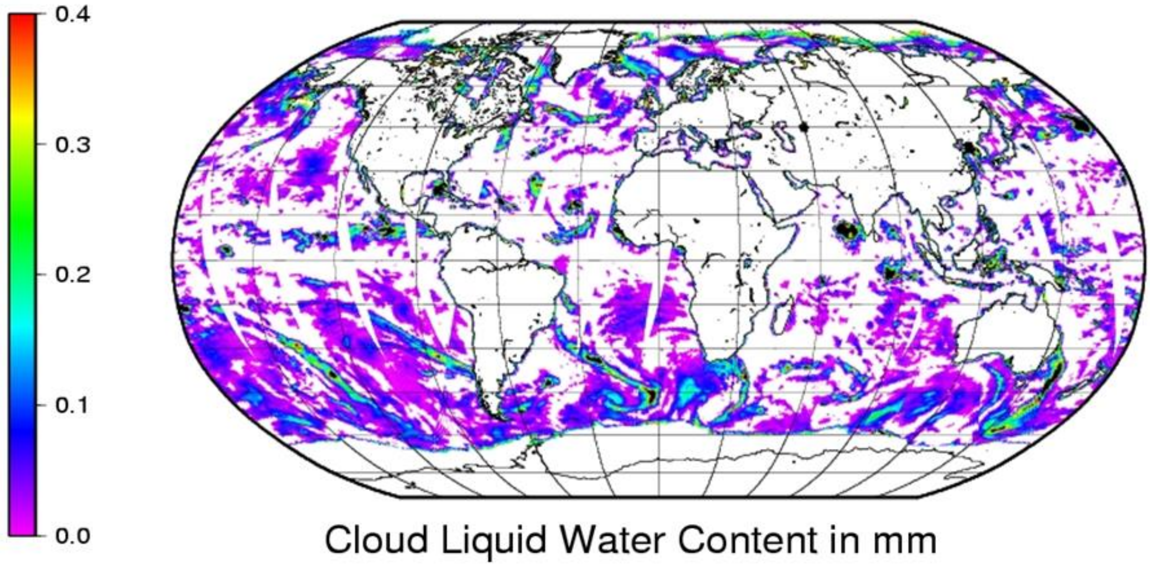

Figure 21: Cloud Liquid Water Content retrieved from Metop-A AMSU-A data of 31. August 2008

5.3.4 Sea Ice Concentration

Monitoring of sea ice under all-sky and all illumination conditions is important for both climate researchers and forecasters. The rationale of the commonly used algorithms is the determination of the scan angle dependent surface emissivity at 23 GHz using passive microwave measurements at 23.8 GHz (MWS channel 1), at 31.4 GHz (MWS channel 2), and at 50.3 GHz (MWS channel 3). The difference between the actually retrieved emissivity value and the (scan angle dependent) emissivity of water at 23 GHz is assumed to increase linearly with the sea ice concentration within the pixel. Thus, a linear equation connects a scaled actual emissivity difference with the percentage of sea ice within the measurement field of view. Figure 22 shows the retrieved sea ice extension for the Northern and the Southern polar areas on the 31. August 2008. Full data coverage of the displayed polar areas is achieved using AMSU-A data of eight subsequent Metop-A orbits, so the product can be updated in approximately 14-hour time intervals.

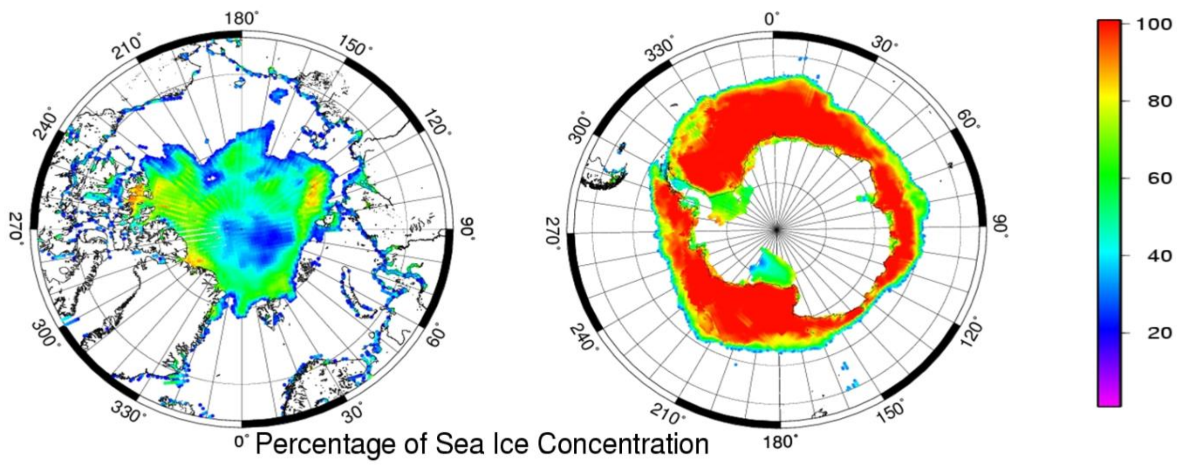

Figure 22: Sea-Ice Concentration retrieved from Metop-A AMSU-A data of 31. August 2008.

5.3.5 Rain Rates

Precipitation information can be derived from low frequency microwave emission by liquid rain droplets over water surfaces and from scattering off precipitation-sized ice particles aloft over water as well as over land surfaces. The calculation of rain rates using the scattering signal is tightly related to retrievals of cloud ice water path (IWP), which rely on the same physical phenomenon (scattering by ice particles). The IWP computations are quite complex and current algorithms rely on the simultaneous use of AMSU-A and MHS measurements. An algorithm of Zhao and Weng (2002) was originally developed for data from AMSU-A/B onboard the NOAA KLM satellite series. It depends on the surface type and estimates in a first step the cloud base height temperature from measurements at 23.8 GHz (MWS channel 1), and 31.4 GHz (MWS channel 2). In combination with brightness temperatures at 89 GHz (MWS channel 17) and at 157 GHz (approximately MWS channel 18), ice cloud scattering parameters for 89 GHz and 150 GHz are computed. This knowledge allows the derivation of an effective particle diameter and hence, the IWP and the hereto related rain rate. The reliability of the retrieved IWP values, and hence, the rain rate, depends on the outcome of several surface type checks: conditions of snow coverage, sea ice, deserts and very cold or high terrains are excluded. For these surface characteristics, no rain rate is determined. Those conditions are identified by means of terrain elevation models, climate maps and outcomes of other surface type retrievals.

Various other precipitation products based on cross-track scanning microwave sounders exist. Kidd et al. (2016) report on a Bayesian physical retrieval algorithm applied to cross-track scanning microwave sounders. Bennartz et al. (2002) describe an AMSU-B based precipitation identification algorithm for nowcasting purposes. This algorithm uses 89 GHz and 150 GHz to identify precipitation. Owing to the challenges and uncertainties associated with scattering-based precipitation retrievals, this algorithm classifies precipitation in four different intensity classes rather than providing quantitative precipitation information. Such nowcasting techniques are in particular valuable for convective precipitation but typically function less well for extended frontal precipitation events. More recently, the combination of microwave and visible and infrared observations has shown promising results in the context of convection detection and precipitation retrievals (e.g. Di Paola et al., 2012). The channels around 183 GHZ also provide information about precipitation rate (e.g. Laviola et al., 2013; Surussavadee and Staelin, 2012).

Figure 23 displays the resulting rain rate distribution derived from the same Metop-A data used to demonstrate the retrievals of TCWV and CLW. For MWS, it can be expected that the additional information from channel 24 at 229 GHz will improve the determination of the IWP and hence, the rain rate estimates.

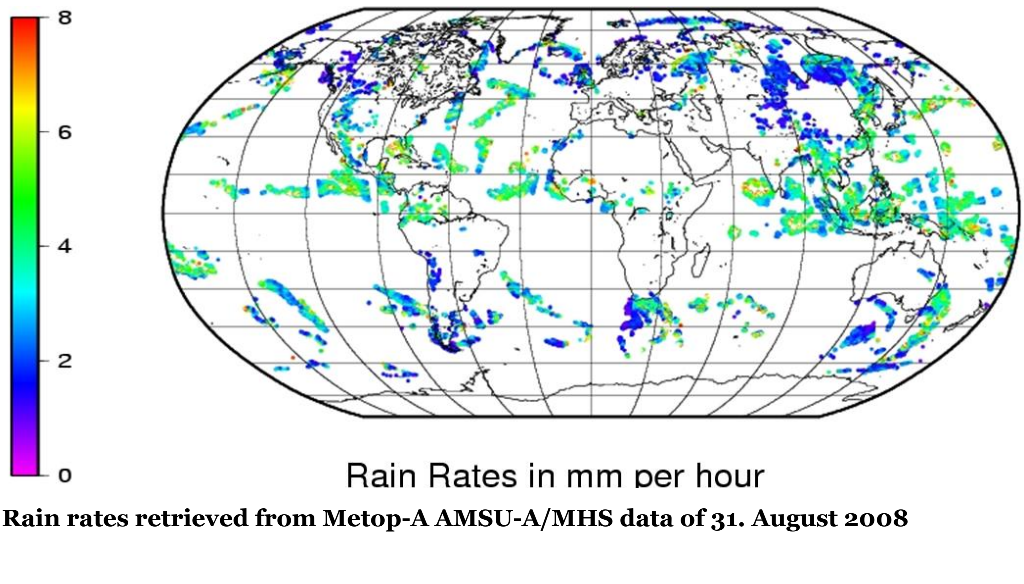

Figure 23: Rain rates retrieved from Metop-A AMSU-A/MHS data of 31. August 2008

5.3.6 Land Surface Temperature

Due to the highly variable land surface emissivities in the microwave domain, algorithms of land surface parameters which rely on regression equations only, provide already quite accurate results for a wide range of surface conditions. One problem, however, is the high temporal and spatial variability of soil moisture that has to be accounted for in the emissivity models used. The coefficients for regression equations are computed from observational data and/or results of radiative transfer models. An example is given in Figure 24, where land surface temperatures calculated from the information content of 23.8 GHz (MWS channel 1), 31.4 GHz (MWS channel 2), and 50.3 GHz (MWS channel 3) are plotted for an AMSU-A retrieval output. Only eight subsequent Metop-A orbits from the 31st August 2008 are needed to provide a good global coverage in the ice-free areas, and the surface temperature can be determined also for most cloudy conditions.

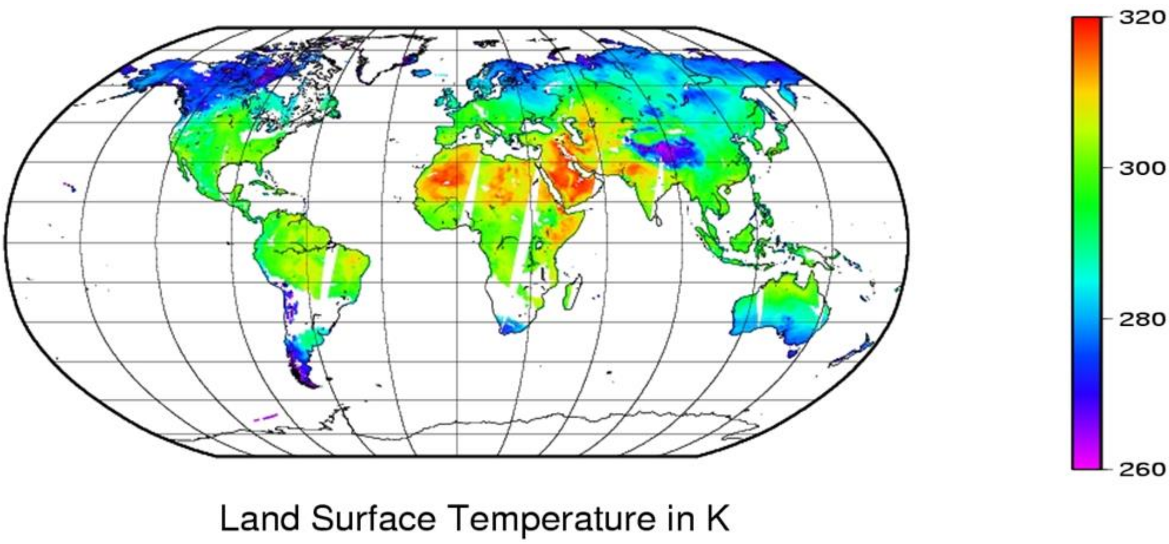

Figure 24: Retrieved land surface temperature distribution from Metop-A AMSU-A data of 31. August 2008

5.3.7 Cirrus Cloud Detection

A 229 GHz channel was added to MWS keeping in mind its sensitivity to cirrus clouds, especially those clouds consisting of ice hydrometeors which are smaller than 200 µm. The higher sensitivity as compared to the window channels at 89 GHz and 150 GHz, will be useful to give more weight to the 183 GHz observation data in data assimilation by eliminating the negative impact of undetected clouds. This will improve the humidity retrieval performance of MWS instrument.

Humidity data from an MWS-like instrument is assimilated in NWP with rather high observation errors, thus diminishing its impact on the forecasting system. Even when the instrument's radiometric performance is highly improved, the observation errors are still set high for the humidity channels. This is done to take into account the systematic errors in the forecast model and the errors associated with undetected cloud. By undetected clouds we mean the thick cirrus clouds which have a significant impact on the brightness temperature of humidity channels, especially those that are peaking in the mid to lower troposphere.

In clear-sky microwave radiance assimilation, cloud affected radiances are removed by cloud detection algorithms. In the case of thick cirrus clouds, very often such algorithms tend to reject good data. This is mainly because the cloud detection algorithms are stringent not to allow cloudy observations into the system. But this leaves the data assimilation system with fewer clear-sky observations assigned with high observation errors leading to minimal impact on forecast. The study by Sreerekha et al. (2007) shows that the screening of undetected clouds using 229 GHz rather than using the 150 GHz channel does not lead to an excessive false alarm rate, so most cloud-free data can still be used. Possibilities are there to devise more effective cloud detection algorithms than the simple algorithm used in the above study. With the better cloud detection skill of 229 GHz channel, the observations can be treated as more trustworthy thus leading to lower observation errors and significant impact from the humidity channels of MWS.

In the context of all-sky assimilation, the observations at 229 GHz can be useful in classifying cloud type into liquid and ice. This will be more useful over land surfaces. Currently over land a scattering index based on frequencies close to 90 GHz and 150 GHz is used as a symmetric predictor for the observation error modelling. As the 229 GHz channel becomes available, a scattering index method based on 229 GHz could prove more efficient in discriminating ice and liquid clouds. A method to retrieve IWP from 229 GHz and another channel sensitive to cirrus clouds (e.g. 165 GHz) can fill the gap to provide this important microphysical variable for the forward modelling of humidity channels sensitive to cirrus clouds.

The use of 229 GHz presents challenges as this is the first time a channel having a frequency higher than 190 GHz is part of a cross-track sounding instrument. The radiative transfer modelling of this channel has to overcome the constraints related to water vapour continuum absorption, scattering of ice clouds, and surface emissivity. A synergy with the ICI instrument for validation of radiative transfer modelling for this channel will be useful, although there are constraints related to being on different platforms and instruments having different scanning geometries.

5.3.8 Snow, Sea ice monitoring

Snow plays a key role in global energy and mass budgets but monitoring its extent and quantifying its water equivalent paradoxically remains a major scientific challenge. The complex natural spatial and temporal variability of snow, the imperfect knowledge of snow physics, the scarcity of in-situ observations, are among the possible reasons for this.

The snow water equivalent (SWE) is the water content of the snow if the snowpack melts instantly, and corresponds to the total water mass per unit surface area. SWE can also be viewed as the product of snow depth by the snowpack bulk density and is a key variable of the surface water budget at various spatial and temporal scales, with large fields of applications including land surface hydrology and numerical weather prediction.

Several methods are currently used to provide daily SWE estimates at the global scale among which one could cite spatial interpolations of in-situ measurements, empirical formulas applied to remote sensing measurements and assimilation techniques that combine a priori information from physically-based models and heterogeneous observations of SWE (synoptic and remote sensing data). So far, most of the studies undertaken to estimate SWE values from remote sensing passive microwave measurements are based upon the use of the brightness temperature (Tb) difference between two frequencies, namely between a frequency in the range of 31-37 GHz at which the electromagnetic signal is scattered by snow crystals and another frequency in the range of 19-22 GHz considered insensitive to snow. In the most well-known study, Chang et al. (1987) have proposed a linear fit formula using Tbs at 18 and 37 GHz assuming a constant density of snow (300 kg m^{-3}). This method has been widely used thereafter to derive SWE from microwave measurements, despite a number of critical views on its performance compared to in-situ measurements. The performance of the Chang et al. algorithm, in terms of mean values and spatial variability, can vary considerably and appears to depend on snow physical characteristics (see for instance Davenport et al. (2012), Armstrong and Brodzik (2000), Pardé et al. (2007) among many others). Data merging techniques, such as variational assimilation, are increasingly favoured since they can overcome the low density of in-situ measurements. Pulliainen (2006) proposed an assimilation tool that combines information from passive microwave data (18 and 37 GHz) and snow depth measurements from the synoptic ground station network. Within this scheme, snow depth in-situ measurements are used to feed the semi-empirical Helsinki University of Technology (HUT) snow emission model (Pulliainen et al. 1999), which uses a one-layer snowpack description (depth, density and grain size) to provide simulated Tbs. These TBs are then compared to satellite observations (e.g. from SSM/I or AMSR-E) near synoptic stations to fit the model estimations by updating effective snow grain size values.

These methods of estimating SWE led to some operational products such as the EUMETSAT HSAF SWE product (http://hsaf.meteoam.it/snow.php), the ESA Globsnow SWE product (Luojus et al. 2010), and NSIDC estimates (Tedesco et al. 2004). Other methods have been proposed to produce estimates of SWE for Numerical Weather Prediction models. Drusch et al. (2004) describes an Optimal Interpolation (OI) method used at the European Centre for Medium range Forecast (ECMWF) to analyse the snow depth by assimilating observations from synoptic stations combined with the NOAA/NESDIS snow cover extent. Lower frequency channel observations from the MWS instrument are sensitive to snow properties and could be used in several snow analysis algorithms to improve the analysis products.

MWS observations are also relevant for sea ice studies. Over the sea ice, several processes occur including emission/absorption phenomena by water, sea ice and snow; scattering phenomena by brine/air inclusions and by snow grains; reflection phenomena at interfaces between snow/ice layers. In addition, melting conditions can strongly impact the electromagnetic signal. Several sea ice products exist such as the EUMETSAT Ocean and Sea Ice Satellite Application Facility product (OSISAF, noted OSISAF hereafter). The OSISAF sea ice types are daily available over Polar Regions and rely on algorithms using SSM/I measurements at 19, 37 and 85 GHz. A gradient ratio (GR) is defined between 19 and 37 GHz and a horizontal/vertical polarization ratio (PR) at 19 and 85 GHz are used as indicators to discriminate ice-free (open water), multiyear (MY) and first year ice (FY). In addition, sea ice age from the National Snow and Sea Ice Data Center (noted NSIDC hereafter) is provided daily over Polar regions and derived from a combination of passive microwave brightness temperatures from SSMIS and AMSR-E.

Figure 25 shows daily surface emissivity variability at 89 GHz over the Northern Hemisphere. The emissivity map can be directly compared with the corresponding OSISAF sea ice age products. One could note that emissivity varies according to the sea ice type and that it shows a much larger variability within a selected sea ice type class. MWS surface sensitive observations could be used to detect ice / no ice region and also to infer sea ice age (Hermozo et al. 2016).

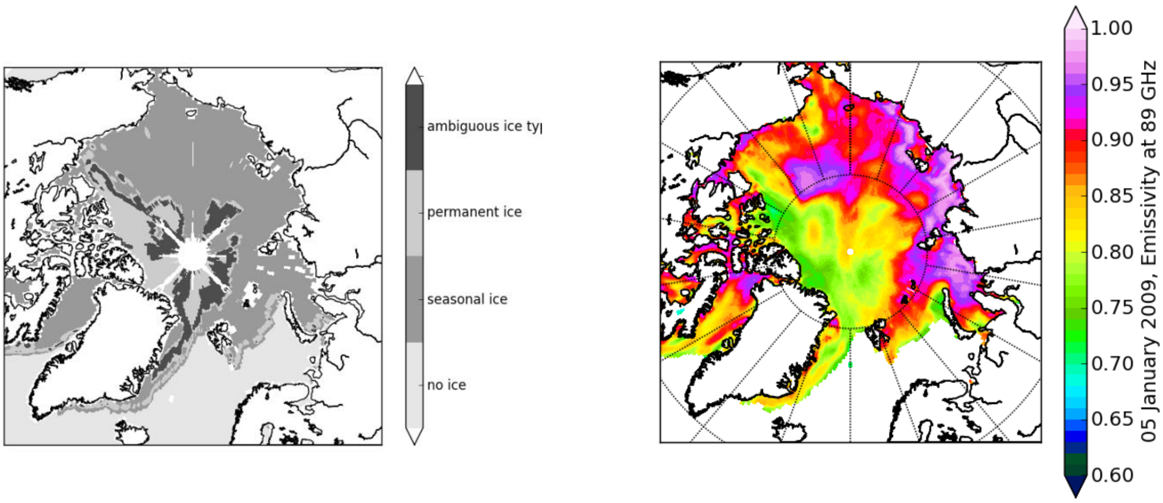

Figure 25: Left: Sea ice types from OSISAF for the Northern Hemisphere for January 5th 2009. Right: daily surface emissivity at 89 GHz computed for the same day.

5.3.9 Rainfall, Soil moisture

Rainfall is a key parameter for meteorology, hydrology and climate, for which many studies have been conducted to derive useful information about precipitation occurrences and rates (hourly, daily or monthly) using MWS like passive microwave sensors. The majority of these studies were conducted using data over ocean surfaces (for which surface emissivities are at least a factor of two smaller than those of land surfaces). Grody et al. (2001) developed an algorithm to retrieve the total precipitable water and the cloud liquid water over oceans from AMSU data. Hilburn and Wentz (2008) retrieved ocean rain products from SSM/I, AMSR- E and Tropical Rainfall Measuring Mission (TRMM) Microwave Imager (TMI). Claud et al. (1991) used SSM/I to retrieve the integrated water vapour content and the surface wind speed. For land surfaces, Ferraro et al. (2004) developed a statistical-physical model to retrieve surface and atmospheric parameters from AMSU measurements over ocean and land surfaces using some a priori information about land surface emissivity and ice water paths. Defer et al. (2008) proposed a rain classification from microwave measurements using physically based cloud and radiative transfer models. A statistical relationship between rain rates and brightness temperatures has then been derived and used to compute probabilities for a given observation to correspond to some predefined precipitation classes. Di Tomaso et al. (2009) developed an algorithm for precipitation estimation from AMSU-B measurements using radiative transfer simulations to infer a precipitation rate over both land and sea surfaces. The use of land surface emissivity instead of brightness temperatures have scarcely been used for rain rates retrieval in previous studies, except for monitoring inundated surfaces (Prigent et al. (2001)).

Birman et al. (2015) showed that it is possible to use land surface emissivities at frequencies close to 89 GHz to detect rainfall occurrences over land (using AMSU-A/-B and SSMI/S).The method is based on the use of daily surface emissivities to detect rain events according to the strong negative correlation between rain events and daily estimates of surface emissivity from several microwave window channels. Figure 26 (from Birman et al. 2015) shows daily time series of rain gauge data (from January to December 2010 near a station located in the south-western part of France) and of surface emissivity at 31GHz (from AMSU-A), 89GHz (from AMSU-B), and 150GHz (from AMSU-B). For a specific location, the surface emissivity varies in time and frequency as well as with surface conditions (vegetation, moisture, rainfall). Strong correlations can be observed: a systematic decrease of the emissivity occurs for rainy days. For instance, an increase in precipitation early June is associated with more than 5% of decrease of the emissivity at 89 GHz. The emissivity sensitivity to rain can be best highlighted by removing mean values from emissivity timeseries: days with no or light rain are associated with very small emissivity departures from mean values. Correlations between emissivity and rain rate were found larger at 89 GHz. At lower frequencies, it was harder to observe a clear relationship between emissivity and rainfall. MWS channels (frequencies from 23 GHz to 150 GHz) would be very useful for monitoring rainfall over all surfaces using the emissivity method or other statistical/physical algorithms. The obtained products would complement other existing rainfall databases such as TRMM, CMORPH, etc.

Regarding soil moisture, Calvet et al. (2011) investigated the sensitivity of passive microwave observations at various frequencies, from 1.4 to 90 GHz, to both surface soil moisture and vegetation water content. L-band observations were found to be very sensitive to soil moisture and higher frequencies tend to be more sensitive to vegetation water content than to soil moisture. However, multi-angular observations permit to achieve a moderate sensitivity to soil moisture at higher frequencies. MWS channels can be integrated into surface property retrieval methods, making use of the potential synergy with other instruments (including scatterometer data and other active measurements such as Sentinel-1 and L-band radiometers).

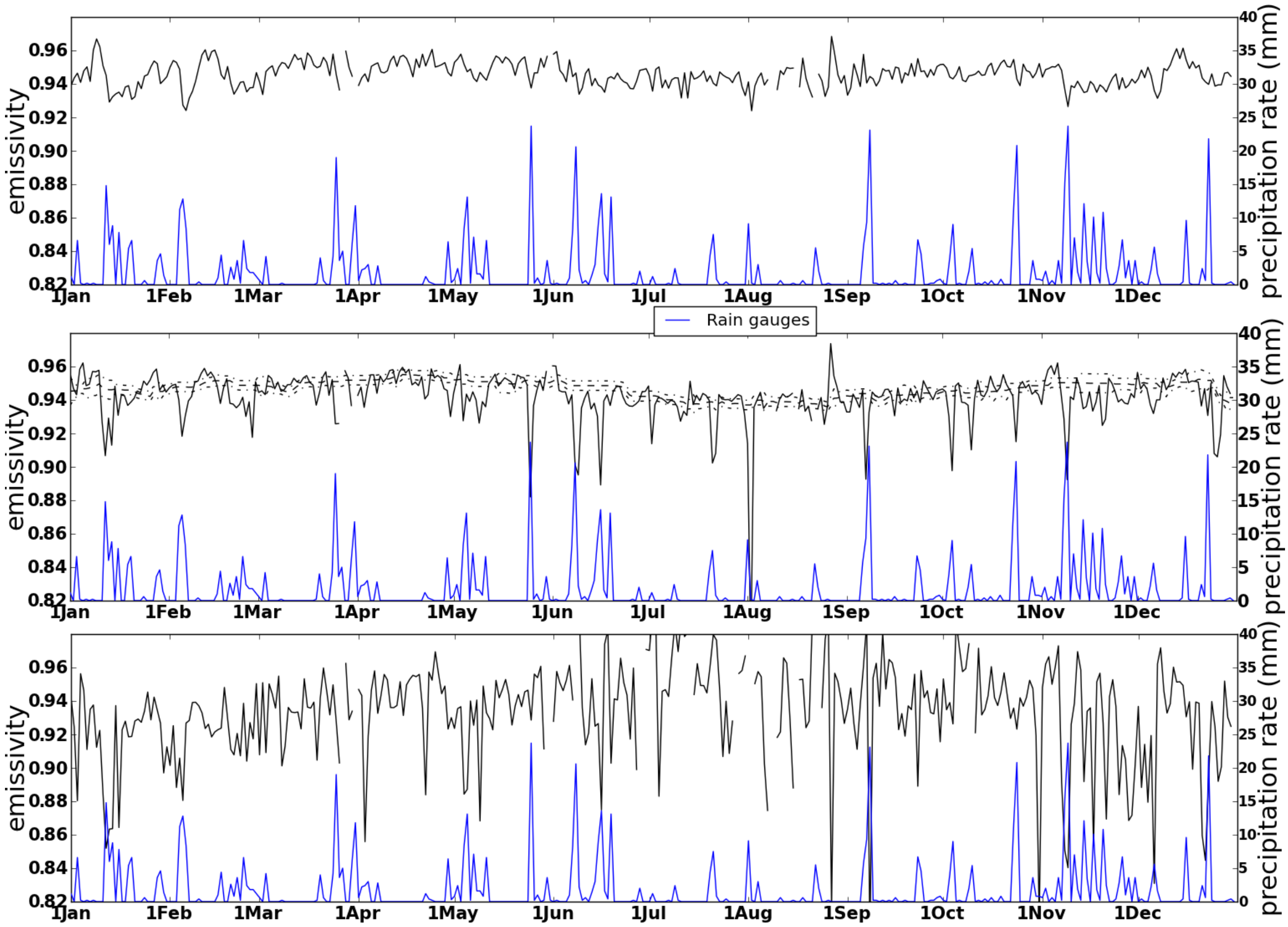

Figure 26: Time series of daily rain rates (blue line) and daily emissivities (black line) at (top) 31 GHz from AMSU-A, (middle) 89 GHz from AMSU-B, and (bottom) 150 GHz from AMSU-B over 1 yr near Agen, France. In the middle panel, the black dashed line represents a dynamic mean dry emissivity. From Birman et al., 2015.

5.4 Product Monitoring

5.4.1 Monitoring of instrument parameters

Monitoring of instrument parameters is an essential activity for both the users of the data and the satellite operators. It is strongly recommended that monitoring data are available on-line to users of MWS, and that the resource covers the entire lifetime of the instrument. The data are useful for near-real-time monitoring (e.g. operational NWP) and for historic studies (e.g. climate). For example, see the NOAA/STAR monitoring resource at: http://www.star.nesdis.noaa.gov/icvs/InstrPerfMonitoring.php.

The following parameters are proposed for MWS near-real time monitoring:

- Time series of warm and cold calibration counts for all channels;
- Time series of OBCT temperatures;
- Time series of instrument gain (all channels) and temperature;
- Time series of striping index for all channels;
- Time series of telemetry relevant for higher level processing. For example, this should include mirror temperature, the status of the scan motor and other parameters helping to detect and monitor any unexpected instrument behaviour;
- Global brightness temperature maps of all channels showing data coverage;
- Time series of NEΔT for all channels;
- Time series of lunar intrusion in space view counts (beam width dependant);
- Time series of data quality flags that are output from the L0 and L1 product processing;
- GSICS inter-calibration products (optional).

By default, all time series should be depicted as 'All Time', '1 Year', '30 days', and '24 Hours'. In addition, it is desirable that the monitoring period is user-configurable by just indicating start time and end time. In particular, displaying shorter periods is considered useful, e.g. in order to spot out orbital variations. To see even more details, a zooming user interface is recommended.

Provided that those monitoring tools are also developed for other EPS-SG instruments, they should be harmonised across instruments as far as possible.

The most important specific instrument parameters for monitoring MWS are presented in more detail below.

5.4.1.1 NEΔT

As mentioned in section 3.2.3, a key instrument parameter for users is the NEΔT for each channel. In orbit, the NEΔT can be computed from the variability of the cold and warm calibration views. There are a number of methods that have been used in the past to do this, see Atkinson (2015). One method is the Allan Deviation method proposed by Tian et al. (2015), and used operationally at NOAA, which analyses the differences between successive scans. However, as shown by Atkinson (2015) this method does not fully account for calibration noise and 1/f noise. Instead, it is suggested to analyse the variability of the differences between each calibration sample and the smoothed, scan-averaged calibration counts, where the scan-to-scan smoothing *excludes the line being analysed*. This differs slightly from the normal calibration procedure. In other words, compute the standard deviation of $\left(C_W - \overline{C_W}\right)/G$, where C_W are the warm calibration counts and G is the channel gain (counts per K). The number of scan lines used in the averaging of C_W will be of order 6 (the central line is not used). It should be similar to the number used in the operational calibration algorithm (section 3.2.3).

The number of scans used to compute the standard deviation is not critical, but the more scan lines are used the more accurate will be the result. It could be a whole orbit, a granule or a rolling standard deviation over a rather small number of lines (as in EUMETSAT's AMSU/MHS scheme). In the latter case, an overall NEΔT can be computed from the root-sum-square of the individual NEΔT estimates.

Using the same method, it is possible to estimate the effective NEΔT for a spatially-averaged scene (e.g. 3×3, see section 3.2.3). Instead of excluding just one scan in computing $\overline{C_W}$ we exclude the central three scans, and average 3×3 warm view samples before taking the difference from $\overline{C_W}$. This ensures that the effect of 1/f noise is allowed for.

5.4.1.2 Calibration view counts

Time series plots of warm and cold calibration counts are valuable for identifying instrument effects such as:

- Sudden changes of gain or offset;
- Lunar intrusion into the space view;
- If calibration counts drift outside the normal limits.

It is useful to be able to display plots on both short timescales (e.g. every scan for one orbit) and long timescales (e.g. orbital means, after rejection of outliers).

5.4.1.3 Striping index

Although the ratio of 3×3 NEΔT to single-sample NEΔT is related to striping (section 3.2.3), it is also useful to compute a more direct striping index (Atkinson, 2014). For MWS, this can be defined as:

$$r = \sqrt{\overline{\sigma_{AT}^2} \Big/ \overline{\sigma_{CT}^2}} \qquad (17)$$

where σ_{AT} is the along-track standard deviation of a 5×5 box of calibration samples (i.e. the standard deviation after averaging in the cross-track direction) and σ_{CT} is the cross-track standard deviation (after averaging in the along-track direction). A large number of 5×5 boxes are used (e.g. one granule or one orbit). The striping index is expected to vary between 1.0 (no striping) and around 2.0 (found for ATMS channel 16).

5.4.1.4 Instrument Temperature

The instrument temperature is often found to be correlated with NWP bias. In some cases this is thought to be related to local oscillator drift (e.g. AMSU-A channels that are not phase-locked), while in other cases the cause is not known (e.g. biases in MWHS-2). The instrument temperature can exhibit both short-term (within an orbit) and long-term (seasonal) variations. A representative temperature should be reported in the level 1 data files (for use as a bias predictor in NWP), and time series plots of different receiver components should be available on-line.

5.4.2 Monitoring of Level 1 data against NWP fields

Another essential component of product monitoring will be comparisons of Level 1 radiances against observation equivalents calculated from NWP data. Short-range forecasts from global NWP systems provide a reference with stable characteristics and comparatively high precision, allowing the detection of relatively small anomalies or changes in the data characteristics. This high precision is ensured through combining the strengths of a wide range of observation types assimilated in the NWP systems, and global circulation model arguably provide the most reliable reference that is available for every observation all the time. In addition, NWP systems allow cross-comparisons to other similar observations available at the time, without the need to collocate the data.

Assessment of the MWS observations against NWP data will form an integral part of the post-launch calibration/validation exercise, as well as the routine monitoring of the data in the operational phase. Such assessments contribute to establishing the quality of the data, as well as characterising any anomalies that may exist. Examples where such monitoring has in the past provided valuable insights during the calibration/validation phase are, for instance, the detection of reflector emission signatures and calibration anomalies for SSMIS (Bell et al. 2008), the suggestion of post-launch pass-band shifts for MWTS, AMSU-A, and MSU (Lu and Bell 2014, Lu et al. 2011), or the detection of striping noise in ATMS data (Bormann et al. 2013). Methods developed as part of the Horizon 2020 GAIA-CLIM project to use ground-based reference observations in combination with NWP lead to enhanced traceability of the NWP comparisons, with benefits for the interpretation of NWP-based calibration/validation information. Continuous routine monitoring against NWP data after the calibration/validation phase will be essential to establish any changes in the data characteristics over time.

As an NWP forecast is likely to be available for other EPS-SG processing, the monitoring against NWP data could be performed at EUMETSAT in addition to the instrument monitoring described above. Such an integrated monitoring against an external reference has been included in the FY-3C monitoring at CMA. Such an approach has a number of advantages, as the instrument monitoring together with the NWP monitoring complement each other and aid the detection and attribution of any changes in the data characteristics. Monitoring against NWP data will of course be performed by NWP centres as part of the routine use of the data.

The monitoring against NWP data should consist of a graphical display of a number of statistics derived from differences between observation and model equivalents (so-called “departures”). This should include, as a minimum, per-channel time-series of global standard deviations of departures, mean departures before and after any bias correction that might be applied, and the number of considered observations. These time-series could be confined to the last 30 days, or, could cover similar different time-scales as the monitoring of instrument parameters described above. These time-series will be primarily used to assess the stability of the provided data. To allow investigations of local effects, geographical maps of departures should also be provided, accumulated to means and standard deviations over longer periods of three weeks to a month. Monitoring of other characteristics could be considered, such as the monitoring of scan-dependent statistics.

5.4.3 User notification

It is important that user notification forms an integral part of the provision of MWS data, continuing the reliable User Notification Service available with the first generation of EPS. User notification includes:

- Advanced warnings for all planned instrument, satellite or processing changes or outages with some potential user impact;

- Swift notification of users when an unexpected anomaly has been detected in the instrument monitoring, even when the origin of the anomaly has not yet been understood;
- Updates about anomalies as they get investigated and root-causes become clearer. Such notifications should be made easily accessible (e.g. through an online tool), but also through alerts that are sent to subscribed recipients.

As extension to the User Notification Service, we recommend the setup of a searchable database that records events that affect the MWS data over the life-time of the instrument. Such a database would be particularly useful for climate or reanalysis applications, but it would also assist any *a priori* evaluation of data quality.

5.5 Synergy with other instruments

5.5.1 Instruments on the same platform

As stated in section 1, MWS will share the Metop-SG-A platform with IASI-NG, MetImage, 3MI, Sentinel-5 and RO. It is common practice in pre-processing software, such as the ATOVS AVHRR Preprocessing Package (AAPP, Labrot et al., 2011), to create "Level 1d" products in which one instrument is mapped to the sampling grid of another. For example:

- AMSU mapped to HIRS, e.g. used in the International ATOVS Processing Package (IAPP, Li et al., 2000)
- AMSU mapped to IASI; the AMSU assists with cloud detection
- VIIRS mapped to the Cross-track Infrared Sounder (CrIS) or the Advanced Very High Resolution Radiometer (AVHRR) to IASI, giving information about the uniformity of the sounder field of view, particularly cloud variability.

Some NWP centres assimilate these mapped radiances in the context of a 1D-VAR processing step (e.g. Harris et al., 2004, Eyre et al., 1993). Other centres assimilate the sounder instruments separately in 4D-VAR.

For Metop-SG, it is envisaged that some centres will have a requirement to map MWS and MetImage to IASI-NG. This is a reasonably straightforward process, because the instruments are closely aligned. Note that the actual scan pattern of MWS is not expected to be synchronised to that of IASI-NG (unlike AMSU/IASI), so the mapping software will have to make use of the latitude/longitude values during the mapping process (as is already done in AAPP for FY-3 sounders). An example of the different areas of coverage of simultaneous measurements of IASI-NG and MWS, respectively, is illustrated in Figure 27. For MWS, the footprint sizes of channels 17 to 24 (about 17 km diameter at nadir) are shown. It is obvious that for whole swath, there is no synchronisation between the scan patterns. In addition, the scan durations of 15.6 seconds for IASI-NG, and 2.254 seconds for MWS do not provide a high repetition rate of the pixel colocation pattern. Hence, a mapping tool cannot rely solely on scan times and quasi-static look-up tables, but must be continuously adapted to the actual pixel geolocation.

We do not envisage a requirement to map directly between the MWS and the other instruments on Metop-SG-A.

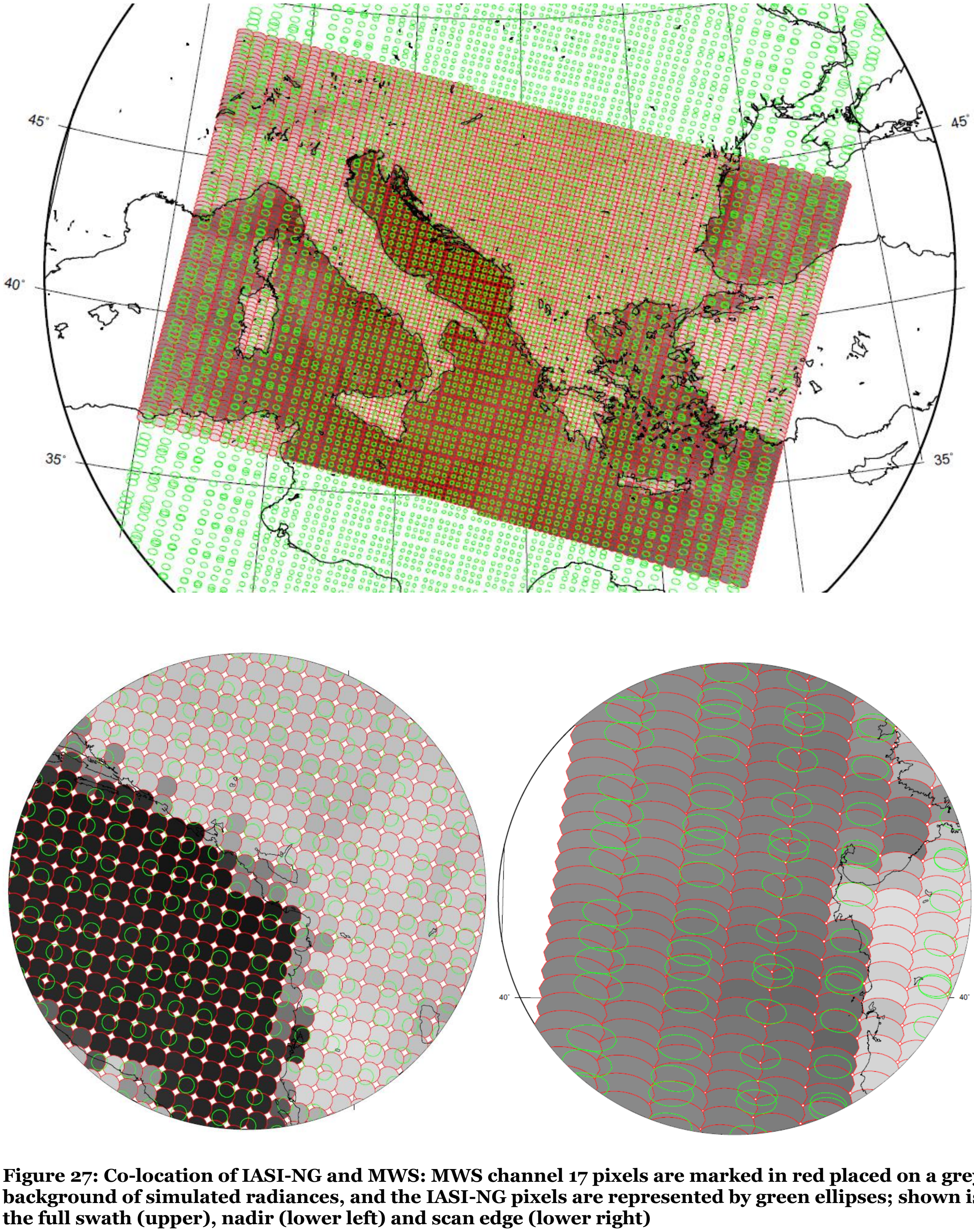

Figure 27: Co-location of IASI-NG and MWS: MWS channel 17 pixels are marked in red placed on a grey background of simulated radiances, and the IASI-NG pixels are represented by green ellipses; shown is the full swath (upper), nadir (lower left) and scan edge (lower right)

5.5.2 Instruments on different LEO platforms

There are strong synergies between MWS on Metop-SG-A and the MWI and ICI microwave imagers on Metop-SG-B. For example:

- Shared channels at 23.8, 31.4, 50-54, 89, 165, 183 GHz
- MWS high-frequency channels provide information on ice cloud, which is the primary focus of ICI.

Together, the three instruments will allow unprecedented characterisation of cloud and rain hydrometeors from microwave frequencies, covering heavy rain to small ice particles. This will allow significant synergies, for instance in the separation between liquid and ice hydrometeors. Successful exploitation of this synergy is likely to be one of the key challenges in applications of EPS-SG data, with strong potential, for instance, in all-sky assimilation, but also for development of improved model cloud parameterisations.

The Metop-SG-A and -B satellites will be nominally in the same orbit, in terms of local equator crossing time, but there will be a time difference of a half-orbit corresponding to about 51 minutes, which should be taken into account. NWP systems provide a natural framework to account for this.

Although the microwave sounder and imagers have different viewing geometries (in terms of zenith angle and footprint size), the differences can be accounted for within RT modelling. The shared channels can therefore provide an indication of calibration accuracy.

The dual-polarisation capability of the microwave imagers could be used to interpret the QV and QH mixed polarisations in the sounder. Also, the impact of channel failure could perhaps be mitigated.

Note that MWS has a wider swath than either MWI or ICI, so has the potential to fill in the gaps between successive swaths in imagery. Imagery from microwave imagers and sounders is particularly valuable for hurricane monitoring, providing information from deep inside the cloud and precipitation structures (e.g. Zhu and Weng, 2013).

5.5.3 Synergies with instruments on geostationary platforms

Currently there are no microwave radiometers operating in geostationary orbit, though this may change in the time frame of EPS-SG. Microwave radiometers in LEO provide information on vertical temperature and humidity structures in both clear and cloudy areas, but infrequently in time. Whereas the geostationary IR sensors provide high timeliness (10 minutes repeat cycle for full-disk FCI imagery on MTG-I satellites) but with limited vertical discrimination. There is value in combining the two.

One obvious way to combine information from the different sensors is via NWP, as discussed previously.

Another way is via Level 3 products from systems like NASA's (GPM) Integrated Multi-Satellite Retrievals for the Global Precipitation Mission (GPM IMERG) facility. According to the web page https://pmm.nasa.gov/data-access/downloads/gpm: "The IMERG algorithm is intended to intercalibrate, merge, and interpolate all satellite microwave precipitation estimates, together with microwave-calibrated infrared (IR) satellite estimates, precipitation gauge analyses, and potentially other precipitation estimators at fine time and space scales for the TRMM and GPM eras over the entire globe."

At the time of writing, it is not clear for how many years the GPM program will be continuing: WMO's OSCAR database[2] gives a mission life of only 3 years for the core observatory and 5 years for

[2] https://www.wmo-sat.info/oscar/satelliteprogrammes/view/67

constellation satellites, but Draper et al. (2015) suggest that it may be up to 15 years. Nevertheless, we can say that in the EPS-SG era it is likely that there will be a continuing requirement for multi-sensor precipitation estimates, and it is recommended that MWS should be part of the mix of LEO microwave observations that are used.

6 MWS RESEARCH AND PRODUCT DEVELOPMENT NEEDS

6.1 Instrument Validation

6.1.1 Pre-launch Activities

To make effective use of a new instrument in areas such as NWP and climate, it is important to understand its characteristics in as much detail as possible. Some of them are measured during pre-launch testing by the manufacturer, motivated by the need to demonstrate that the instrument meets the required specifications. However, instrument characterisation goes far beyond the need to demonstrate conformance, and the results of such analysis have scientific value long after the launch of the instrument, especially for climate monitoring applications.

While much can be done from using the instrument radiances in NWP (e.g. Lu and Bell, 2013), NWP studies alone can only provide probable explanations for the effects that are seen. It is much better if the post-launch observations can be compared with pre-launch measurements performed under carefully controlled conditions. Therefore we make the general recommendation that:

- Pre-launch characterisation of MWS should be written up and published (e.g. in peer-review literature or as technical notes), to ensure availability for future research.

Some specific tests are considered below. It is envisaged that most (or all) of these will be conducted for MWS.

6.1.1.1 Thermal vacuum calibration using precision calibration targets

Thermal vacuum test results for AMSU-B are described in Saunders et al. (1996). Measurements included:

- Bias determination as a function of scene temperature, related to receiver nonlinearity and internal target accuracy (see Figure 28);
- Cold bias as a function of scan angle, related to mirror reflectivity and the dependence of the reflectivity on polarisation (see Figure 28);
- NEΔT as a function of instrument temperature and scene temperature;
- Power spectrum for each channel. This can be from (i) normal scanning using just the calibration views or (ii) using the Earth views when the antenna is parked or viewing a uniform scene such as cold space (see Figure 29).

For ATMS, pre-launch cold-bias measurements were compared with the results of an in-orbit pitch-over manoeuvre (Weng and Yang, 2016) to provide valuable information on mirror reflectivity.

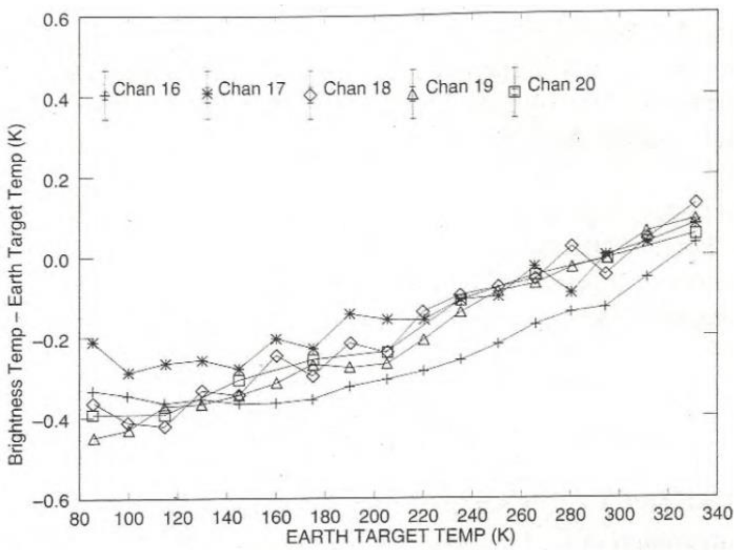

Figure 28: AMSU-B bias at Nadir as a function of scene temperature from thermal vacuum testing (from Saunders et al., 1995). The plot shows: (i) cold bias due to polarisation-dependent reflector emissivity, (ii) nonlinearity for Channel 16.

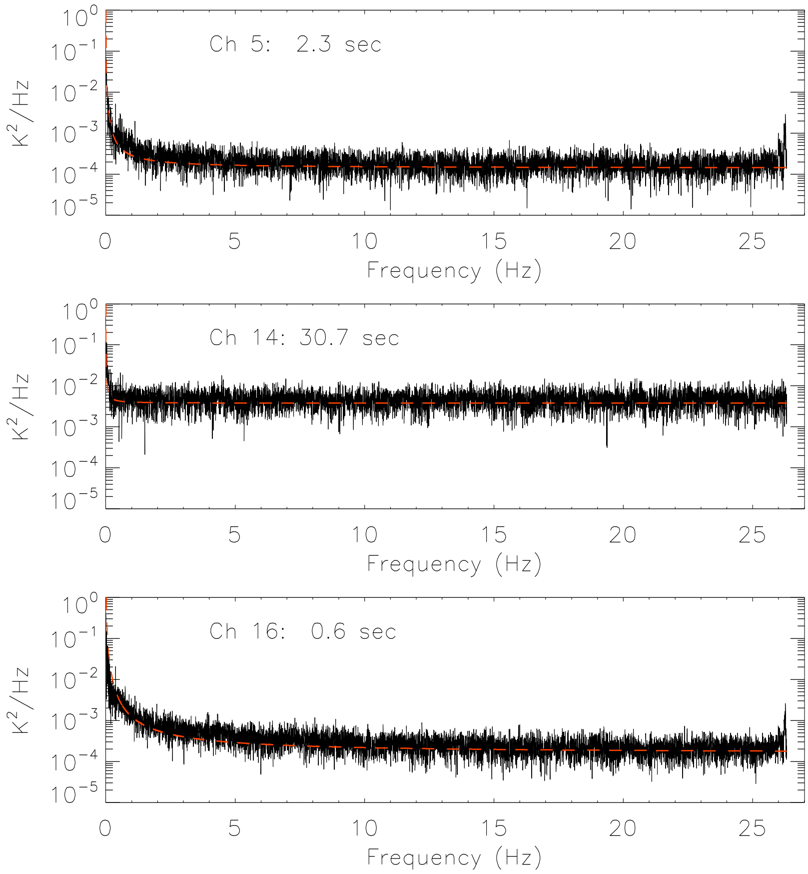

Figure 29: ATMS power spectra from Earth views during the pitchover manoeuvre on 20th Feb 2012, showing (top to bottom) a channel moderately affected by 1/f noise, a channel almost unaffected, and a channel strongly affected by 1/f noise. The red dashed line shows a best fit when the noise is modelled as the sum of random noise and 1/f noise, and the printed times are the timescales at which the two noise components are equal. From Atkinson (2014).

6.1.1.2 Local oscillator frequency monitoring

For AMSU-B, the local oscillator frequencies were measured *under vacuum* as a function of oscillator temperature. Cavity-stabilised oscillators run at different frequencies in air and in vacuum (about 15 MHz in the case of AMSU-B). Unfortunately the results were only written up in an internal technical note, which appears to have been subsequently lost.

For AMSU-A, the local oscillator frequencies and their temperature dependence were measured (presumably in air) and reported in the manufacturer's End Item Data Pack.

It is valuable to compare these pre-launch measurements with NWP-based analysis. For example, AMSU-A channel 6 on NOAA-15 showed little dependence on instrument temperature pre-launch, but appeared to show a much stronger dependence as the instrument aged (Met Office study from 2005).

Since MWS will have phase-locked oscillators, it is possible that the type of monitoring described here will not be applicable.

6.1.1.3 Cross-channel interference

In AMSU-B, an interference mode was identified whereby a harmonic of 89 GHz local oscillator was emitted from the feedhorn, reflected off the calibration target and affected the signal at 183±7 GHz (causing the four space-view samples to have systematic offsets). This could be easily identified by switching off the 89 GHz channel and observing the effect on the other channel.

For the MWTS-2 instrument on FY-3C, a rather different issue was observed: the brightness temperature in several upper-tropospheric sounding channels appeared to depend on the signal in a window channel. An effect like this would not be detectable in standard thermal vacuum testing because in thermal vacuum all channels view the same target. The effect is only apparent when the different channels view *different* brightness temperatures, which is hard to simulate on the ground. It would require special tests on the receiver. Some tests of this nature are planned for MWS in order to give confidence that such effect will not occur.

6.1.1.4 EMC testing

Electromagnetic compatibility testing is performed as a matter of course by the manufacturer, but results are not usually made available. This assumed great significance with AMSU-B, where the first flight instrument passed the ground testing but was found in space to be highly susceptible to emissions from spacecraft transmitters.

6.1.1.5 Antenna pattern determination

Antenna pattern is usually measured in a compact test range. Although comprehensive measurements are made, the challenge is to summarize those measurements in a form that is useful to users (Mo, 1999). Typical outputs include the 3dB beam width of each channel and the efficiencies (fraction of incident power originating from within a specified solid angle). This information is needed if the user wants to use signal processing techniques to manipulate the beam width of one channel in order to match the beam with of another (Atkinson, 2011). It is also needed for accurate estimation of the space-view calibration offset and the Earth-view corrections.

It is important to measure the cross-polarisation sensitivity of each channel, as this can cause a scan-dependent bias in orbit (ocean emissivity depends strongly on polarisation). Also, a twist in the feedhorn axis can cause an asymmetry in the scan-dependent bias, though this is harder to measure.

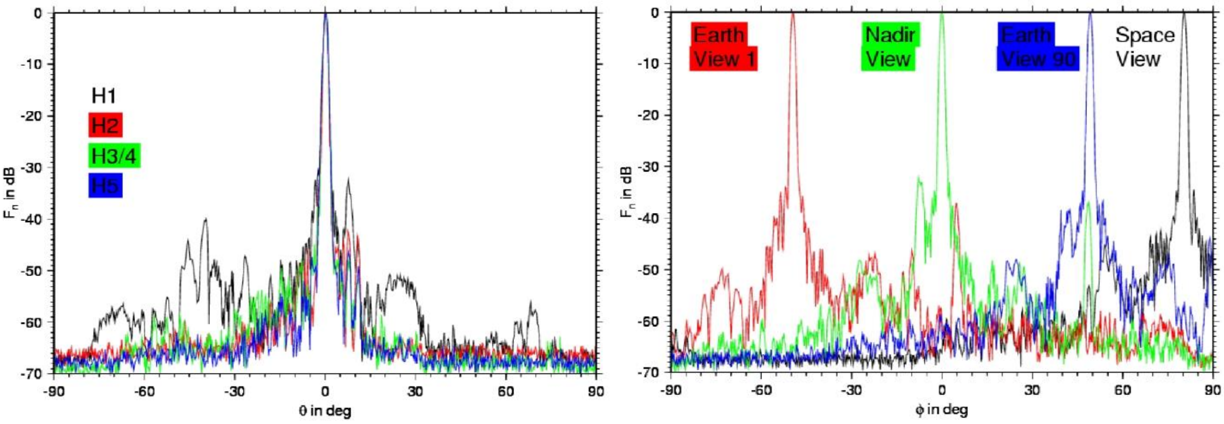

Figure 30: MHS-Flight Model 3 (Metop-A) main cut antenna power for different channels (left) and for different viewing directions of Channel 1 antenna (right). The angles θ and ϕ refer to the directions along and across the mirror axis, respectively.

In Figure 30, it can be seen that the noise floor for MHS antenna pattern measurement is around -66 dB, which means that a proper characterisation of the noise floor from pre-launch measurements requires a dynamic range of about 70 dB. For MWS, it is planned to make measurements over both hemispheres, but this is only meaningful if the noise floor is low enough. A low noise floor is not easy to achieve; it can take many weeks of measurement, which may not be feasible. It is likely that a combination of modelling and measurement will be used to provide the best characterisation.

6.1.1.6 Pass-band characterisation

The pass-band is characterised during sub-system testing (e.g. Jarrett and Charlton, 1993). The results are valuable to radiative transfer modellers. For AMSU and MHS, the measured passband 3dB limits (required by, for example, RTTOV) are tabulated in Appendix D of the NOAA KLM User Guide. However, the detailed filter response functions are not freely available. In the case of AMSU-A, the filter responses can be found in the Calibration Log Books (some unofficial copies are known to exist), but the corresponding log books for AMSU-B no longer exist.

The International TOVS Working Group (ITWG) strongly advocates making available the filter functions for all relevant instruments. For example, the following recommendation appeared in the working group summary report of ITSC-19 (2014), available at: http://cimss.ssec.wisc.edu/itwg/itsc/itsc19/index.html:

> To satellite agencies: instrument characteristics should be provided as early as possible (even approximate versions) to allow preparations for radiative transfer modelling and other evaluations. This includes in particular spectral response functions. Ultimately, detailed digitised channel system responses should be made available to allow the best-possible radiative transfer calculations.

Detailed measured spectral response functions are also essential for investigations when RFI is suspected. While MWS operates in protected bands, the identification of any illegal source of RFI is only possible when detailed accurate spectral response functions are available.

It is therefore recommended that digitised spectral response functions be made freely available for MWS.

Sideband imbalance figures should also be made available if possible, as this can significantly affect the brightness temperatures (Atkinson and Rayer, 2015).

6.1.2 *Post-launch Activities*

Essentially, post-launch activities of science validation comprise activities that allow the validation and verification of those mission requirements, which are related to product quality and completeness. Hence, for the Level 1 products, the corresponding tests are mainly focussed on geometric and radiometric performance assessments, whereas for higher level products, the validation strategy depends strongly on the product type and its spatial and temporal resolution. The underlying testing procedures can be mainly subdivided into two categories: tests of absolute accuracy and tests of relative accuracy. A quick summary of post-launch tests is given in the table below. Some more post-launch characterisation activities planned for MWS are described in the following sub-sections. The list is not exhaustive.

Requirement		Test Description
Spectral	Frequency Stability	Simultaneous Nadir Overpasses with Metop (AMSU,MHS) and NPP (ATMS); Bias evaluation with RT models
		Simulated brightness temperatures using NWP model fields over clear sky regions as input; comparison with collocated MWS measurements; shift central frequency for best fit
	Spectral Response Shape	With RTTOV, compute brightness temperature using upper side band only and lower side band only and nominal. Calculate the brightness temperature difference between upper and nominal sideband. Do the same for lower sideband. Calculate the maximum BT difference for sideband imbalance if the specification were just met.
Radiometric	Dynamic Range	Run the L1B prototype processor with L0 MWS data and obtain brightness temperature for all channels. Test whether these brightness temperature are within the limits specified in the End User Requirements documentation
	Radiometric Sensitivity	Calculation of NEΔT for each channel using the variability of the warm target and of space view counts, and the actual instrument gain
	Radiometric Bias	Evaluation of Simultaneous Nadir Overpasses with METOP satellites
		Evaluation of Simultaneous Nadir Overpasses with NOAA/NPP satellites
		Evaluation of Simultaneous Nadir Overpasses with Fengyung polar orbiting satellites
		Comparison with co-located radio occultation temperature profiles
		Data collected during a roll manoeuvre looking at the cold space will be evaluated to detect scan dependent biases due to e.g. antenna side lobes. The data can also support the detection of potential EMI (Electromagnetic Interferences)
		Radiosonde observations of temperature and humidity are used as input to radiative transfer simulations of MWS observations and are collocated to MWS observations to estimate biases ($O\text{-}B^{radiosonde}$).
		Evaluation of the radiometric bias using aircraft campaigns measurements from instruments that are similar to MWS. These observations are collocated to MWS overpasses to calculate biases ($O\text{-}B^{aircraft}$).
		Temperature, humidity and other atmospheric and surface parameters from NWP model forecast fields are used as input to radiative transfer simulation of collocated MWS observations; calculate biases ($O\text{-}B^{NWP}$).
	Interchannel and Interpixel radiometric bias	Evaluation of the interchannel and interpixel radiometric bias using the PRT temperature as a reference and calculating the variability of individual warm target views and the target temperatures derived from different channels.
Geometric	Viewing Angle	Convert the antenna position counts to corresponding viewing angles and calculate the angular span between the first and last sample. Check that this is larger than the

Requirement		Test Description
		requirement; check position of the center pixel and the angular spacing between adjacent spatial samples.
	Footprint	To ensure that there are no spatial gaps due to calibration of the instrument, check the difference in time between consecutive scans and check that it matches with the scan cycle time of MWS
	Geolocation	For about one month, data are selected over a geographical region of interest (eg. Australia), subdivided into ascending and descending scenes, and binned into a regular grid of required resolution. The mean brightness temperature difference between ascending and descending data samples for each grid point is computed. If, for surface sensitive channels, the differences are less than a threshold and the maximum difference coincides with the true coastline, the test is considered passed geo location accuracy requirement is met).
	Co registration	Validate the channel co-registration requirement using the lunar intrusion in space views. Analyse data sequence of five minutes across a Moon intrusion in a single space pixel and all channels. It is possible to detect from visual inspection that the centre of the curves derived from the individual channels do not coincide which would be an indication of co-registration problem would require further quantification, analysis and potential mitigation.

6.1.2.1 Launch and early orbit phase (LEOP)

The LEOP phase comprises many activities that ensure that the instrument is configured optimally, and is verified against specifications. For example:

- Thermal stabilisation of the instrument;
- Configuring the adjustable channel gains and offsets;
- Determination of initial post-launch NEΔTs;
- Determination of the optimum space viewing angle;
- Estimation of space view radiometric corrections;
- Verification that the ground processing is working with real instrument data.

These activities are essential, but can be considered routine, and this document does not discuss them in any further detail.

6.1.2.2 Satellite manoeuvres

The normal scan geometry for MWS is shown (to scale) in Figure 31. We can see that the space views are close to, but still largely clear of, the Earth's limb. There will be some contamination of the space-views, via the antenna sidelobes.

The idea of a satellite manoeuvre is to rotate the satellite about the roll or pitch axis so that the Earth views are viewing cold space, in order to characterise any scan-dependent biases. Pitch-over manoeuvres have been performed for NOAA-14 (Kleespies, 2011) and Suomi-NPP (Yang et al., 2016). In both of these cases, scan-dependence was detected in the measured Earth-view counts, and this was attributed to polarization-dependent main reflector emission.

For Metop-SG, instead of a pitch-over manoeuvre, it is planned to perform a 120° roll manoeuvre during the commissioning phase. A roll in the anti-sun direction is illustrated in Figure 32. We can see that the space views and the majority of the Earth views are pointing at deep space (never at the sun). The first 6 (approximately) Earth samples are close to where the space samples are in the nominal case.

Similarly, a roll in the sun direction is illustrated in Figure 33. But in this case, the space views are pointing directly at the Earth, and for some parts of the orbit the Earth-views will be pointing directly at the sun.

The scientific benefits of the roll manoeuvre are as follows:

- Provides information on the Earth contamination of the space views during normal operations. Normally this effect is modelled using pre-launch antenna pattern measurements, but the manoeuvre provides the opportunity for this effect to be measured directly, via the variation in the first few Earth samples (Figure 32) or last few samples (Figure 33).
- Provides information on the mirror reflectivity – a slow variation of measured counts with scan angle for Earth pixels that are pointing at deep space.

For MWS, a roll in the anti-sun direction is to be preferred, because (i) the space views are still directed at space, so the normal calibration procedures can be used, and (ii) there is no risk of the instrument viewing the sun directly (which would affect the results and could damage the instrument).

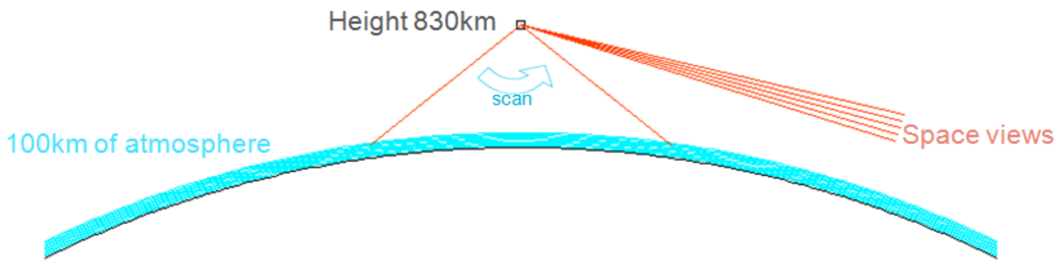

Figure 31: Normal scan geometry for MWS.

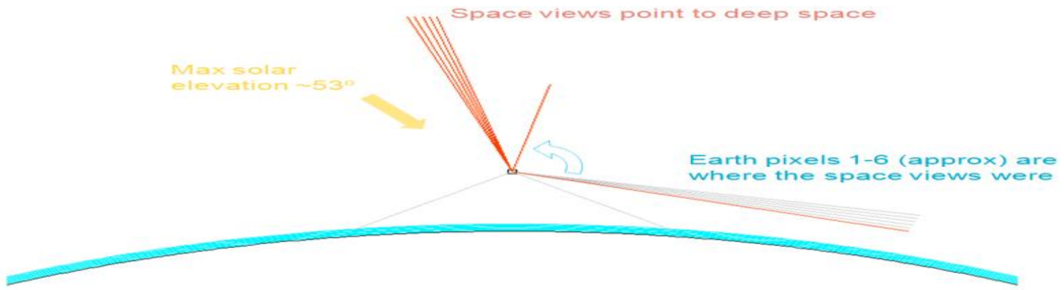

Figure 32: Scan geometry for a 120° roll manoeuvre in the anti-sun direction.

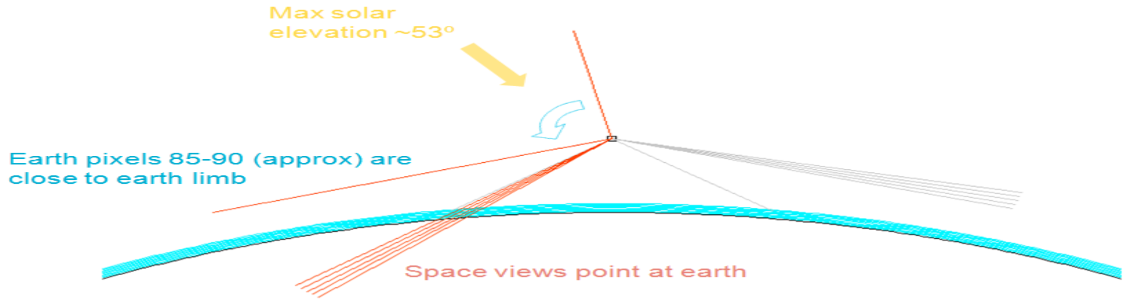

Figure 33: Scan geometry for a -120° roll manoeuvre in the sun direction.

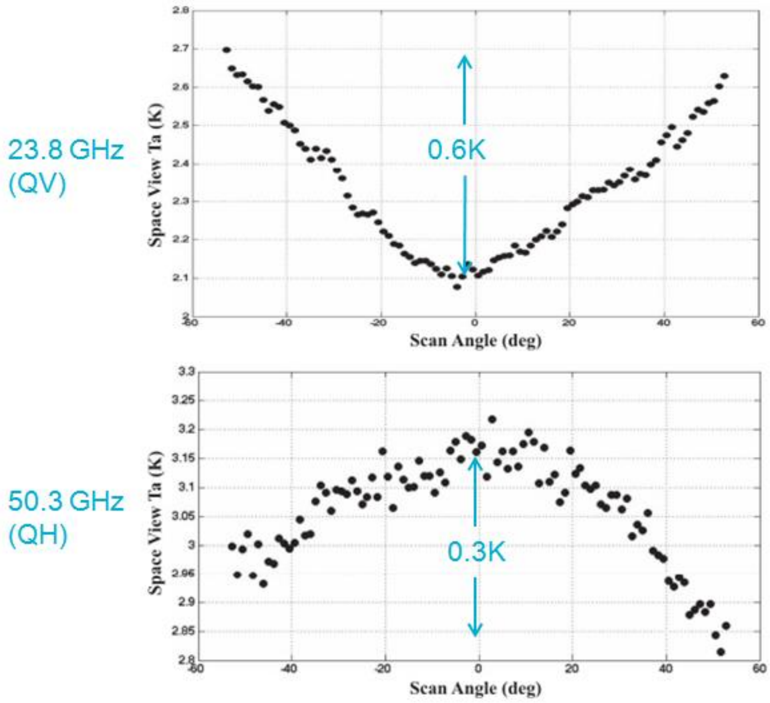

Figure 34: Antenna temperatures measured during ATMS pitchover manoeuvre (Yang et al., 2016).

However, a roll in the sun direction could be considered if it was carried out in the night-time part of the orbit, to confirm symmetry of the two effects.

Regarding the duration of the test: in the ATMS test documented by Yang et al. (2016), the instrument was viewing cold space for 33 minutes and a 25 minute period was used in the analysis. This allowed the random variability in antenna temperature, after averaging for each scan position, to be reduced to 0.05 to 0.1K (depending on channel – see Figure 34). This is sufficient to characterise the antenna reflectivity to the required accuracy. It is recommended that the MWS test should also be at least 25 minutes, or alternatively several shorter tests totalling at least 25 minutes. If possible, the test be repeated on a separate occasion to confirm consistency.

6.1.2.3 Aircraft campaigns

For several instruments on Metop-SG, similar instruments are installed on research aircraft. For example, the Microwave Airborne Radiometer Scanning System (MARSS), the DEIMOS, and the International SubMillimeter Airborne Radiometer (ISMAR) microwave radiometers on the Facility for Airborne Atmospheric Measurements (FAAM) Bae-146 operated by the UK Met Office / National Environment Research Council (NERC) (Fox et al., 2014). These instruments can be used to validate the satellite measurements through underflights.It is likely that validation campaigns designed for IASI-NG, and perhaps also for MWI/ICI, will also be useful for MWS.

6.1.2.4 Monitoring and use in NWP

Passive monitoring of new sounder data in NWP provides a powerful method to quantify the bias and noise characteristics of the data. For example, see Lu and Bell (2014) and Bell et al. (2008). The random noise derived from statistics of observed minus background radiance is a combination of noise in the observations and noise in the model background. However, the latter is usually well-characterised due to the presence of many other observation types in the NWP system.

For temperature-sounding channels, temporal or spatial changes in radiometric bias can be detected, usually to a precision of much better than 0.1K. These bias changes may be correlated with factors such as:

- Observed brightness temperature;
- Air mass;
- Humidity;
- Position in the orbit (e.g. solar angle at the satellite);
- Instrument temperature;
- Lunar position.

It will be important to include some NWP centres as Cal/Val partners, and to provide data to these centres as early as possible in the commissioning phase. Then the correlations mentioned above can be looked for, and explanations sought. If adjustments need to be made to the Level 1 processing then this should be done before the start of routine distribution of the data.

Once the data start to be routinely disseminated, impact studies should be performed, to quantify the improvement to model performance that results from assimilating the MWS data. This helps to justify, in financial terms, the investments that have taken place in supporting the satellite programme.

Forecast Sensitivity to Observations (FSO) metrics (Lorenc and Marriott, 2013) are also valuable: either to quantify the impact of the instrument as a whole (relative to other instruments) or even the relative impact of different channels of MWS.

Once data are flowing routinely, changes to the Level 1 processing system should be kept to a minimum. Modern variational bias correction (VarBC) systems are good at adjusting to step changes in bias, but not all NWP centres (or models) have VarBC, and for even for those that do there is a risk of assimilating biased data during transition periods. It is much better if such changes can be avoided.

6.2 Radiative transfer

6.2.1 General Problems in Radiative Transfer for MWS

An accurate, reliable and computationally efficient radiative transfer model will be essential for every quantitative analysis of MWS data and its use in NWP via data assimilation. These models capture the propagation of electromagnetic radiation through the atmosphere, and, depending on the application, they account for interactions with molecules, clouds, hydrometeors and the surface. The radiative transfer calculations include absorption, emission and scattering processes, based on knowledge of, for instance, absorption line shapes and coupling effects. The models also require an accurate description of the instrument's channel responses, one reason why the MWS SAG strongly recommends the provision of measured spectral response functions (see also section 6.1.1).

Available radiative transfer models vary considerably in complexity, with the most accurate models being so-called line-by-line models that solve the monochromatic radiative transfer equation using appropriate line-shape models and related spectroscopic parameters describing the lines. An example is MPM (Millimeter-wave Propagation Model, Liebe, 1989; Rosenkranz, 1998). Line-by-line models for the atmospheric gases underpin all radiative transfer simulations, and are the starting point for any advancement in spectroscopic modelling. Radiative transfer in cloudy or precipitating situations will additionally require a model capable of handling scattering effects, which critically depend on particle constitution (liquid, frozen mixed), shape, and even orientation.

Most users will rely on so-called fast radiative transfer models in which some calculations are parameterised, for instance, trained on more accurate but computationally much more demanding line-by-line models. This is to achieve greater computational speed, a key requirement for many near-realtime applications. Examples of such models are RTTOV (Saunders et al. 2013 and references therein), developed and maintained by the NWP-SAF, and the Community Radiative Transfer Model (CRTM, Han et al. 2006, Ding et al. 2011), developed and maintained by the Joint Center for Satellite Data Assimilation (JCSDA). Both also provide code for Jacobian, tangent linear and adjoint calculations, as required, for instance, in variational retrievals or variational assimilation applications. New radiative transfer coefficient files will need to be derived for the MWS instrument for these models, but the adaptation of existing methods to achieve this is straightforward and no major obstacles are foreseen, including for the new MWS channels in the 50 GHz band or the 229 GHz channel.

As radiative transfer calculations are essential for almost all applications of MWS data, improvements in this area have a very wide application potential. In the following, we review some areas that warrant further science developments.

6.2.2 Line-shape modelling

Microwave sounders such as the MWS sample between spectral lines in the 50-60 GHz band, in regions where optical depth is high but changes relatively slowly with frequency (e.g. Figure 1). This allows the use of broader pass-bands, with benefit in terms of achievable NeΔT, whilst retaining the sharpest possible weighting functions for temperature sounding. This is the only approach that can meet user requirements with current technology, but it has one clear drawback. The radiative transfer errors are dominated by errors in far line wing contributions and in line coupling between lines. These are the two areas of highest uncertainty in the clear-air radiative transfer.

Recent work has highlighted considerable uncertainties in these areas (Boukabara et al. 2005, Makarov et al. 2013). As the accuracy of NWP systems has increased very significantly in the last 10-15 years (e.g. Figure 11), it is conceivable that uncertainty in the radiative transfer will become a major source of error at 50-60 GHz in clear-sky regions for the use of MWS data in NWP. It is hence important to attempt to better characterise the spectroscopy for far line wings and line coupling. Improvements in the accuracy of these effects, and also a better characterisation of their uncertainties are likely to be of significant benefit to the impact of MWS temperature sounding channels. In particular, this is likely to be a requirement for enabling an effective exploitation of the lower NeΔT of MWS in future NWP systems in which increasingly small corrections to the initial state are needed.

6.2.3 Issues in the 183 GHz band

Systematic differences between measurements in the 183.31 GHz water vapour line by space-borne sounders and calculations using radiative transfer models (RTMs), with inputs from either radiosondes observations (RAOBs) or short-range forecasts by NWP models have been reported by several recent studies. More specifically, comparing the measurements to RTM calculations, using profiles of temperature and humidity either from RAOBs or from NWP models, shows a channel-dependent bias increasing from the center towards the wings of the line.

The spectral shape of the bias became clear only with the arrival of ATMS and SAPHIR, both launched in October 2011 (Clain et al. 2015, Moradi et al. 2015). These two instruments sample the 183.31 GHz line five and six times, respectively, between the line center (providing humidity information for the upper troposphere, above 300 hPa) and line wings (up to 11 GHz from the line center, for lower tropospheric sounding) compared to only three times for SSMIS, MHS and AMSU-

B. The observed minus calculated brightness temperatures (BTs) are shown for SAPHIR, ATMS, MHS and SSMIS using temperature and humidity profiles either from RAOBs or NWP systems (Météo-France and ECMWF). The radiances are calculated using the RTTOV v.11 RTM. A consistent spectrally dependent bias is found that is increases with distance from the line center. However, cross-comparisons between the existing nadir satellite microwave sounders of the tropospheric humidity using the 183.31 GHz line, SAPHIR, ATMS, SSMIS and MHS, show very good agreement between them, with a 0.3–0.7 K range of mean difference, well within the radiometric noise of the individual instruments (Wilheit et al, 2013, Moradi et al. 2015).

Biases can originate from RTMs (both from models and the underlying spectroscopy), RAOBS calibration, NWP models, and data assimilation. A two day workshop was held in Paris on 29th and 30th June 2015 gathering experts to discuss biases in the above mentioned aspects. A summary of the specific aspects there discussed and the drawn recommendations on radiative transfer and spectroscopy modelling at 183 GHz is given below. An exhaustive discussion regarding all the potential sources of the bias under investigation can be found in Brogniez et al. (2016).

Many cross-comparisons of microwave (MW) RTMs have been performed over the years. For instance, in their evaluation of SAPHIR using RAOBs, Clain et al. (2015) have shown that the three RTMs, RTTOV V.10, ARTS (Atmospheric Radiative Transfer Simulator; Eriksson et al., 2011) and MonoRTM (Monochromatic Radiative Transfer Model; Clough et al., 2005), provide fairly consistent BTs for a common set of tropical profiles, the differences being in the range of -1.50 K – 0.78 K, with the largest differences observed for the central channel (183±0.2 GHz). These three RTMs rely on the currently most widely accepted model MT_CKD (Mlawer-Tobin_CloughKneisysDavies; Mlawer et al., 2012) for the parametrization of the absorption due to the water vapour continuum.

While this result excludes the RTM as the cause of the bias under investigation, the accuracy of the spectroscopic input for the modelling of molecular absorption for the line-by-line radiative transfer (RT) needs more consideration.

The main contributions to molecular absorption in the MW region of the spectrum are from H_2O, O_2 and N_2, with some minor contributions from O_3 and N_2O. The uncertainty of the dry air absorption including dry continuum and resonance absorption by O_2, O_3, N_2O, NO, CO and other minor atmospheric constituents, as well as uncertainties related to wings of neighbouring water lines is not thought to be large enough to account for the observed model–minus–measurement bias.

H_2O line parameters (line position and strength, the foreign-broadened half-width, the self-broadened half-width, the temperature exponent of the width and the pressure shift) may be obtained from laboratory experiments or from theoretical calculations and are collected in databases such as the widely used high-resolution transmission compilation (HITRAN, Rothman et al. 2013). Sensitivity tests on Voigt parameters described in HITRAN, performed using MonoRTM, have shown that illustrative uncertainties on the foreign (3 %) and self-broadened (15 %) half widths, on the temperature exponent (maximum of 15 %) and the pressure shift (maximum of 20 %) are certainly too small to explain the observed bias (Payne et al. 2008), and the spectroscopic community believes that the accuracy of these parameters is higher than the above numbers.

The physical origin and properties of the water vapour continuum have been debated and probed with measurements for decades. There is thus an inconsistency between two large sets of experimental data, namely laboratory (together with surface path measurements) and radiometric measurements. This is confirmed by Payne et al. (2011) who concluded that for atmospheric path lengths the combination of MPM foreign and self-continuum is inconsistent with the (up-looking) radiometric measurements at high column water vapour amounts.

Currently, the cause of the apparent discrepancy between laboratory measurements and ground-based in situ results remains an open question. For instance, recent opacity measurements performed with the radio occultation active spectrometer ATOMMS (Active Temperature, Ozone

Moisture Microwave Spectrometer) have shown two spectral discrepancies (Kursinski et al. 2016). The first discrepancy is a poor match between the Liebe-MPM93 model and the measured line shape within 4 GHz of the 183.31 GHz line center. In this interval, the HITRAN-based AM6.2 model of Scott Paine (Harvard-Smithsonian Center for Astrophysics) matches the ATOMMS measurements very well, to 0.3 %. There is also a second significant spectral discrepancy in the wing of the line with respect to the AM6.2 modelled opacity, which is apparently lower than the measured opacity. Viewed from space, this would translate into a modelled BT that is higher than the measured BT (the modelled radiation coming from deeper in the atmosphere). This result is consistent with the discrepancies between the satellite-based measurements and the modelled estimates described above. A more detailed understanding of these discrepancies requires additional measurements and more quantitative examinations. In particular, it is recommended that ATOMMS measurements be made from aircraft at a range of pressures in order to determine the true line shape variation with pressure. In particular, measurements at high precipitable water contents (> 3 cm) are required to constrain the self-broadened continuum. Besides the use of ground-based 183 GHz instruments to better constrain the parameterizations, continuation and augmentation of laboratory measurements are strongly encouraged to check the uncertainty levels for the main spectroscopic parameters, and to explore new line shape parameterizations. Recent laboratory studies have resulted in unambiguous detections of H2O dimer absorption in the millimeter-wave range (Serov et al. 2014) and to the development of a model to describe it (Odintsova et al. 2014). This absorption shows spectral variation on scales that are not accounted for in the current version of MT_CKD or in Liebe-based models. Odintsova et al. (2014) indicate that the inclusion of dimer absorption can result in small-scale spectral (1 GHz) variation of 0.5 to 1 K in up-looking (ground-based) spectra. The impact of accounting for dimer absorption on RT modelling for the 183 GHz satellite radiometer channels has yet to be determined.

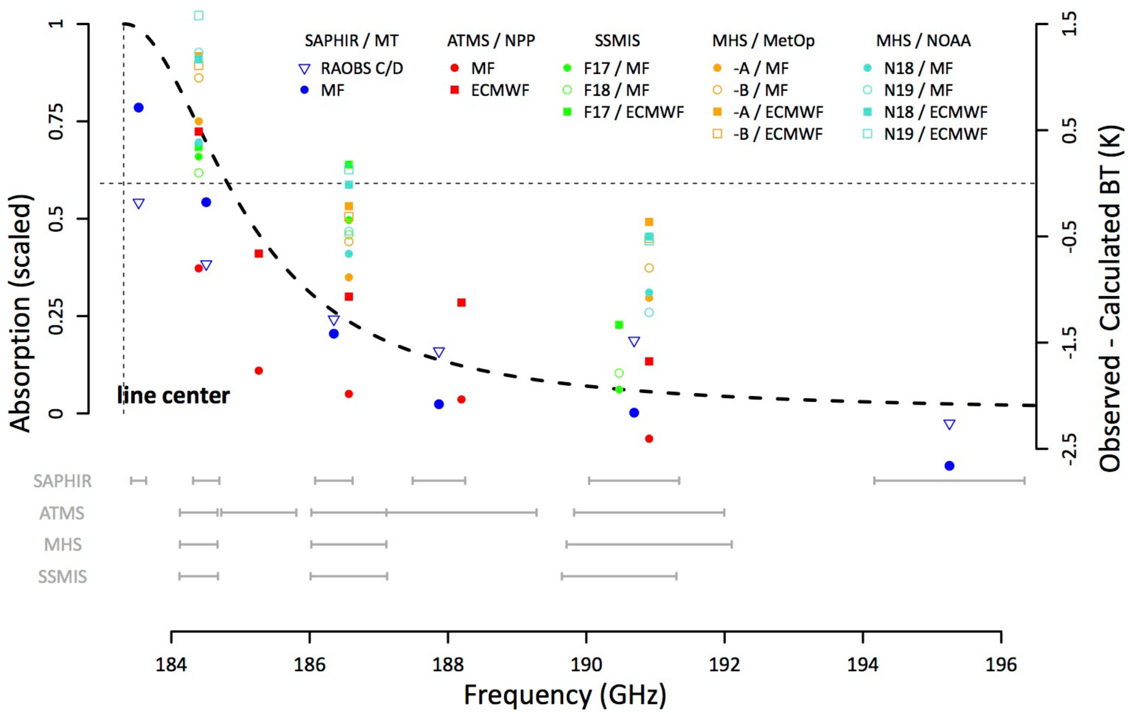

Figure 35: Mean observed BT minus calculated BT. All the calculated BTs are from RTTOVv11 run on RAOBs measurements collected during the CINDY/DYNAMO/AMIE field campaign, winter 2011–2012 (triangles) or Météo France NWP profiles (MF, circles) or European Centre for Medium-range Weather Forecasts NWP profiles (ECMWF, squares). Each colour refers to a specific sensor, as in the legend. The horizontal gray bars indicate the width of the band passes. For simplicity, only one side of the absorption line is represented. (Figure courtesy of Helene Brogniez and Stephen English).

6.2.4 Radiative transfer in clouds and precipitation

Recent years have seen rapid development in the quantitative use of cloud- and precipitation-affected microwave radiances. Many NWP centres will assimilate the MWS radiances in `all-sky' conditions to get better impact from the data; for example, using 183 GHz channels in all-sky conditions roughly doubles their impact on forecast quality compared to a clear-sky approach in the ECMWF system (Geer et al. 2014). Moreover, the cloud and rain information is of great interest for nowcasting and wider scientific investigations that should ultimately feed back into a better modelling of the water cycle for weather forecasting and climate simulations.

To simulate cloud and precipitation affected MWS radiances requires a radiative transfer model capable of modelling the multiple-scattering effects from hydrometeors, i.e. cloud and precipitation particles in liquid, frozen and mixed forms. However, there is great variability in the sizes and shapes of these particles, and in the three-dimensional structure of clouds and precipitation. The forward simulation would be most accurately performed by three-dimensional fully-polarised Monte-Carlo radiative transfer, but this is computationally not affordable, even for most research purposes. Instead, a number of increasingly severe approximations are made: (i) the 3D structure of the atmosphere is ignored by reducing the problem to a plane-parallel single-column approach; (ii) the scattering solution is reduced to a multi-stream solver such as DISORT (Stamnes et al. 2000) or even to a two-stream equivalent such as the delta-Eddington approximation (Joseph et al. 1976); (iii) the great variety of hydrometeor variability is reduced to a limited number of set habits, fixed particle size distributions (PSDs) and orientations, and the scattering properties may be modelled in highly approximate fashion, such as by applying the T-matrix approach for ellipsoids or even the Mie solution for the interaction of light with spheres. The RTTOV-SCATT model (Bauer et al. 2006) is an example of a fast model with a level of approximation presently adequate for the operational assimilation of all-sky microwave radiances at frequencies from 19 GHz to 183 GHz (Geer et al. 2014). The 3D-structure of clouds and precipitation is reduced to a two-column effective cloud overlap model (Geer at al. 2009). The scattering solution uses the delta-Eddington approximation. Scattering optical properties are generated using the Mie solution, except for large frozen hydrometeors (broadly `snow', but attempting to represent graupel, aggregates and hail too) for which the Mie solution is inadequate, and the particle structure is accounted for by using the Discrete Dipole Approximation (DDA, Draine and Flatau, 1994). However, given that mostly sufficiently detailed microphysical information on particle shapes, size distributions and orientations are not available from the models - snow is e.g. modelled as a single particle shape with a fixed size distribution and random orientation (Liu 2008, Geer and Baordo 2014) - all of these approximations result in modelling errors. Forward modelling for precipitation retrievals such as GPROF relies on a similar level of approximation. To get more accurate hydrometeor retrievals and a better use of all-sky radiances in NWP would require improved forward modelling.

Of the three areas of approximation, the modelling of hydrometeor size, shape, orientation and composition (mixed-phase particles) likely causes the largest errors. Better single-particle scattering properties for frozen and mixed-phase particles are required, with more complete and thus complex modelling of frozen hydrometeor habits (e.g. Eriksson et al. 2015). It is just starting to become clear that particle orientation is important, even at MWS frequencies. Gong and Wu (2017) showed that up to 10K differences are observed between brightness temperature of v and h polarisations in cloudy and precipitating scenes, even at frequencies as low as 89 GHz. This would most likely be explained by a persistent, widespread orientation of hydrometeors that is not represented in any current operational radiative transfer model for NWP purposes. Considerable experience does however exist with modelling of observations (and retrievals) of oriented hydrometeors from ground-based observations e.g. of rain (e.g. Saavedra et al. 2012, Battaglia et al. 2011) and snow (e.g. Xie et al. 2012, 2015), which could be exploited. Especially in rainy conditions also the experience gathered in research in the modelling of active microwave spectral range (radar) may be helpful since particle orientation is the essence of radar polarimetry and even multiple scattering becomes an issue when radars are deployed in space (e.g. Battaglia et al. 2010)

The second most important area is the treatment of the 3D atmospheric structure. Bennartz and Greenwald (2011) show that ignoring 3D radiative transfer effects can easily cause 10 K errors; this would be one main target for future development. The full 3D problem is still considered to be too complex for fast modelling, but some of the biggest errors could be reduced by using multiple independent columns to represent sub-field of view heterogeneity, and by better accounting for the slant path taken by radiation through cloud and precipitation structures.

A final area of uncertainty is the coupling of atmospheric scattering with the surface. Atmospheric scattering generates a sensitivity to radiation travelling outside the direct beam, which often also has interactions with the surface at angles other than that of the direct beam. A practical demonstration of this problem is that a multiple-stream scattering radiative transfer like DISORT really needs a full bidirectional reflectance distribution function to describe surface interaction; research is needed both to produce these functions and to understand the importance of coupling of scattering in the surface (e.g. volume scattering from the snowpack) and in the atmosphere from clouds and precipitation. Exploitable experience is available, albeit more in the lower frequency range, from the land surface community interested in e.g. the retrieval of soil moisture from L-band (1 GHz) observations of the SMOS (Soil Moisture and Ocean Salinity) and SMAP (Soil Moisture Active Passive) satellites.

6.2.5 Ocean surface emissivity

Ocean emissivity models depend on three main components: the dielectric properties of saline water; waves and ripples on the oceans surface; ocean whitecapping and sea foam. The first is fairly well known, with extensive laboratory measurements (Ellison et al. 2003) providing good quality information from 1 to 100 GHz. At higher frequencies the models are largely extrapolated based on either a single or double Debye formula and uncertainty is higher, but laboratory measurements do exist and are sufficient to estimate that uncertainty arising from the dielectric model is not very high.

In microwave emissivity models such as the FAST microwave Emissivity Model (FASTEM) (English and Hewison 1998, Deblonde and English 2000) the waves and ripples are parameterised as a function of the instantaneous wind and then roughness scales are divided into large scales, which can be solved using geometric optics, and small scales, for which a scattering solver is needed. In practise these are too slow for operational applications so FASTEM uses a predictor based framework to replicate the output of the more elaborate model quickly. This has proved successful in providing adequately fast computations for 20-100 GHz, and has been used at both lower (Liu et al. 2012) and higher frequencies. At higher frequencies a geometrics approach is adequate for all scales, so this is fairly straightforward. The errors at lower frequencies are not well characterised.

The MWS extension to 229 GHz should not pose any problems for the current approach, though the coefficients need to be re-computed. The study recently undertaken by Prigent and Aires (pers. comm.) will be adequate for this. The main issues lie in the parameterisation of the waves themselves, especially for smaller scales. It is possible that larger scale waves could or should be modelled from a wave model, with only small scale roughness parameterised as a function of instantaneous wind speed.

Foam and whitecapping has always posed a problem for microwave emissivity models. The foam coverage is parameterised as a function of instantaneous wind speed. However it is clear that much foam is generated from the breaking of large waves which may have little or no relation to the instantaneous wind, but have a memory of recent wind forcing. Partly for this reason there is a huge spread in foam fraction formulations for a given wind speed between different models in the literature. Therefore it appears more appropriate to parameterise foam fraction from the wave dissipative energy from a wave model. This has been tried by Meunier et al. (2014) who were able to model observed radiances as well as the current foam models without any tuning. This approach deserves more attention as accurate representations of whitecapping and foam generation is the largest source of uncertainty in ocean emissivity modelling.

6.2.6 Land surface emissivity

Current microwave observations were found beneficial to improve NWP analyses and forecasts (Karbou et al. 2010, Bauer et al. 2006, Kazumuri et al. 2008, English et al. 2014). Not surprisingly, MWS measurements are expected to have a great potential to help improving air temperature and humidity analysis and forecast fields. However, to accurately assimilate MWS temperature and humidity channels, channels receiving contributions from the surface must be carefully handled in order to properly model the effect of the surface (Karbou et al. 2010, 2014, Krzeminski et al. 2008, Di Tomaso et al. 2013). This is due to remaining uncertainties about the surface emissivity and the skin temperature (English et al. 2008). The uncertainties about the surface are more critical over land than over ocean. At microwave frequencies, sea emissivities are low, generally close to 0.5, whereas land emissivities are rather close to 1.0. Consequently, the surface contribution to the measured signal is less important over sea than over land.

Figure 36 (from Karbou et al. 2010) illustrates the effect of the surface on the number of assimilated observations from temperature sounding channels. It shows the density of assimilated observations from AMSU-A channel 7 (which is sensitive to temperature at about 10 km height) over grid cells of 2 deg by 2 deg when these data are assimilated with an empirical estimation of the surface emissivity (subplot (a), CTL experiment) and with a suitable parameterization of the emissivity (subplot (b), TEST experiment). One should notice that the CTL density map highlights land–sea regions since land surfaces can clearly be distinguished on this map. Improvements in the land emissivity modelling in the TEST experiment help improving the assimilation of data over land by increasing the number of assimilated observations with improved radiative transfer performances. Note that the process of satellite data assimilation can only be beneficial if the model, through the observation operator, is able to accurately simulate the observed brightness temperatures and screen for clouds. The cloud screening is made through a Quality Control (QC) test mainly based upon the evaluation of the difference between observations and simulations (Obs-Sim) of surface sensitive channels (the difference should be as low as possible). AMSU-A Channel 4 (52 GHz) and AMSU-B channel 2 (150 GHz) are respectively used in QC tests for AMSU-A, and AMSU-B/MHS. The effect of the surface is quite large for these channels, which cause a rejection of sounding channels for QC failures.

Several studies have shown that land surface emissivities can be accurately estimated from satellite observations (Choudhury 1993, Felde and Pickle 1995, Jones and Vonder Haar 1997, Karbou 2005, Karbou et al. 2005, Prigent et al. 1997-2005, Karbou et al. 2005-2006, Guedj et al. 2010 amongst others). The surface emissivity computation method is fully described in Karbou et al. (2006). The RTTOV model, fed by NWP short range forecasts of air temperature/humidity and surface temperature, is used to calculate upwelling radiation, downwelling radiation, and atmospheric transmission. Emissivity can then be estimated using the radiative transfer equation.

Surface emissivity varies due to several factors including surface type, soil moisture and roughness, ground conditions (rain, snow). Recently, Birman et al. (2014) showed that it is possible to get useful information about rainfall using daily land surface emissivities at 89 GHz. Emissivity also varies with observation frequency, viewing angle, and polarization. Examples of surface emissivity outputs are shown in Figure 37 and Figure 38, which display monthly mean emissivity estimates at AMSU-A/-B/MHS surface sensitive channels (from 23 to 150 GHz) using January and August 2014 data, respectively. As expected, emissivity varies in a complex way in space and with frequency. Snow areas have rather low emissivities at 89 GHz (see for instance the snow signature over North America, Eurasia, and polar regions in January in contrast to August). For sea ice, the emissivity variation is more complex with emissivity varying with season, ice type, and roughness.

For the assimilation of MWS observations, surface emissivity treatment can initially be very similar to the one used for current microwave sounders (used at Météo-France and at ECMWF): emissivity is dynamically computed at a well selected surface sensitive channel and used as a proxy for sounding channels. For temperature sounding, MWS-3 (50.3 GHz) can be used to compute the emissivity which will be used for the temperature channels (MWS-4 to MWS-16). For humidity, MWS-17 channel (89 GHz) is a good candidate for an emissivity first-guess in that spectral region, or MWS-18 (165 GHz) over snow and sea-ice regions.

The dynamic surface emissivity retrieval, however, has the draw-back of largely discarding information on surface conditions (i.e. snow, sea-ice) and skin temperature contained in the observations. Innovative approaches that instead make use of this information in NWP are highly desirable. This is particularly true in the context of increased coupling of the assimilation for atmospheric as well as land/ocean models. Here, information currently discarded could be useful for initialisation of the surface models. This likely results also in benefits for extracting information on the atmosphere, as there is potential to reduce the uncertainty inherent in the present approach.

Making better use of the surface information contained in the surface-sensitive channels will require the development of adequate modelling approaches that link the available model surface information to emissivity estimation. While full surface emissivity modelling over land/snow may be unfeasible with surface models presently available for NWP, this could be based on suitably simplified parameterisations.

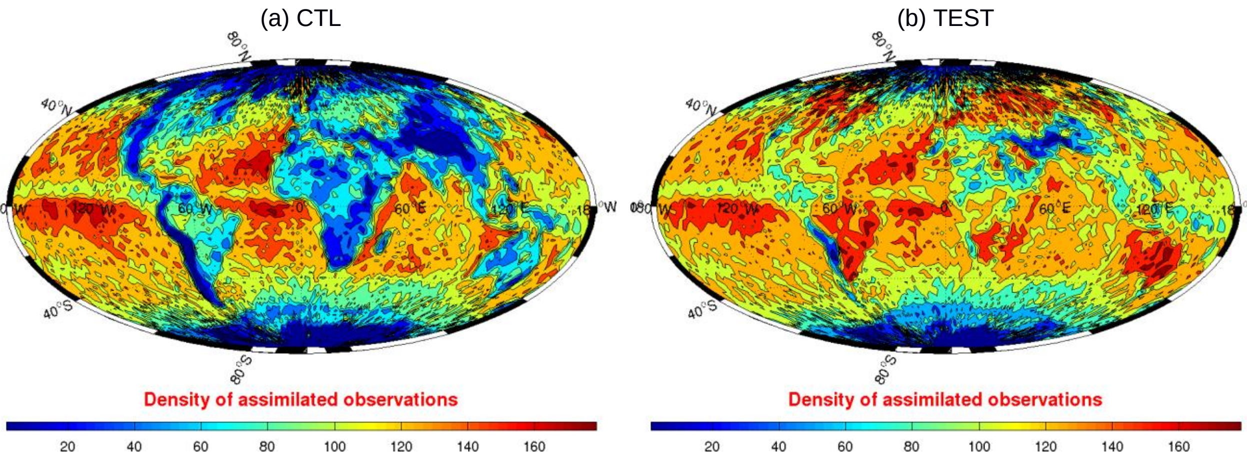

Figure 36: Map of the density of the assimilated observations from AMSU-A channel 7. The density values have been computed by counting the number of assimilated observations falling in grid cells of 2° × 2° during 45 days (1 Aug–14 Sep 2006). Results are for (a) CTL and (b) TEST experiments (From Karbou et al. 2010).

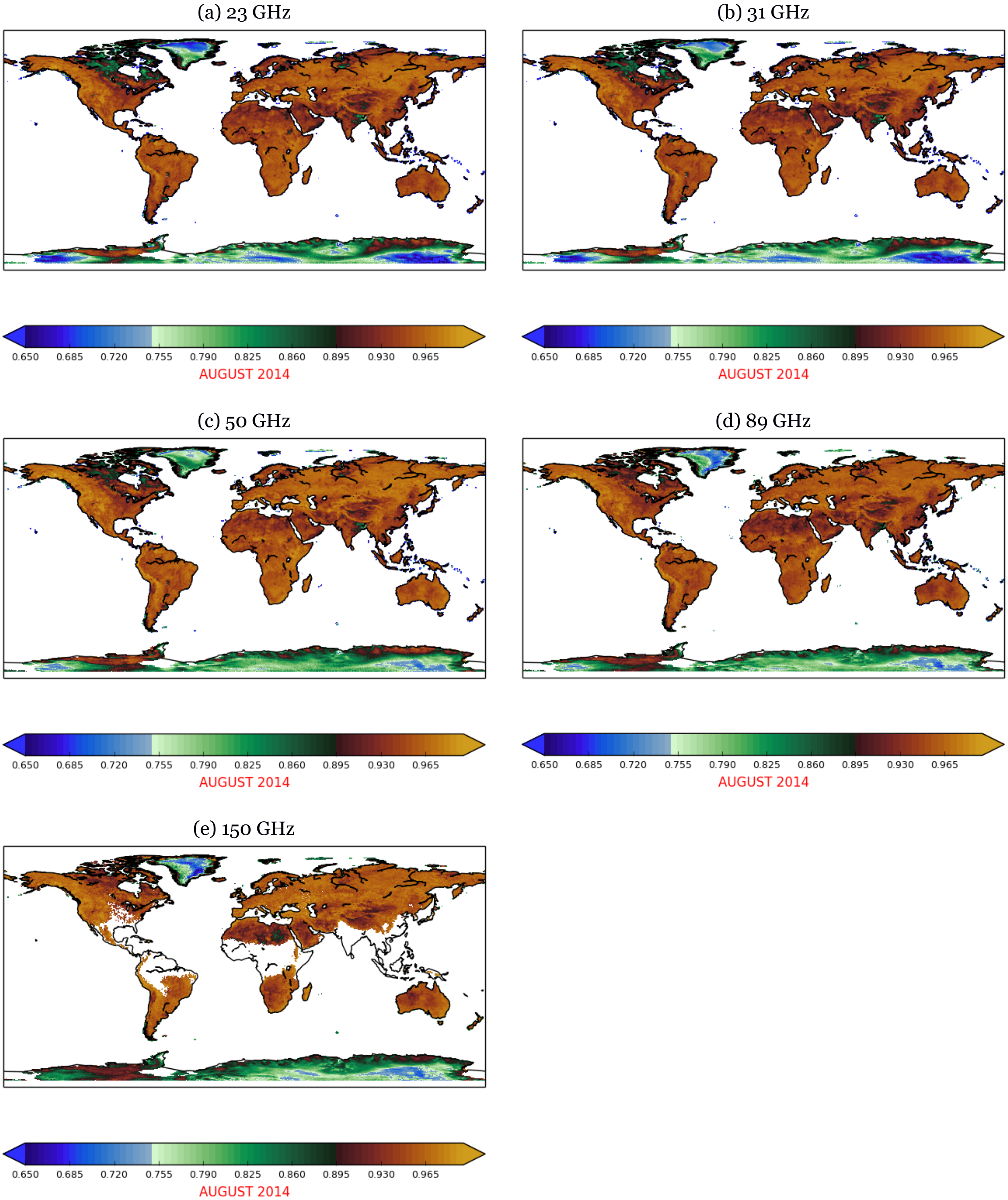

Figure 37: Monthly mean surface emissivity computed using AMSU-A/-B data from August 2014 and at (a) 23 GHz, (b) 31,4 GHz, (c) 50 GHz, (d) 89 GHz and (e) 150 GHz.

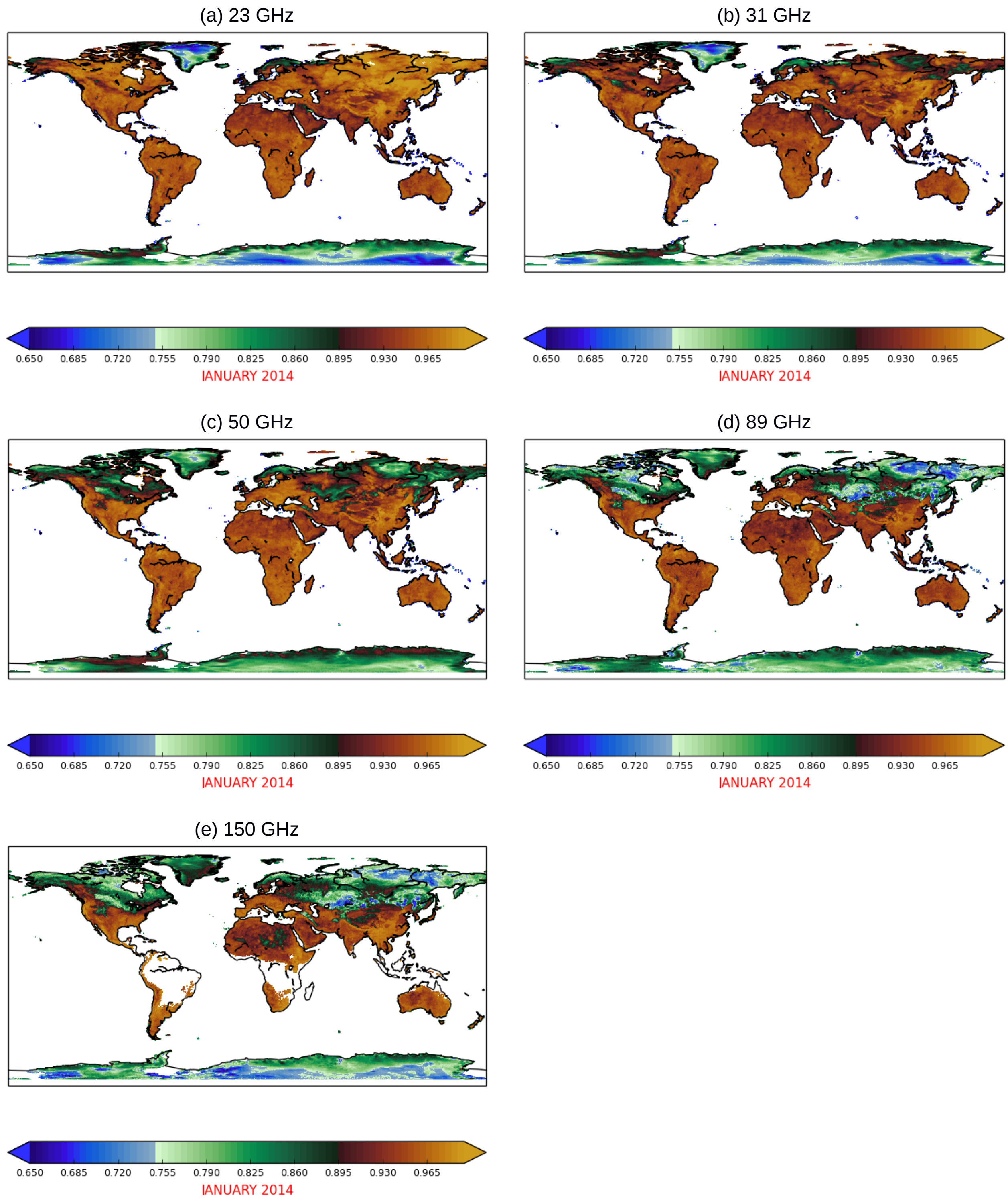

Figure 38: Same as Figure 37, but using AMSU-A/-B data from January 2014.

6.3 Identified research needs

This section summarises the main research needs identified during the preparation of this Science Plan. Addressing these research needs is required for an optimised use of the MWS observations. While MWS can build on the considerable experience with heritage microwave sounders as a good basis, these key research needs for an optimised use arise from two main rationales:

- Firstly, the MWS instrument has enhanced capabilities, such as additional channels and a much improved instrument characterisation (section 6.1.1), and the instrument is expected to achieve a lower effective noise performance than heritage instruments. Also, MWS is flown in the context of other microwave instruments sensing in spectral regions never before available from space (ICI, section 5.5). We need to ensure early optimised benefits from these enhancements.
- Secondly, application areas have advanced substantially since the inception of the MWS instrument, in particular data assimilation for NWP. Data assimilation systems are significantly more accurate, with random uncertainties in short-range forecasts from state-of-the-art NWP systems already around 0.1 K for tropospheric temperature channels, and with increasingly reliable estimates of these uncertainties in short-range forecasts, including their situation-dependence. This demands increasingly careful treatment of all observational uncertainties involved in the assimilation (e.g. from instrument noise, radiative transfer, quality control, etc.). Furthermore, NWP systems are now aiming to use, rather than discard information on clouds. Atmospheric data assimilation systems are also increasingly extending to Earth System assimilation systems, including coupled components such as land or ocean models.

These developments offer new opportunities to extend operational applications of MWS products into presently under-used areas. The following main areas have been identified:

1) Assessment of leading areas of uncertainty

Given increasingly accurate NWP systems and expected lower instrument noise, other sources of uncertainty will become increasingly important and potentially limiting factors for the optimised use of MWS data (e.g. sections 4.1, 5.2). These include uncertainties from radiative transfer and forward modelling, uncertainties from cloud detection (for clear-sky applications), or uncertainties arising from spatial representativeness. These uncertainties can have random or systematic components and an assessment of these is needed, for instance through simulation studies or metrological approaches. Better information on these uncertainties will allow a better treatment of them in data assimilation (e.g. specification of observation error covariance, constraints on bias corrections), and will highlight areas where further development is most needed to reduce uncertainties. It will also be of benefit for other applications, such as climate or product derivation.

2) Reduction of uncertainties from forward modelling

Radiative transfer and forward modelling is required for all quantitative uses of MWS data. Progress in radiative transfer models is therefore highly desirable for both clear-sky and cloudy/precipitating regions (see section 6.2).

For clear-sky applications, the modelling of line-coupling at 50-60 GHz, the modelling of line wings and inconsistencies with the water vapour continuum parameterisation (esp. around 183 GHz), as well as inaccuracies in surface emissivity modelling (over land, but also ocean) are considered leading sources of uncertainty.

For applications in cloudy/rainy regions, better and faster approximations for scattering properties for frozen and mixed-phase particles are required coupled with a better modelling of frozen hydrometeor habits (section 6.2.4). Radiative transfer developments for cloudy/precipitating regions should be coordinated with efforts undertaken for ICI/MWI, in order to achieve consistent approaches across the full MW spectrum.

Better forward modelling should also be possible through a better use of high-resolution model fields in NWP (section 5.2.1). With nominal spatial resolutions of global NWP models approaching 5 km in the MWS time-frame and regional models approaching 1 km and below, an explicit modelling of the spatial footprints of MWS (> 20 km off-nadir) will become increasingly important when calculating observation equivalents from model fields. These effects will be particularly important in all-sky use of the data.

3) All-sky use of new MWS channels and synergies with MWI/ICI data

All-sky applications in NWP are a very active field of research, aimed at using rather than discarding the cloud information contained in the observations. This is a highly challenging field with many development areas remaining, for the optimised assimilation of the observations, or better feedback from the observations on cloud parameterisations (section 5.2.5).

The new additional MWS channels are prime candidates for an all-sky use, and assimilation approaches will need to be developed. The channels will allow a better distinction of liquid and ice clouds.

All-sky applications offer very strong potential for synergy between MWS and MWI/ICI. This builds on the different sensitivities to clouds and precipitation across the full microwave spectrum, allowing unprecedented discrimination between liquid and ice clouds, information on cloud size distributions, etc. A dedicated effort will be needed to make best use of this information for assimilation and model cloud parameterisation development. Making consistent use of the highly complementary information on clouds and rain from these different instruments, if realised, is arguably one of the major advancements available with EPS-SG.

4) Improved use of surface information in Earth System Assimilation

Coupled data assimilation will be wide-spread in NWP in the EPS-SG time-frame, with assimilation systems in which initial conditions are calculated for atmospheric models coupled to, for instance, land and ocean models (section 5.2.5). In this context, MWS observations offer very significant information on surface characteristics, such as sea ice, snow, skin temperature, contained in the surface-sensitive channels of MWS (e.g. sections 5.3.4, 5.3.6, 5.3.8).

Presently, surface information from microwave sounders is largely discarded in assimilation systems or it adds to uncertainties in forward modelling. Coupled assimilation approaches will allow instead optimised extraction and use of such surface information. This should lead to more accurate initial conditions for all affected components. This means land or ocean models should benefit from previously unavailable information from observations, whereas the atmospheric part will benefit from a better treatment of the lowest sounding channels. Both are likely crucial aspects for the new 50 GHz channels available with MWS.

To achieve these benefits will require long-term developments, including the development of capabilities to model the surface contributions in the radiative transfer from currently available land/snow/sea-ice models used in NWP (sections 6.2.5, 6.2.6).

Reference Documents

Atkinson, N. C., 2011. Annex to AAPP scientific documentation: Pre-processing of ATMS and CrIS, document NWPSAF-MO-UD-027, available at http://nwpsaf.eu/site/software/aapp/documentation/.

Atkinson, N. C., 2014. "Striping" tests for microwave sounders. Satellite Applications Technical Memo 14, available from the Met Office, Exeter, UK.

Atkinson, N. C. and Rayer, P. J., 2015. Sideband imbalance sensitivity for the Microwave Sounder (MWS). Satellite Applications Technical Memo 36, available from the Met Office, Exeter, UK.

Atkinson, N. C., 2015. NEΔT specification and monitoring for microwave sounders. Satellite Applications Technical Memo 24, available from the Met Office, Exeter, UK.

Atkinson, N. C., 2016. Radiometric calibration for microwave sounders. Satellite Applications Technical Memo 44, available from the Met Office, Exeter, UK.

Auligné T., A. McNally and D. Dee, 2007: Adaptive bias correction for satellite data in a Numerical Weather Prediction system. Q. J. R. Meteorol. Soc. 133, 631–642.

Battaglia, A. S. Tanelli, S. Kobayashi, D. Zrnic, R.J. Hogan, and C. Simmer, 2010: Multiple-scattering in radar systems: a review. J. Quant. Spec. Rad. Transf., 111 (6), p.917-947, doi:10.1016/j.jqsrt.2009.11.024

Battaglia, A., P. Saavedra, C. A. Morales, and C. Simmer, 2011: Understanding 3D effects in polarized observations with the ground-based ADMIRARI radiometer during the CHUVA campaign. Journal of Geophysical Research,116, D09204, doi:10.1029/2010JD015335.

Bauer, P., Moreau, E., Chevallier, F. and O'Keeffe, U., 2006: Multiple-scattering microwave radiative transfer for data assimilation applications. Quarterly Journal of the Royal Meteorological Society, 132(617), pp.1259-1281.

Bauer, P., Auligné, T., Bell, W., Geer, A., Guidard, V., Heilliette, S., Kazumori, M., Kim, M.J., Liu, E.H.C., McNally, A.P. and Macpherson, B., 2011. Satellite cloud and precipitation assimilation at operational NWP centres. Quarterly Journal of the Royal Meteorological Society, 137(661), pp.1934-1951.

Bell, W., Di Michele, S., Bauer, P., McNally, T., English, S.J., Atkinson, N., Hilton, F. and Charlton, J., 2010. The radiometric sensitivity requirements for satellite microwave temperature sounding instruments for numerical weather prediction. Journal of Atmospheric and Oceanic Technology, 27(3), pp.443-456.

Bell, W., Candy, B., Atkinson, N., Hilton, F., Baker, N., Bormann, N., Kelly, G., Kazumori, M., Campbell, W.F. and Swadley, S.D., 2008. The assimilation of SSMIS radiances in numerical weather prediction models. Geoscience and Remote Sensing, IEEE Transactions on, 46(4), pp.884-900.

Bennartz, R., A. Thoss, A. Dybbroe, and D.B. Michelson, 2002: Precipitation analysis using the Advanced Microwave Sounding Unit in support of nowcasting applications. Met. Apps, 9: 177–189. doi:10.1017/S1350482702002037

Bennartz, R., and G. W. Petty, 2001: The sensitivity of microwave remote sensing observations of precipitation to ice particle size distributions. J. Appl. Meteor., 40, 345–364, doi:https://doi.org/10.1175/1520-0450(2001)

Birman, C., F. Karbou, J-F. Mahfouf, 2015, Daily rainfall detection and estimation over land using microwave surface emissivities, J. Appl. Meteor. And Clim., 54, 880-895, DOI: 10.1175/JAMC-D-14-0192.1.

Bojinski, S., M. Verstraete, T.C. Peterson, C. Richter, A. Simmons, and M. Zemp, 2014: The Concept of Essential Climate Variables in Support of Climate Research, Applications, and Policy. Bull. Amer. Meteor. Soc., 95, 1431–1443, doi: 10.1175/BAMS-D-13-00047.1

Bollmeyer, C., S. Wahl, S. Crewell, P. Friederichs, K. Hartung, A. Hense, J.D. Keller, J. Keune, S. Kneifel, C. Ohlwein, I. Pscheidt, S. Redl, S. Steinke (2015): Towards a high-resolution regional reanalysis for the European CORDEX domain. Q. J. R. Meteorol. Soc. 141, 1-15, doi: 10.1002/qj.2486

Bonavita, M., Isaksen, L. and Hólm, E., 2012. On the use of EDA background error variances in the ECMWF 4D-Var. Quarterly journal of the royal meteorological society, 138(667), pp.1540-1559.

Bormann, N., 2017: Slant path radiative transfer for the assimilation of sounder radiances. Tellus A, **69**, in print, http://dx.doi.org/10.1080/16000870.2016.1272779.

Bormann, N. and P. Bauer, 2010: Estimates of spatial and interchannel observation-error characteristics for current sounder radiances for numerical weather prediction. I: Methods and application to ATOVS data. Quarterly Journal of the Royal Meteorological Society, 136(649), pp.1036-1050.

Bormann, N., Fouilloux, A. and Bell, W., 2013. Evaluation and assimilation of ATMS data in the ECMWF system. Journal of Geophysical Research: Atmospheres, 118(23).

Boukabara, S-A., et al. 2005: Uncertainties in the temperature dependence of the line-coupling parameters of the microwave oxygen band: Impact study." IEEE transactions on geoscience and remote sensing. 43, 1109-1114.

Brogniez, H., English, S., Mahfouf, J.F., Behrendt, A., Berg, W., Boukabara, S., Buehler, S.A., Chambon, P., Gambacorta, A., Geer, A. and Ingram, W., 2016. A review of sources of systematic errors and uncertainties in observations and simulations at 183GHz. Atmospheric Measurement Techniques, 9(5), pp.2207-2221.

Brocca, L., T. Moramarco, F. Melone, and W. Wagner, 2013: A new method for rainfall estimation through soil moisture observations. Geophys. Res. Lett., 40, 853–858, doi:https://doi.org/10.1002/grl.50173.

Brocca, L., and Coauthors, 2014: Soil as a natural rain gauge: Estimating global rainfall from satellite soil moisture data. J. Geophys. Res., 119, 5128–5141, doi:https://doi.org/10.1002/2014JD021489.

Buehner, M., Morneau, J. and Charette, C., 2013. Four-dimensional ensemble-variational data assimilation for global deterministic weather prediction. Nonlinear Processes in Geophysics, 20(5), pp.669-682.

Buehler, S. A., and V. O. John (2005), A simple method to relate microwave radiances to upper tropospheric humidity, J. Geophys. Res., 110,D02110, doi:10.1029/2004JD005111.

Buehler, S. A., M. Kuvatov, V. O. John, M. Milz, B. J. Soden, D. L. Jackson, and J. Notholt (2008), An upper tropospheric humidity data set from operational satellite microwave data, J. Geophys. Res., 113, D14110, doi:10.1029/2007JD009314.

Calvet, J.-C, J.-P. Wigneron, J.P. Walker, F. Karbou, A. Chanzy, C. Albergel, 2011, Sensitivity of passive microwave observations to soil moisture and vegetation water content : L-band to W-band", IEEE Trans. Geosc. Remote Sens., 49(4), 1190 – 1199, doi:10.1109/TGRS.2010.2050488.

Chander, G., T.J. Hewison, N. Fox, X. Wu, X. Xiong, and W.J. Blackwell, 2013: Overview of Intercalibration of Satellite Instruments, IEEE Trans. Geosciences and Remote Sens., 51(3), 1056-1080, doi:10.1109/TGRS.2012.2228654.

Clain, G., Brogniez, H., Payne, V.H., John, V.O. and Luo, M., 2015. An assessment of SAPHIR calibration using quality tropical soundings. Journal of Atmospheric and Oceanic Technology, 32(1), pp.61-78.

Clayton, A.M., Lorenc, A.C. and Barker, D.M., 2013. Operational implementation of a hybrid ensemble/4D-Var global data assimilation system at the Met Office. Quarterly Journal of the Royal Meteorological Society, 139(675), pp.1445-1461.

Clough, S.A., Shephard, M.W., Mlawer, E.J., Delamere, J.S., Iacono, M.J., Cady-Pereira, K., Boukabara, S. and Brown, P.D., 2005. Atmospheric radiative transfer modeling: a summary of the AER codes. Journal of Quantitative Spectroscopy and Radiative Transfer, 91(2), pp.233-244.

Courcoux, N. and Schröder, M.: The CM SAF ATOVS data record: overview of methodology and evaluation of total column water and profiles of tropospheric humidity, Earth Syst. Sci. Data, 7, 397-414, doi:10.5194/essd-7-397-2015, 2015.

Courcoux, Nathalie; Schröder, Marc. (2013): Vertically integrated water vapour, humidity and temperature at pressures levels and layers from ATOVS - Daily Means / Monthly Means. Satellite Application Facility on Climate Monitoring. DOI:10.5676/EUM_SAF_CM/WVT_ATOVS/V001. http://dx.doi.org/10.5676/EUM_SAF_CM/WVT_ATOVS/V001

Crow, W. T., G. F. Huffman, R. Bindlish, and T. J. Jackson, 2009: Improving satellite rainfall accumulation estimates using spaceborne soil moisture retrievals. J. Hydrometeor., 10, 199–212, doi:https://doi.org/10.1175/2008JHM986.1.

Crow, W. T., M. J. van Den Berg, G. F. Huffman, and T. Pellarin, 2011: Correcting rainfall using satellite-based surface soil moisture retrievals: The Soil Moisture Analysis Rainfall Tool (SMART). Water Resour. Res., 47, W08521, doi:https://doi.org/10.1029/2011WR010576.

Deblonde, G. and S.J. English, 2000: Evaluation of FASTEM and FASTEM2. Satellite Application Facility for Numerical Weather Prediction Report NWPSAF-MO-VS-001.

Dee, D.P. et al. 2011. The ERA-Interim reanalysis: Configuration and performance of the data assimilation system. Quarterly Journal of the Royal Meteorological Society, 137(656), pp.553-597.

Defer, E., C. Prigent, F. Aires, J. R. Prado, C. J. Walden, O.-Z. Zanif, J.-P. Chaboureau, and J.-P. Pinty, 2008: Development of precipitation retrievals at millimeter and sub-millimeter wavelength for geostationary satellites. J. Geophys. Res., 113, D0811, doi:https://doi.org/10.1029/2007JD008673.

Ding, S., P. Yang, F. Weng, Q. Liu, Y. Han, P. Van Delst, J. Li, and B. Baum, 2011: Validation of the community radiative transfer model. Journal of Quantitative Spectroscopy and Radiative Transfer 112 (6): 1050-1064.

Di Paola, F., Casella, D., Dietrich, S., Mugnai, A., Ricciardelli, E., Romano, F., and Sano, P.: Combined MW-IR Precipitation Evolving Technique (PET) of convective rain fields, Natural Hazards and Earth System Sciences, 12, 3557-3570, 10.5194/nhess-12-3557-2012, 2012.

DiTomaso, E., F. Romano, and V. Cuomo, 2009: Rainfall estimation from satellite passive microwave observations in the range 89 GHz to 190 GHz. J. Geophys. Res., 114, D18203, doi:https://doi.org/10.1029/2009JD011746.

Doherty, A., Atkinson, N., Bell, W. and Smith, A., 2015. An Assessment of Data from the Advanced Technology Microwave Sounder at the Met Office. Advances in Meteorology, 2015.

Draine, B.T. and Flatau, P.J., 1994. Discrete-dipole approximation for scattering calculations. JOSA A, 11(4), pp.1491-1499.

Draper, D.W., Newell, D.A., Wentz, F.J., Krimchansky, S. and Skofronick-Jackson, G.M., 2015. The global precipitation measurement (GPM) microwave imager (GMI): Instrument overview and early on-orbit performance. IEEE Journal of Selected Topics in Applied Earth Observations and Remote Sensing, 8(7), pp.3452-3462.

ECMWF strategy 2016-2025: The strength of a common goal. Available from: https://www.ecmwf.int/sites/default/files/ECMWF_Strategy_2016-2025.pdf

Ellison, W.J., English, S.J., Lamkaouchi, K., Balana, A., Obligis, E., Deblonde, G., Hewison, T.J., Bauer, P., Kelly, G. and Eymard, L., 2003. A comparison of ocean emissivity models using the Advanced Microwave Sounding Unit, the Special Sensor Microwave Imager, the TRMM Microwave Imager, and airborne radiometer observations. Journal of Geophysical Research: Atmospheres, 108(D21).

English, S.J. and Hewison, T.J. 1998: A fast generic millimetre-wave emissivity model". In Proceedings of SPIE Microwave Remote Sensing of the Atmosphere and Environment Edited by: Hayasaka, T., Wu, D.L., Jin, Y. and Jiang, J. 15 September 1998, 288–300.

English, S.J., J.R. Eyre, J.A. Smith, J.A., 1999: A cloud-detection scheme for use with satellite sounding radiances in the context of data assimilation for numerical weather prediction. Quarterly Journal of the Royal Meteorological Society, 125(559), pp.2359-2378.

English, S.J., Renshaw, R.J., Dibben, P.C., Smith, A.J., Rayer, P.J., Poulsen, C., Saunders, F.W. and Eyre, J.R., 2000. A comparison of the impact of TOVS arid ATOVS satellite sounding data on the accuracy of numerical weather forecasts. Quarterly Journal of the Royal Meteorological Society, 126(569), pp.2911-2931.

Ehrendorfer M, Errico RM, Raeder KD. 1999. Singular-vector perturbation growth in a primitive equation model with moist physics. Journal of Atmospheric Sciences 56: 1627–1678.

EPS-SG End User Requirements Document (EURD) (EUM/PEPS/REQ/09/0151)

EPS-SG Micro-Wave Sounder (MWS) Level 1B Products Algorithm Theoretical Basis Document (ATBD) (EUM/LEO-EPSSG/SPE/14/737100)

Eriksson, P., Jamali, M., Mendrok, J. and Buehler, S.A., 2015: On the microwave optical properties of randomly oriented ice hydrometeors. Atmospheric Measurement Techniques, 8(5), p.1913.

Eriksson, P., Buehler, S.A., Davis, C.P., Emde, C. and Lemke, O., 2011. ARTS, the atmospheric radiative transfer simulator, version 2. Journal of Quantitative Spectroscopy and Radiative Transfer, 112(10), pp.1551-1558.

Eyre J. R., Kelly G. A., McNally A. P., Andersson E., and Persson A., 1993, Assimilation of TOVS radiance information through one-dimensional variational analysis. Q J R Met Soc, 119, 1427-1463.

Ferraro, R. R., and G. F. Marks, 1995: The development of SSM/I rain-rate retrieval algorithms using ground-based radar measurements. J. Atmos. Oceanic Technol., 12, 755–770, doi:https://doi.org/10.1175/1520-0426.

Fox, S., Lee, C., Rule, I., King, R., Rogers, S., Harlow, C. and Baran, A., 2014, March. ISMAR: A new submillimeter airborne radiometer. In Microwave Radiometry and Remote Sensing of the Environment (MicroRad), 2014 13th Specialist Meeting on (pp. 128-132). IEEE.

Garot, T., H. Brogniez, R. Fallourd, and N. Viltard, 2017, Evolution of the Distribution of Upper-Tropospheric Humidity over the Indian Ocean: Connection with Large-Scale Advection and Local Cloudiness, J. Appl. Meteo. And Clim., https://doi.org/10.1175/JAMC-D-14-0096.1

Geer, A.J., F. Baordo, N. Bormann and S. English, 2014: All-sky assimilation of microwave humidity sounders. ECMWF Technical Memorandum 741, Reading, U.K., 57pp.

Geer, A.J. and Baordo, F., 2014. Improved scattering radiative transfer for frozen hydrometeors at microwave frequencies. Atmospheric Measurement Techniques, 7(6), pp.1839-1860.

Geer, A.J. and P. Bauer, 2011: Observation errors in all-sky data assimilation. Quarterly Journal of the Royal Meteorological Society, 137(661), pp.2024-2037.

Geer, A.J., Bauer, P. and O'Dell, C.W., 2009. A revised cloud overlap scheme for fast microwave radiative transfer in rain and cloud. Journal of Applied Meteorology and Climatology, 48(11), pp.2257-2270.

Geer, A.J., Lonitz, K., Weston, P., Kazumori, M., Okamoto, K., Zhu, Y., Liu, E.H., Collard, A., Bell, W., Migliorini, S., Chambon, P., Fourrié, N., Kim, M.-J., Köpken-Watts, C. and Schraff, C., 2018: All-sky satellite data assimilation at operational weather forecasting centres. Q.J.R. Meteorol. Soc., 144, doi:10.1002/qj.3202

Gelaro, R., Langland, R.H., Pellerin, S. and Todling, R., 2010. The THORPEX observation impact intercomparison experiment. Monthly Weather Review, 138(11), pp.4009-4025.

GCOS, 2016: The Global Observing System for Climate: Implementation Needs, GCOS 200 (GOOS-214), Oct. 2016 (at time of download http://unfccc.int/files/science/workstreams/systematic_observation/application/pdf/gcos_ip_10oct2016.pdf via http://www.wmo.int/pages/prog/gcos/)

Goody, R., J. Anderson, T. Karl, R. Balstad Miller, G. North, J. Simpson, G. Stephens, and W. Washington, 2002: Why We Should Monitor the Climate. Bull. Amer. Meteor. Soc., 83, 873–878, doi: 10.1175/1520-0477(2002)083<0873:WWSMTC>2.3.CO;2.

Grody, N., J. Zhao, R. Ferraro, F. Weng, R. Boers, 2001. Determination of precipitable water and cloud liquid water over oceans from the NOAA 15 advanced microwave sounding unit. Journal of Geophysical research, 106(D3), pp.2943-2953.

GSICS, 2015: Vision of GSICS in the 2020s – Shaping GSICS to meet future challenges, GSICS-RD002-v1.1, v1.1, June 2015. (At time of download available at http://www.wmo.int/pages/prog/sat/documents/GSICS-RD002_Vision.pdf)

GISCS, 2016: GSICS quarterly. Vol 9, no. 4 (2016). U.S. Department of Commerce, National Oceanic and Atmospheric Administration, National Environmental Satellite, Data, and Information Service, Center for Satellite Applications and Research, doi: 10.7289/V5ZC80W8

Guerbette J., J.F. Mahfouf, M. Plu, 2016: Towards the assimilation of all-sky microwave radiances from the SAPHIR humidity sounder in a limited area NWP model over tropical regions. Tellus A 68: 28 620, doi:http://dx.doi.org/10.3402/tellusa.v68.28620.

Han Y, van Delst P, Liu Q, et al. Community radiative transfer model (CRTM): Version 1, NOAA Technical Report. NOAA, Washington, DC; 2006; 122 pp.

Harris, B., Tingwell, C., Steinle, P., Bourke, W., Naughton, M., Roff, G. and Paevere, J., 2005. Use of Level-1d ATOVS Radiances in GASP. Proc. of ITSC-XIV, Beijing, China, pp.25-31.

Hermozo, L., L. Eymard, F. Karbou, 2017, Modeling Sea Ice Surface Emissivity at Microwave Frequencies: Impact of the Surface Assumptions and Potential Use for Sea Ice Extent and Type Classification, IEEE-TGRS, Volume: 55, Issue: 2, DOI: 10.1109/TGRS.2016.2616920.

Hewison, T.J. and Saunders, R., 1996. Measurements of the AMSU-B antenna pattern. Geoscience and Remote Sensing, IEEE Transactions on, 34(2), pp.405-412.

Instrument Requirements Specification for the Micro-Wave Sounder (MOS-RS-ESA-MWS-0430)

Hilburn, K. A., and F. J. Wentz, 2008: Intercalibrated passive microwave rain products from the Unified Microwave Ocean Retrieval Algorithm (UMORA). J. Appl. Meteor. Climatol., 47, 778–794, doi:https://doi.org/10.1175/2007JAMC1635.1

Jarrett, M.L. and Charlton, J.E., 1993. Characterization of the channel passband response of AMSU-B. In Optical Engineering and Photonics in Aerospace Sensing (pp. 169-177). International Society for Optics and Photonics.

Joseph, J.H., W.J. Wiscombe, and J.A. Weinman, 1976: The delta-Eddington approximation for radiative flux transfer. Journal of the Atmospheric Sciences, 33(12), pp.2452-2459.

Karbou, F., E. Gérard, and F. Rabier, 2006: Microwave land emissivity and skin temperature for AMSU-A and -B assimilation over land. Quart. J. Roy. Meteor. Soc., 132, 2333–2355, doi: https://doi.org/10.1256/qj.05.216.

Karbou, F., Gérard, E. and Rabier, F., 2010. Global 4DVAR assimilation and forecast experiments using AMSU observations over land. Part I: Impacts of various land surface emissivity parameterizations. Weather and Forecasting, 25(1), pp.5-19.

Karbou, F., F. Rabier, and C. Prigent, 2014: The assimilation of observations from the Advanced Microwave Sounding Unit over sea ice in the French global numerical weather prediction system. Mon. Wea. Rev., 142, 125–140, doi: https://doi.org/10.1175/MWR-D-13-00025.1.

Kidd, C., Matsui, T., Chern, J., Mohr, K., Kummerow, C., and Randel, D.: Global Precipitation Estimates from Cross-Track Passive Microwave Observations Using a Physically Based Retrieval Scheme, Journal of Hydrometeorology, 17, 383-400, 10.1175/jhm-d-15-0051.1, 2016.

Kleespies, T. J., Smith-Dearring, R., Woodward, J., Shepherd, J., Gliniak, C., Chadwick, W., Han, D. 2007: Evaluation of Scan Asymmetry in the NOAA-14 Microwave Sounding Unit by a Pitch Maneuver. IEEE Geosci. Remote Sens. Lett.. 4(4), 621-623. doi: 10.1109/lgrs.2007.903394

Kleespies, T. J., 2011. Recharacterization of the Microwave Sounding Unit cross-track asymmetry during a spacecraft tumble. IEEE Geoscience and Remote Sensing Letters, 8(2), 230-232.

Kulie, M.S., Bennartz, R., Greenwald, T.J., Chen, Y. and Weng, F., 2010: Uncertainties in microwave properties of frozen precipitation: Implications for remote sensing and data assimilation. Journal of the Atmospheric Sciences, 67(11), pp.3471-3487.

Kursinski, E. R., Ward, D., Otarola, A. C., McGhee, J., Stovern, M., Sammler, K., Reed, H., Erickson, D., McCormick, C., and Griggs, E., 2016. Atmospheric profiling via satellite to satellite occultations near water and ozone absorption lines for weather and climate. Earth Observing Missions and Sensors: Development, Implementation, and Characterization IV, 10th SPIE Asia-Pacific Remote Sensing Symposium, New Delhi, India, 2016.

Labrot, T., Lavanant, L., Whyte, K., Atkinson, N. and Brunel, P., 2011. AAPP documentation: scientific description, document NWPSAF-MF-UD-001, available at https://www.nwpsaf.eu/site/software/aapp/documentation/.

Laviola, S., Levizzani, V., Cattani, E., and Kidd, C.: The 183-WSL fast rain rate retrieval algorithm. Part II: Validation using ground radar measurements, Atmospheric Research, 134, 77-86, 10.1016/j.atmosres.2013.07.013, 2013.

Lawrence H., N. Bormann, A.J. Geer, Q. Lu, S.J. English, 2018: An evaluation of FY-3C MWHS-2 at ECMWF. Quart. J. Roy. Meteorol. Soc. , doi: 10.1109/TGRS.2018.2798292.

Liebe, H.J., 1989: MPM – an atmospheric millimeter wave propagation model. Int. J. Infrared and Millimeter Waves, 10(6), 631-650.

Li, J., Wolf, W. W., Menzel, W. P., Zhang, W., Huang, H. L., & Achtor, T. H. (2000). Global soundings of the atmosphere from ATOVS measurements: The algorithm and validation. Journal of Applied Meteorology, 39(8), pp. 1248-1268.

Liebe, H.J., 1989. MPM—An atmospheric millimeter-wave propagation model. International Journal of Infrared and millimeter waves, 10(6), pp.631-650.

Lonitz K, A.J. Geer, 2015: New screening of cold-air outbreak regions used in 4D-Var all-sky assimilation. EUMETSAT/ECMWF Fellowship Programme Research Report, 35, available from http://www.ecmwf.int .

Liu, G., 2008: A database of microwave single-scattering properties for nonspherical ice particles. Bulletin of the American Meteorological Society, 89(10), pp.1563-1570.
Liu, Q., English, S. and Weng, F., 2012: Fast microwave ocean emissivity model version 5 (FASTEM-5). IEEE Trans. Geosci. Remote Sens, 50.

Lu, Q. and Bell, W., 2014. Characterizing channel center frequencies in AMSU-A and MSU microwave sounding instruments. Journal of Atmospheric and Oceanic Technology, 31(8), pp.1713-1732.

Lu, Q., Bell, W., Bauer, P., Bormann, N. and Peubey, C., 2011. Characterizing the FY-3A microwave temperature sounder using the ECMWF model. Journal of Atmospheric and Oceanic Technology, 28(11), pp.1373-1389.

Lupu, C, A.J. Geer, N. Bormann, S. English, 2016: An evaluation of radiative transfer modelling errors in AMSU-A data. ECMWF Technical Memorandum 770, 36pp.
Ma, Y. and Zou, X., 2015. Striping noise mitigation in ATMS brightness temperatures and its impact on cloud LWP retrievals. Journal of Geophysical Research: Atmospheres, 120(13), pp.6634-6653.

Makarov, D. S., M. Yu Tretyakov, and C. Boulet, 2013: Line mixing in the 60-GHz atmospheric oxygen band: Comparison of the MPM and ECS model. Journal of Quantitative Spectroscopy and Radiative Transfer. 124, 1-10.

Melsheimer C., and G. Heygster, 2008: Improved Retrieval of Total Water Vapor Over Polar Regions From AMSU-B Microwave Radiometer Data, *Geoscience and Remote Sensing IEEE Transactions on*, vol. 46, pp. 2307-2322, ISSN 0196-2892.

Meunier, L.F., English, S. and Janssen, P., 2014. Improved ocean emissivity modelling for assimilation of microwave imagers using foam coverage derived from a wave model. Report of Visiting Scientist mission NWP_VS12_02, Document NWPSAF-MO-VS-049.

McNally, A.P., C. Lupu, C. Cardinali, A. Geer, R. Forbes, K. Lonitz, M. Diamantakis, Carole Peubey, 2014: Impact of satellite data in global NWP. Presentation at the ECMWF annual seminar on the use of satellite observation in numerical weather prediction. Available online: http://www.ecmwf.int/ sites/default/files/elibrary/2014/14686-impact-satellite-data-global-nwp.pdf

Mlawer, E.J., Payne, V.H., Moncet, J.L., Delamere, J.S., Alvarado, M.J. and Tobin, D.C., 2012. Development and recent evaluation of the MT_CKD model of continuum absorption. Philosophical Transactions of the Royal Society of London A: Mathematical, Physical and Engineering Sciences, 370(1968), pp.2520-2556.

Mo, T., 1999: AMSU-A antenna pattern corrections. IEEE Trans. Geosci. Remote Sens.,37, 103–112.

Moradi, I., Ferraro, R.R., Eriksson, P. and Weng, F., 2015. Intercalibration and validation of observations from ATMS and SAPHIR microwave sounders. IEEE Transactions on Geoscience and Remote Sensing, 53(11), pp.5915-5925.

Moradi, I., S. A. Buehler, V. O. John, and S. Eliasson (2010), Comparing upper tropospheric humidity data from microwave satellite instruments and tropical radiosondes, J. Geophys. Res.,115 , D24310, doi:10.1029/2010JD013962.

Odintsova, T.A., Tretyakov, M.Y., Krupnov, A.F. and Leforestier, C., 2014. The water dimer millimeter-wave spectrum at ambient conditions: A simple model for practical applications. Journal of Quantitative Spectroscopy and Radiative Transfer, 140, pp.75-80.

Ohring, G., B. Wielicki, R. Spencer, B. Emery, and R. Datla, 2005: Satellite Instrument Calibration for Measuring Global Climate Change: Report of a Workshop. Bull. Amer. Meteor. Soc., 86, 1303–1313, doi: 10.1175/BAMS-86-9-1303.

Payne, V.H., Delamere, J.S., Cady-Pereira, K.E., Gamache, R.R., Moncet, J.L., Mlawer, E.J. and Clough, S.A., 2008. Air-broadened half-widths of the 22-and 183-GHz water-vapor lines. IEEE Transactions on Geoscience and Remote Sensing, 46(11), pp.3601-3617.

Payne, V.H., Mlawer, E.J., Cady-Pereira, K.E. and Moncet, J.L., 2011. Water vapor continuum absorption in the microwave. IEEE Transactions on Geoscience and Remote Sensing, 49(6), pp.2194-2208.

Pellarin, T., A. Ali, F. Chopin, I. Jobard, and J.-C. Bergès, 2008: Using spaceborne surface soil moisture to constrain satellite precipitation estimates over West Africa. Geophys. Res. Lett., 35, L02813, doi:https://doi.org/10.1029/2007GL032243.

Pellarin, T., S. Louvet, C. Gruhier, G. Quantin, and C. Legout, 2013: A simple and effective method for correcting soil moisture and precipitation estimates using AMSR-E measurements. Remote Sens. Environ., 136, 28–36, doi:https://doi.org/10.1016/j.rse.2013.04.011.

Peubey, C. and McNally, A.P., 2009. Characterization of the impact of geostationary clear-sky radiances on wind analyses in a 4D-Var context. Quarterly Journal of the Royal Meteorological Society, 135(644), pp.1863-1876.

Randriamampianina R. 2006. Impact of high resolution observations in the ALADIN/HU model. *Időjárás* **110**: 329–349.

Randriamampianina R, H Schyberg and M Mile, 2017. Observing system experiments with an Arctic mesoscale model, under preparation.

Rawlins, F., Ballard, S.P., Bovis, K.J., Clayton, A.M., Li, D., Inverarity, G.W., Lorenc, A.C. and Payne, T.J., 2007. The Met Office global four-dimensional variational data assimilation scheme. Quarterly Journal of the Royal Meteorological Society, 133(623), pp.347-362.

Robel, J. (editor), 2009: NOAA KLM user's guide with NOAA-N, -N' supplement, available from http://www.ncdc.noaa.gov/oa/pod-guide/ncdc/docs/klm/cover.htm

Rosenkranz, P.W., 1998. Water vapor microwave continuum absorption: A comparison of measurements and models. Radio Science, 33(4), pp.919-928.

Rothman, L.S., Gordon, I.E., Babikov, Y., Barbe, A., Benner, D.C., Bernath, P.F., Birk, M., Bizzocchi, L., Boudon, V., Brown, L.R. and Campargue, A., 2013. The HITRAN2012 molecular spectroscopic database. Journal of Quantitative Spectroscopy and Radiative Transfer, 130, pp.4-50.

Saavedra, P., A. Battaglia, and C. Simmer, 2012: Partitioning of cloud and rain water content by ground-based observations with the radiometer ADMIRARI in synergy with a micro rain radar. Journal of Geophysical Research - Atmospheres, 117, D05203, 18pp., doi:10.1029/2011JD016579

Saunders, R.W., Hewison, T.J., Stringer, S.J. and Atkinson, N.C., 1995. The radiometric characterization of AMSU-B. Microwave Theory and Techniques, IEEE Transactions on, 43(4), pp.760-771.

Saunders, R.W., M.Matricardi and P.Brunel, 1999: An improved fast radiative transfer model for assimilation of satellite radiance observations. Q.J.Roy.Met.Soc., 125, 1407—1426.

Saunders, R., Hocking, J., Rundle, D., Rayer, P., Matricardi, M., Geer, A., Lupu, C., Brunel, P., and Vidot, J., 2013. RTTOV-11: Science and validation report, NWP-SAF report, Met Office, UK, 62 pp.

Serov, E.A., Koshelev, M.A., Odintsova, T.A., Parshin, V.V. and Tretyakov, M.Y., 2014. Rotationally resolved water dimer spectra in atmospheric air and pure water vapour in the 188–258 GHz range. Physical Chemistry Chemical Physics, 16(47), pp.26221-26233.

Sreerekha, T.R., S.J. English and P.J. Rayer, 2007. Report on oxygen sounding channel frequencies and polarisations. EUMETSAT Contract EUM/CO/06/1557/PSF. Available from http://www.eumetsat.int.

Sreerekha TR, A.M. Doherty, S.J. English, P.J. Rayer 2008: Report on tThe Potential of a Microwave Sounder 229GHz Channel. EUMETSAT Contract EUM/CO/07/4600000409/CJA. Available from http://www.eumetsat.int.

Stamnes K, Tsay SC, Wiscombe W, Laszlo I., 2000: DISORT, a general-purpose Fortran program for discrete-ordinate-method radiative transfer in scattering and emitting layered media: documentation of methodology. Goddard Space Flight Center, NASA. 2000 Mar.

Storto A, R. Randriamampianina 2010. The relative impact of meteorological observations in the Norwegian regional model as determined using an energy norm-based approach. *Atmos. Sci. Let.* **11**: 51–58.

Sun, J., M. Xue, J. W. Wilson, I. Zawadzki, S. P. Ballard, J. Onvlee-Hooimeyer, P. Joe, D. M. Barker, P.-W. Li, B. Golding, M. Xu, and J. Pinto, 2014: Use of NWP for Nowcasting Convective Precipitation. Bull. Amer. Meteor. Soc., 95, 409–426, doi:10.1175/BAMS-D-11-00263.1

Surussavadee, C., and Staelin, D. H.: Global Precipitation Retrievals Using the NOAA AMSU Millimeter-Wave Channels: Comparisons with Rain Gauges, Journal of Applied Meteorology and Climatology, 49, 124-135, 10.1175/2009jamc2262.1, 2010.

Tian, M., Zou, X. and Weng, F., 2015. Use of Allan Deviation for Characterizing Satellite Microwave Sounder Noise Equivalent Differential Temperature (NEDT). Geoscience and Remote Sensing Letters, IEEE, 12(12), pp.2477-2480.

Ulaby, F.T., Moore, R.K. and Fung, A.K., 1981, Microwave Remote Sensing: Active and Passive, Volume 1, Microwave Remote Sensing Fundamentals and Radiometry, Norwood, Artech House.

Uppala, S.M. et al., 2005: The ERA-40 re-analysis. Quarterly Journal of the Royal Meteorological Society, 131(612), pp.2961-3012.

R. F. Voss, "1/f (flicker) noise : a brief review," in Proceedings of the 33rd Annual Symposium on Frequency Control, pp. 40–46, June 1979.

Wahl, S., C. Bollmeyer, S. Crewell, C. Figura, P. Friederichs, A. Hense, J. Keller, and C. Ohlwein (2017): A novel convective-scale regional reanalysis COSMO-REA2: Improving the representation of precipitation. Meteorologische Zeitschrift, doi: 10.1127/metz/2017/0824

Weatherhead, E. C., Harder, J., Araujo-Pradere, E. A., English, J. M., Flynn, L. E., Frith, S., Lazo, J. K., Pilewskie, P., Weber, M., and Woods, T. N.: How long do satellites need to overlap? Evaluation of climate data stability from overlapping satellite records, Atmos. Chem. Phys., 17, 15069-15093, 2017.

Weng, F. and Yang, H., 2016. Validation of ATMS calibration accuracy using Suomi NPP pitch maneuver observations. Remote Sensing, 8(4), p.332.

Wilheit, T., Brogniez, H., Datta, S., Linwood Jones, W., Payne, V., Stocker, E., and Wang, J., 2013: The use of SAPHIR on Megha-Tropiques for intercalibration of polar-orbiting microwave water vapor sounders. EUMETSAT meteorological satellite Conference / 19th AMS Satellite Meteorology Oceanography and Climatology Conference, Vienna, Austria, 272, 2013.

WMO, 2015. Guide to the Direct Broadcast Network (DBNet) for near real-time relay of low earth orbit satellite data, https://wis.wmo.int/DBNet-Guide

Xie, X., Löhnert, U., Kneifel, S. und Crewell, S., 2012: Snow particle orientation observed by ground-based microwave radiometry. Journal of Geophysical Research, 117, DOI: 10.1029/2011JD016369

Xie, X., S. Crewell, U. Loehnert, C. Simmer, and J. Miao, 2015: Polarization Signatures and Brightness Temperatures Caused by Horizontally-Oriented Snow Particles at Microwave Bands: Effects of Atmospheric Absorption. Journal of Geophysical Research, 120, 12, 6145-6160, DOI: 10.1002/2015JD023158

Yang, H. and Weng, F. (2016). Corrections for On-Orbit ATMS Lunar Contamination. IEEE Transactions on Geoscience and Remote Sensing, 54(4), 1918-1924.

Yang, H., Weng, F., & Anderson, K. (2016). Estimation of ATMS antenna emission from cold space observations. IEEE Transactions on Geoscience and Remote Sensing, 54(8), 4479-4487.

Zhao, L., and F. Weng, 2002: Retrieval of ice cloud properties using the Advanced Microwave Sounding Unit (AMSU). *J. Appl. Meteor*, **41,** pp. 384–395

Zhang F,. Y. Yang, C. Weng, 2014, The Effects of Assimilating Conventional and ATOVS Data on Forecasted Near-Surface Wind with WRF-3DVAR, *Mon. Wea. Rev. 143, 153-164.*

Zhu, T. and Weng, F., 2013. Hurricane Sandy warm-core structure observed from advanced Technology Microwave Sounder. Geophysical Research Letters, 40(12), pp.3325-3330.

Zhu Y., E.H. Liu, R. Mahajan, C. Thomas, D. Groff , P. van Delst, A. Collard, D. Kleist, R. Treadon, J. Derber, 2016: All-sky microwave radiance assimilation in the NCEP's GSI analysis system. *Mon. Wea. Rev.* **144**: 4709 – 4735, doi: http://dx.doi.org/10.1175/MWR-D-15-0445.1.

Zou, C.-Z., and W. Wang, 2011: Intersatellite calibration of AMSU-A observations for weather and climate applications. J. Geophys. Res., 116, D23113, doi:10.1029/2011JD016205.

Zou, X., F. Weng, B. Zhang, L. Lin, Z. Qin, and V. Tallapragada (2013), Impacts of assimilation of ATMS data in HWRF on track and intensity forecasts of 2012 four landfall hurricanes, J. Geophys. Res. Atmos., 118, 11,558–11,576

List of Acronyms

Acronym	Meaning
AAPP	ATOVS AVHRR Preprocessing Package
ADC	Analogue to Digital Converter
A-DCS	Advanced Data Collection System
AIRS	Atmospheric Infrared Sounder
ALADIN	Aire Limitée Adaptation dynamique Développement InterNational
AMIE	Atmospheric Radiation Measurement Madden Julian Observation Investigation Experiment
AMSR-E	Advanced Microwave Scanning Radiometer – Earth Observing System
AMSU	Advanced Microwave Sounding Unit
AMV	Atmospheric Motion Vector
ARTS	Atmospheric Radiative Transfer Simulator
ASCAT	Advanced Scatterometer
ATOMMS	Active Temperature, Ozone Moisture Microwave Spectrometer
ATOVS	Advanced TIROS-N Operational Vertical Sounder
ATMS	Advanced Technology Microwave Sounder
AVHRR	Advanced Very High Resolution Radiometer
BT	Brightness Temperature
Cal/Val	Calibration/Validation
CDR	Climate Data Record
CINDY	Cooperative Indian Ocean Experiment on Intraseasonal Variability
CLW	Cloud Liquid Water
CMA	China Meteorological Administration
CMORPH	Climate Prediction Center (CPC) Morphing Technique
CNES	Centre Nationale d'Études Spatiales
CONV	Conventional observations
CPI	Contractor Provided Item
CrIS	Cross-track Infrared Sounder
CRTM	Community Radiative Transfer Model
DBNet	Direct Broadcast Network
DC	Direct Current
DDA	Discrete Dipole Approximation
DFS	Degrees of Freedom for Signal
DEIMOS	Airborne microwave radiometer (23.8 GHz and 50.3 GHz)
DISORT	DIScrete Ordinate Radiative Transfer
DMSP	Defence Meteorological Satellite Program
DYNAMO	Dynamics of the Madden Julian Observation
EarthCARE	Earth Clouds, Aerosol and Radiation Explorer
ECMWF	European Centre for Medium-Range Weather Forecasts
ECV	Essential Climate Variable
EOF	Empirical Orthogonal Function
E Field	Electric Field
EMI	Electromagnetic Interference
EnVAR	Ensemble Variational
EPS	EUMETSAT Polar System
EPS-SG	EUMETSAT Polar System – Second Generation
ESA	European Space Agency

EUMETSAT	European Organisation for the Exploitation of Meteorological Satellites
EURD	EPS-SG End Users Requirements Document
FAAM	Facility for Airborne Atmospheric Measurements
FASTEM	FAST microwave Emissivity Model
FCI	Flexible Combined Imager
FSOI	Forecast Sensitivity Observation Impact
FY-	Feng Yun
FY	Firstyear
GCOM-W	Global Change Observation Mission – Water (SHIZUKU)
GCOS	Global Climate Observing System
GDAS	Global Data Assimilation System
GEO	Geostationary Orbit
GMI	Global precipitation mission Microwave Imager
GNSS	Global Navigation Satellite System
GPM	Global Precipitation Mission
GPS	Global Positioning System
GRUAN	GCOS Reference Upper-Air Network
GSICS	Global Space-based Inter-Calibration System
HARMONIE-AROME	HIRLAM-ALADIN Research on Mesoscale Operational NWP in Euromed, Applications of Research to Operations at Mesoscale
HIRLAM	High-resolution Limited Area Model
HIRS	High-resolution Infrared Radiation Sounder
HITRAN	High-resolution Transmission
HPBW	Half-Power Beam Width
H-SAF	Hydrology Satellite Application Facility
HUT	Helsinki University of Technology
IAPP	International ATOVS Processing Package
IASI	Infrared Atmospheric Sounder Interferometer
IASI-NG	Infrared Atmospheric Sounder Interferometer-Next Generation
ICI	Ice Cloud Imager
IFOV	Instantaneous Field-Of-View
IMERG	Integrated Multi-Satellite Retrievals for GPM
IOP	Intensive Operation Period
IPCC	Intergovernmental Panel on Climate Change
ISMAR	International Sub-millimetre Airborne Radiometer
ITSC	International TOVS Study Conferences
ITWG	International TOVS Working Group
IR	Infrared
IWP	Ice Water Path
JCSDA	Joint Center for Satellite Data Assimilation
JMA	Japan Meteorological Agency
JPSS	Joint Polar System Satellite
KENDA	Km-scale Ensemble Data Assimilation
LAM	Limited Area Model
LEO	Low Earth Orbit
LEOP	Launch and Early Orbit Phase
LO	Local Oscillator
LWP	Liquid Water Path
L1	Level 1
L2	Level 2

MARSS	Microwave Airborne Radiometer Scanning System
MEPS	MetCoOp Ensemble Prediction System
MetCoOp	Meteorological Cooperation on Operational NWP
Metop-SG	Meteorological Operational Satellite-Second Generation
MF	Météo France
MHS	Microwave Humidity Sounder
MOGREPS	Met Office Global and Regional Ensemble Prediction System
MPM	Millimeter-wave Propagation Model
MSLP	Mean Seal-level Pressure
MSU	Microwave Sounding Unit
MTG-I	Meteosat Third Generation – Imaging Satellite
MW	Microwave
MWHS	Microwave Humidity Sounder
MWI	Microwave Imager
MWS	Microwave Sounder
MWSG	Microwave Subgroup
MWRI	Microwave Radiation Imager
MWTS	Microwave Temperature Sounder
MY	Multiyear
NASA	National Aeronautics and Space Administration
NCEP	National Center for Environmental Prediction
NE∆T	Noise Equivalent Delta Temperature
NEMS	Nimbus-E Microwave Sounder
NERC	National Environment Research Council
NOAA	National Oceanic and Atmospheric Administration
NOAA/STAR	NOAA Center for Satellite Applications and Research
NPOESS	National Polar-orbiting Operational Environmental Satellite System
NPP	NPOESS Preparatory Programme
NRT	Near Real Time
NSIDC	National Snow and Ice Data Center
NWP	Numerical Weather Prediction
NWP SAF	NWP Satellite Application Facility
OBCT	On-board Calibration Target
OI	Optimal Interpolation
OSCAR	Observing Systems Capability Analysis and Review
OSI SAF	Ocean and Sea Ice Satellite Application Facility
OZA	Observation Zenith Angle
PC	Principal Component
PMET	Post-EPS Missions Experts Team
POES	Polar-orbiting Operational Environmental Satellites
PR	Polarisation Ratio
PRT	Platinum Resistance Thermistor
PSF	Point Spread Function
QC	Quality Control
QH	Quasi-horizontal
QV	Quasi-vertical
RAOB	Radiosonde Observation
RFI	Radio Frequency Interference
RMSE	Root Mean Square Error

RO	Radio Occultation
RR	Rotating reflector
RT	Radiative Transfer
RTM	Radiative Transfer Model
RTTOV	Radiative Transfer for TOVS
SAF	Satellite Application FacilityPDF
SAG	Scientific Advisory Group
SAPHIR	Sondeur Atmosphérique du Profil d'Humidité Intertropicale par Radiométrie
SCA	Scatterometer (EPS-SG)
SIOV	Satellite In-Orbit Verification
SNO	Simultaneous Nadir Overpass
SSM/I	Special Sensor Microwave / Imager
SSMIS	Special Sensor Microwave Imager / Sounder
SMAP	Soil Moisture Active Passive
SMOS	Soil Moisture and Ocean Salinity
SWE	Snow Water Equivalent
SYNOP	Synoptic
TB	Brightness Temperature
TCWV	Total Column Water Vapour
TIR	Thermal Infrared
TIROS	Television Infrared Observation Satellite
TMI	TRMM Microwave Imager
TPW	Total Precipitable Water
TRMM	Tropical Rainfall Measuring Mission
UNFCCC	United Nations Framework Convention on Climate Change
UTC	Universal Time Coordinated
UTH	Upper Tropospheric Humidity
UV	Ultraviolet
UVNS	Ultraviolet Visible Near-Infrared Shortwave-Infrared
VarBC	Variational Bias Correction
VIS	Visible
VII	Visible/Infrared Imager
VIIRS	Visible Infrared Imaging Radiometer Suite
WMO	World Meteorological Organization
3MI	Multi-Viewing Multi-Channel Multi-Polarisation Imager
4DVAR	Four-dimensional Variational Data Assimilation